Copy No. _____

Defence Research and
Development Canada

Recherche et développement
pour la défense Canada

DEFENCE R&D DÉFENSE

A load shortening curve library for longitudinally stiffened panels

Malcolm J. Smith

Defence R&D Canada – Atlantic

Technical Memorandum
DRDC Atlantic TM 2010-140
August 2010

Canada

This page intentionally left blank.

A load shortening curve library for longitudinally stiffened panels

Malcolm J. Smith

Defence R&D Canada – Atlantic

Technical Memorandum
DRDC Atlantic TM 2010-140
August 2010

Principal Author

Original signed by Malcolm J. Smith

Malcolm J. Smith

Approved by

Original signed by Neil G. Pegg

Neil G. Pegg

Head/ Warship Performance

Approved for release by

Original signed by Ron Kuwahara for

Calvin Hyatt

Chair/ Document Review Panel

Abstract

Efficient methods for determining the load versus end-shortening response of longitudinally stiffened panels are considered. A library of load-shortening curves for a wide range of design parameters is developed using an automated finite element analysis (FEA) procedure. The load-shortening response of twenty benchmark stiffened panels is estimated by interpolation of the library curves. These are compared with similar curves calculated using nonlinear FEA and using design formulas published by the International Association of Classification Societies (IACS). The ultimate strength of eight benchmark hull girders is predicted using the interpolation and IACS methods for estimating the load-shortening response of stiffened panel structures, all within the framework of a Smith's method algorithm implemented in ULTMAT. Comparisons with previously published results indicate that acceptable accuracy can usually be obtained with the approximate methods. The scatter in strength predictions using Smith's method is considered, and is sometimes found to be greater than the recommended safety factor of 1.1.

Résumé

Des méthodes efficaces permettant de déterminer la réaction de raccourcissement de charge versus la réaction de raccourcissement d'extrémité de panneaux raidis dans le sens de la longueur sont prises en compte. Un ensemble de courbes de raccourcissement de charge pour une vaste gamme de paramètres de conception est créé à l'aide d'une procédure d'analyse par éléments finis automatisée. La réaction de raccourcissement de charge de vingt panneaux raidis de référence est estimée par interpolation de l'ensemble des courbes. On les compare à des courbes semblables calculées à l'aide d'une analyse par éléments finis non linéaire et de formules de conception publiées par l'*International Association of Classification Societies* (IACS). La résistance à la rupture de huit poutres-coques de référence est prédite à l'aide des méthodes d'interpolation et de l'IACS permettant d'estimer la réaction de raccourcissement de charge de structures de type panneau raidi, la totalité dans le cadre d'un algorithme de la méthode de Smith mis en œuvre dans ULTMAT. Les comparaisons avec les résultats publiés antérieurement indiquent qu'une précision acceptable peut habituellement être obtenue en utilisant les méthodes approximatives. La répartition des prédictions de résistance à l'aide de la méthode de Smith est prise en compte; de plus, elle dépasse parfois le facteur de sécurité recommandé de 1.1.

This page intentionally left blank.

Executive summary

A load shortening curve library for longitudinally stiffened panels

Malcolm J. Smith; DRDC Atlantic TM 2010-140; Defence R&D Canada – Atlantic; August 2010.

Introduction or background: A ship's ultimate strength is the maximum bending moment that can be sustained by the hull structure. Assessment methods based on ultimate strength are being increasingly accepted in the design standards for large naval and commercial ships. Rapid calculation is required in design work, and the present study explores the accuracy of approximate methods for evaluating ultimate strength. The accuracy of using libraries of predetermined design curves in ultimate strength calculations is considered in particular. These design curves describe the compressive stress-strain behaviour of basic structural element types, which is fundamental to a ship's ultimate strength.

Results: The report presents an automated procedure for calculating large libraries of "load-shortening" design curves for the compressive stress-strain response of basic stiffened panel elements. These are applied to a number of test cases, and are compared with results obtained with standard design formulas and more direct numerical methods. First, the compressive stress-strain responses of twenty benchmark stiffened panels are analysed. Second, the ultimate strengths of eight benchmark hull girder models, representing a wide range of ship types, are predicted.

Significance: The library of design curves developed for this study enables the ultimate strengths of a wide range of commercial and naval ships to be evaluated rapidly and with sufficient accuracy overall. The results show that the accuracy obtained by interpolating structural response behaviour from design curves is comparable to other methods. The ultimate strength predictions for the benchmark models exhibit considerable scatter in some cases, sometimes exceeding the recommended safety factor of 1.1.

Sommaire

A load shortening curve library for longitudinally stiffened panels

Malcolm J. Smith; DRDC Atlantic TM 2010-140; R & D pour la défense Canada – Atlantique; Août 2010.

Introduction : La résistance à la rupture d'un navire est le moment de flexion maximal auquel la structure de la coque peut résister. Les méthodes d'évaluation basées sur la résistance à la rupture sont de plus en plus acceptées dans les normes de conception des gros navires commerciaux et militaires. Un calcul rapide est nécessaire pour le travail de conception; de plus, la présente étude analyse la précision de méthodes approximatives permettant d'évaluer la résistance à la rupture. On tient compte en particulier de la précision de l'utilisation d'ensembles de courbes de conception prédéterminées dans les calculs de résistance à la rupture. Ces courbes de conception décrivent le comportement d'effort de compression/de déformation de compression de types d'éléments de structure de base, ce qui est fondamental à la résistance à la rupture d'un navire.

Résultats : Le rapport présente une procédure automatisée permettant de calculer de grands ensembles de courbes de conception de type raccourcissement de charge pour la réaction d'effort de compression/de déformation de compression d'éléments de panneau de type raidi de base. On les applique à un certain nombre d'essais et on les compare aux résultats obtenus en utilisant des formules de conception standard et des méthodes numériques plus directes. En premier lieu, les réactions d'effort de compression/de déformation de compression de vingt panneaux raidis de référence sont analysées. En deuxième lieu, la résistance à la rupture de huit modèles de poutre-coque de référence, représentant une vaste gamme de types de navires, est prédite.

Portée : L'ensemble des courbes de conception créé pour la présente étude permet d'évaluer la résistance à la rupture d'une vaste gamme de navires militaires et commerciaux rapidement et avec une précision globale suffisante. Les résultats montrent que la précision obtenue en interpolant le comportement de réaction de structure à partir des courbes de conception est comparable à celle d'autres méthodes. Les prédictions de résistance à la rupture s'appliquant aux modèles de référence présentent une répartition considérable dans certains cas, dépassant parfois le facteur de sécurité recommandé de 1.1.

Table of contents

List of figures

List of tables

This page intentionally left blank.

1   Introduction

Load versus end-shortening curves are used to define the average stress-strain response of longitudinally stiffened panels undergoing compressive loading. For example, when calculating the ultimate strength of a ship's hull girder in sag, load-shortening curves are used for the compressive response of continuous topsides structure, such as the weather deck, upper portions of the side shell, and the upper interior decks, all of which are in compression under sag loading. This use of load-shortening curves is a feature of Smith's method, a common numerical technique for evaluating hull girder ultimate strength [1].

Direct calculation of load-shortening curves by numerical methods is too time intensive for design work. More efficient methods have been developed, starting with Smith et al [2], who used libraries of pre-determined design curves describing the load-shortening response of basic stiffened panel elements. The design curves were interpolated to obtain the load-shortening response and ultimate strength for specific configurations.

Alternatives to load-shortening curves include the use of analytical formulas for the compressive stress-strain response. This is the approach taken for the ultimate strength check in the International Association of Classification Societies (IACS) Common Structural Rules (CSR) for oil tankers and bulk carriers [3],[4]. These rules incorporate analytical formulas for the stress-strain response of local structure into an incremental-iterative scheme for analysis of the hull girder that is similar to Smith's method. While the IACS formulas are, strictly speaking, intended for the design of bulk carriers and double hull oil tankers, there is nothing in the formulation of the method prescribed in the IACS common structural rules that invalidates it for use with other types of large, longitudinally framed vessels.

Other alternatives for evaluating hull girder ultimate strength include simplified closed-form assessment methods such as those of Caldwell [5], Paik and Mansour [6], and Paik et al [7]; the Idealized Structural Unit Method (ISUM) first developed by Ueda and Rashed [8]; and direct assessment with nonlinear finite element analysis (FEA) first reported by Chen et al. [9].

A recent study comparing the ultimate strengths of several naval and commercial ship designs found considerable scatter in hog and sag ultimate strengths [10]. In that study, ultimate strengths were calculated using the ULTMAT program (DRDC's ultimate strength analysis software [19]) in conjunction with three different load-shortening curve libraries and the IACS rules. The scatter was attributed to incompleteness of the libraries of load-shortening curves used in the calculations; and also to an apparent conservativeness in the IACS rules. Both of these shortcomings are addressed in the present report.

The primary purpose of this study is to report on the development of a new load-shortening curve library to replace the existing libraries in DRDC's ULTMAT code. While the existing curve libraries were intended for naval structures, the goal of this development is to create one curve library applicable to both naval and commercial ship structure designs. The new curve library will complement the load-shortening formulas based on the IACS rules, which were implemented in version 2.2 of ULTMAT. The extension of ULTMAT's applicability to commercial structures was deemed necessary as part of its incorporation into the STRUC II software developed for Co-operative Research Ships (CRS) [11].

Subsequent to the publication of Ref [10], some errors were discovered in the ULTMAT implementation of the IACS rules which affected the accuracy of numerical results in that study. A secondary purpose of the present study is therefore to re-evaluate the numerical results with the corrected ULTMAT code, and to again compare ultimate strength results calculated using both the IACS and load-shortening curve approach. Based on these comparisons, some conclusions are drawn as to the best approach for a given ship design and about the accuracy of Smith's method as a whole.

2 Methodology

2.1 Preliminaries

Modern ship structures are comprised of welded stiffened panels. In longitudinally framed ships, the hull and deck plating is supported by relatively small, closely spaced longitudinal stiffeners in the fore-and-aft direction. These longitudinal stiffeners are themselves supported by a system of heavier, more widely spaced transverse frames perpendicular to the longitudinal stiffeners. The transverse framing system is supported by deep longitudinal girders and longitudinal bulkheads, while these in turn are supported by transverse bulkheads. If this system of support functions properly, the structure will resist bending loads through its continuous longitudinal structure, which consists of the plating and longitudinal stiffeners, longitudinal girders, and longitudinal bulkheads.

In ultimate strength analysis using Smith's method, a fundamental assumption is that the hull structure behaves like a beam in bending under still water and wave load action. The bending strength of the hull girder can therefore be calculated by considering just the response of the structure at certain critical transverse cross sections. It also means that individual structural elements undergo loading mainly in the fore-aft direction, and are therefore subject primarily to uni-axial tension and compression. This approximation neglects other loading effects besides hull girder bending, such as hull girder shear loading and local pressure loading of the hull plating.

The majority of the longitudinal structure consists of basic longitudinally stiffened panel components, shown in Figure 1. Subject to extreme compressive loads these components will fail in one or more of the following modes: interframe beam-column buckling; interframe flexural-torsional buckling; local buckling of the plating; local buckling of the longitudinal stiffener web; gross yielding; and overall grillage collapse [12]. If it is assumed that the transverse supporting structure is sufficiently sturdy, the grillage mode of failure can be ruled out. This assumption allows the other modes of failure to be studied by considering only the longitudinal structure at certain transverse cross sections.
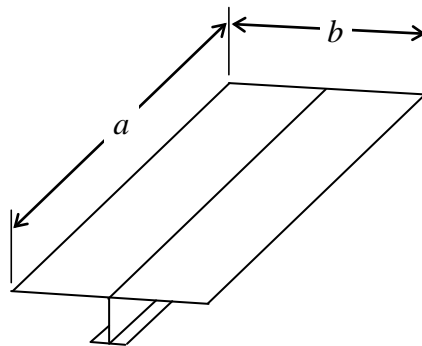
Figure 1: Basic longitudinally stiffened panel component.

Longitudinally stiffened panel components are commonly characterized by three dimensionless design parameters [13]:

$$\text{Plate slenderness: } \beta = (b/t)\sqrt{\sigma_y / E} \tag{1}$$

$$\text{Column slenderness: } \lambda = (a/\pi r_g)\sqrt{\sigma_y / E} \tag{2}$$

$$\text{Area ratio: } \gamma = A_s / A = \frac{(d - t_f)t_w + wt_f}{bt + (d - t_f)t_w + wt_f} \tag{3}$$

in which b is the width of attached plating; t is the plate thickness; a is the length; r_g is a radius of gyration of the plate/stiffener combination; A_s is the cross sectional area of the stiffener; and σ_y and E are the yield stress and elastic modulus, respectively.

In addition to these parameters, panels can also be characterized by the imperfections that arise due to welding and other fabrication effects. Separate dimensionless measures of the plate imperfection, stiffener imperfection, and residual stress are commonly used, although these are generally correlated. These are expressed as $\delta_p/\beta^2 t$, δ_s/a, and σ_r/σ_y, where the plate imperfection δ_p refers to the maximum out-of-plane deflection of the plate relative to an adjacent stiffener; the stiffener imperfection δ_s is the maximum out-of-straightness from the undeformed axis of the stiffener; and the residual stress σ_r is the average induced compressive stress in the plating outside of the heat-affected zone. Distributions of stiffener imperfections and residual stresses are illustrated in Figure 2 and Figure 3, respectively. The three measures of imperfection are assumed to be correlated, and are grouped into three levels (slight, average, severe) as defined in Table 1.

Table 1: Imperfection levels [14].

Level	Values		
	Plate def $\delta_p/\beta^2 t$	**Panel def** δ_s/a	**Res. stress** σ_r/σ_y
Slight	0.025	0.00025	0.05
Average	0.10	0.0008, $\lambda \le 0.3$ 0.0012, $0.3 < \lambda \le 0.6$ 0.0015, $\lambda > 0.6$	0.15
Severe	0.30	0.002, $\lambda \le 0.3$ 0.0038, $0.3 < \lambda \le 0.6$ 0.0046, $\lambda > 0.6$	0.30

DRDC Atlantic TM 2010-140
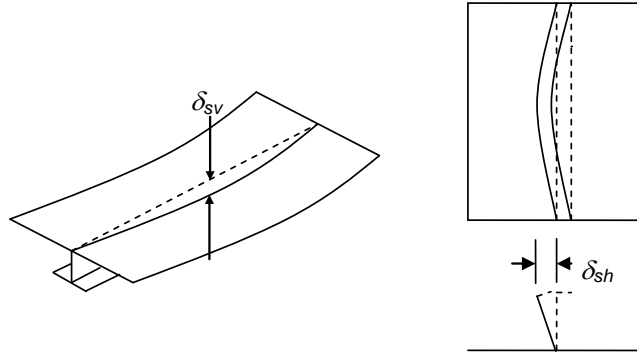
Figure 2: Shape imperfections for longitudinal stiffeners.
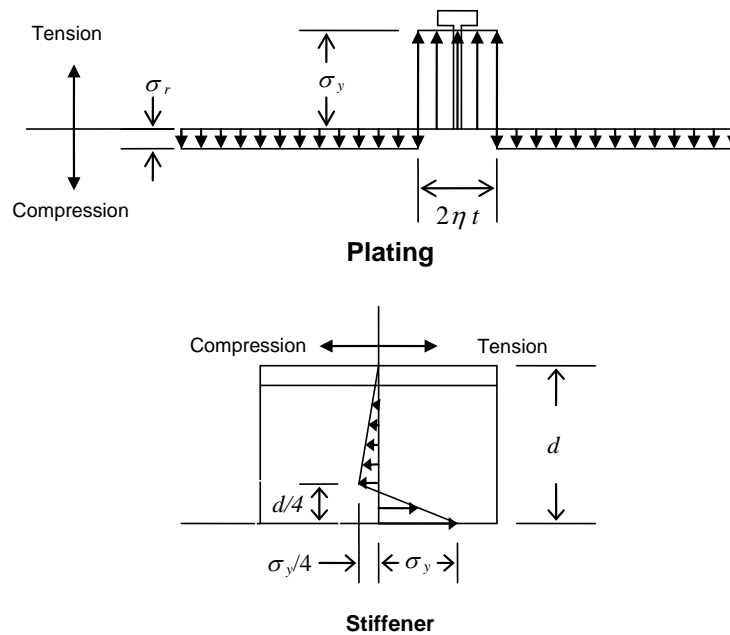
Plating

Stiffener

Figure 3: Residual stress distribution due to welding a stiffener to plating

2.2   Curve library parameter space

While it is possible to directly calculate the average stress-strain response for each stiffened panel in a cross section, this generally entails lengthy computations with a nonlinear numerical procedure. Practical ship design work requires much faster methods.

In the load-shortening curve library approach, a library of curves spanning a design parameter space is determined. In previous work, design parameters have typically included β, λ, and sometimes γ, along with different measures of imperfections and residual stresses. The combination of all of these comprises the design parameter space. Individual curves are then

calculated for unique combinations of the design parameters and these curves are then organized into a database or library in an easily accessible format. The stress-strain response of a particular panel can then be rapidly evaluated by interpolating the library curves using the values of the design parameters for the panel in question. For this method to be effective, the following conditions must be met:

1. The design parameter space must be sufficiently complete that the resulting load shortening curves represent the full range of load-shortening behaviour in stiffened panels.

2. The number of curves populating the library must be large enough to keep interpolation errors to a minimum.

Suppose the design parameter space is limited to β, λ, and γ. It may happen that two stiffened panel models have identical design parameters but also have one or more of the physical parameters that differ. Examples of this are if the two stiffened panels have different amounts of geometric imperfection, or if the stiffeners have a different section shape (tee vs. flatbar). If the load-shortening curves for these two panels are significantly different, the selected design parameters are not sufficient to fully characterize load-shortening response, and additional parameters would have to be considered.

It may also happen that an incremental change in the design parameters produces a large change in load-shortening behaviour. This is possible because of the nonlinearity inherent in the inelastic stress-strain response and may be associated with a sudden change in a stiffened panel's collapse mode or load-shedding behaviour. When this occurs it is an indication that the number of curves used to span the design parameter space is insufficient. As an example, if a large change in load-shortening response is observed between $\lambda=0.3$ and $\lambda=0.6$, this is an indication that intermediate values of λ should also be included.

The distributions of non-dimensional design parameters in several naval and commercial hull girders were previously investigated [10]. The ranges of parameters encountered in commercial structure were found to be somewhat wider than had been previously used in curve library developments for naval structure. For the present work, it was therefore decided to develop a new curve library based on an expanded design parameter space suitable for both commercial and naval structure.

The new curve library was populated using the parameters listed in Table 2. With one curve for each unique combination of the parameters, the total number of curves required is 1575. In the present study, only curves for an "average" imperfection level are calculated, so that the total number of curves calculated is only 525. Expansion of the library to include curves for "slight" and "severe" imperfections is left for future work. Calculating a library with this number of curves requires a highly automated analysis procedure. The remainder of Section 2 describes how this is done.

2.3 Panel sizing

Each curve of the database gives the load-shortening response for a unique combination of the design parameters. To determine each curve, the dimensionless design parameters must be

replaced by physical dimensions and properties of a numerical model. By inverting Eqns (1)-(3) the following formulas for t, b, and a are obtained in terms of the three dimensionless parameters and a material parameter $\mu = \sqrt{\sigma_y / E}$,

$$t = \sqrt{A_s (1 - \gamma) \mu / \gamma \beta} \,, \tag{4}$$

$$b = \sqrt{A_s (1 - \gamma) \beta / \gamma \mu} \,, \tag{5}$$

$$a = \pi \lambda r_g / \mu \,, \tag{6}$$

These formulas also depend upon the cross sectional area of the stiffener A_s, and the radius of gyration of the plate and stiffener combined r_g. Therefore, cross sectional dimensions of the stiffener must be assumed before (4)-(6) can be evaluated. These dimensions cannot be assumed arbitrarily, however, as this can lead to stiffener dimensions that are out-of-proportion to the plating thickness. Instead Eqns (4)-(6) are solved repeatedly with iterative adjustments to the stiffener dimensions until a reasonable compatibility between the stiffener and plate are achieved. For a tee or angle stiffener, dimensional compatibility is achieved when the following conditions are met, which are based on typical ranges observed in ship stiffened panels:

$$0.8 \leq t_f / t \leq 1.2 \,, \tag{7}$$

$$1 \leq d / w \leq 4.5 \,, \qquad 1 \leq t_f / t_w \leq 2.5 \,, \qquad 15 \leq d / t_w \leq 50 \tag{8}$$

Eqn (7) ensures that the stiffener is in proportion to the plate thickness, while Eqn (8) ensures that stiffener dimensions are in proportion to each other. For flatbar stiffened panels, only two conditions need to be satisfied:

$$0.8 \leq t_w / t \leq 1.2 \,, \tag{9}$$

$$7 \leq d / t_w \leq 15 \tag{10}$$

Table 2: Summary of parameters values used in load-shortening curve libraries

Parameter	Parameter values
β	1.0, 1.5, 2.0, 3.0, 4.0
λ	0.05, 0.15, 0.3, 0.45, 0.6, 0.8, 1.0
γ	0.125, 0.2, 0.275, 0.35, 0.425
Imperfections	slight, average, severe
Section shape	tee, angle, flatbar

2.4   Finite element modelling

Load-shortening curves are calculated using nonlinear FEA of three-dimensional models generated using panel dimensions determined by the method in Section 2.3. The FE models use

regular meshes of shell elements, similar to those shown in Figure 4. Models are configured as multispan models that extend from the midspan of one frame bay ($y = -a/2$) to the midspan of the next ($y = a/2$). These are considered to give more realistic collapse behaviour than single span models because deformation modes over adjacent frame bays can be represented [2]. Boundary conditions are also illustrated in Figure 4. A rigid frame is assumed to intersect the model at the central section ($y = 0$), which is simulated with translational constraints on the plate and web frame at those locations. Symmetry conditions are enforced at the ends of the panels and rotation constraints are applied to the transverse edges of plating.
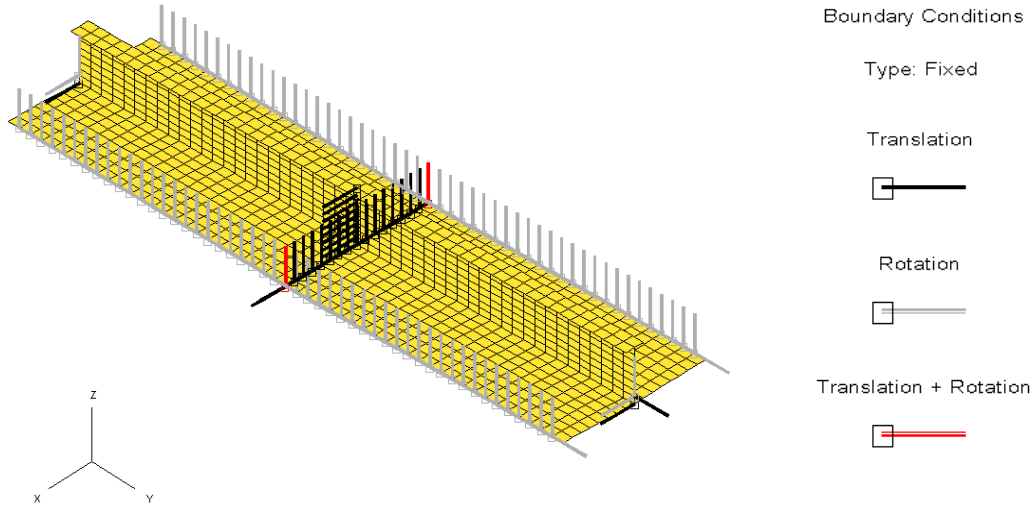
Figure 4: Boundary conditions for a longitudinally stiffened panel model.

The structural material is assumed to have an elastic modulus $E = 207$ GPa, Poisson's ratio $\nu = 0.3$, yield stress $\sigma_0 = 324$ MPa, and an isotropic hardening modulus of 2 GPa.

The entire model is meshed with 4-node quadrilateral shell elements. The element chosen is the 4 node shell in the VAST FEA program [15], which is based on mixed interpolation of tensorial strain components (MITC) and is free of shear locking. A regular meshing scheme is employed in which the mesh density is determined with the aid of a meshing parameter P, such that $n_a \times n_b = P^2$, and where n_a and n_b are the number of elements along the panel length and across the width of plating, respectively. It is further required that $n_a/n_b \cong a/b$, the aspect ratio of the plating. The stiffener web and flange are given meshes of $n_a \times n_w$ and $n_a \times n_f$ elements, respectively, where n_w and n_f are selected so as to maintain an approximately uniform element size. Thus the entire mesh is determined from the value of P. Experience has shown that meshes based on $P = 25$ give sufficient accuracy for a wide range of panel geometries.

Imperfections are explicitly included in the FE models. Out-of-straightness for symmetric beam sections is assumed to be sinusoidal in a direction normal to the plating (Figure 2). For non-symmetric sections, a lateral out-of-straightness is also included. Plating imperfections are doubly

sinusoidal in shape, and are always directed towards the stiffener side of the plate. Residual stress distributions applied to the plating and stiffener are shown in Figure 3.

In addition to these physical imperfections, a small amplitude of a linear buckling mode shape is added to the finite element model geometry in order to seed local buckling modes in the nonlinear analysis.

2.5   Solution procedure

The load-shortening response of the FE model is determined by applying a compressive load along an axis passing through the centroid of the panel. The axial loading and displacement of the panel ends is controlled by a single node at each end. This is accomplished through use of multipoint constraints that tie displacements and rotations of nodes at the panel ends to the centroidal nodes. The axial displacement of one of these centroidal nodes is fixed, while the axial displacement of the other is incrementally increased until $\varepsilon/\varepsilon_y = 6$, where $\varepsilon/\varepsilon_y$ is the normalized axial compressive strain.

Nonlinear calculations are performed using an orthogonal trajectory algorithm in the VAST FEA program. In this method, the arc length of each load increment is determined by the following equations:

$$_{i+1}\Delta l =\, _i\Delta l\left(\frac{N_d}{_i N}\right)^{\mu},\tag{11}$$

$$_i\Delta l \le \alpha(_1\Delta l)\tag{12}$$

where $_i\Delta l$ is the arc length of the ith increment; $_i N$ is the number of iterations needed for the ith increment to converge to a tolerance of κ; N_d is a desired or optimal number of iterations per increment; μ is an exponent governing the rate at which the arc length can grow or shrink; and α sets a limit on the amount by which the arc length may grow from the initial step size $_1\Delta l$.

Unfortunately no single combination of the user-selected nonlinear parameters κ, N_d, μ, α, $_1\Delta l$ can be expected to produce a convergent solution over the entire loading range for all stiffened panels. Instead nonlinear calculations are performed in a series of passes, adjusting the parameters with each pass until fully convergent solutions are obtained over the entire load range for all panels.

The convergence tolerance is maintained at $\kappa = 0.005$ in all passes so as not to compromise the accuracy of the calculations. For the other parameters it was found that the arc length exponent μ had the largest effect on the number of load steps required and the speed of convergence. Larger values of μ (e.g. 0.5) allow the step size to adjust more dynamically but results in non-convergence in about 30% of panels. Smaller values (e.g. 0.01) reduce the number of non-convergent solutions but greatly increase the number of load steps needed. The sequence of four passes used for each mesh parameter P is listed in Table 3.

Better efficiency with the VAST solution algorithm can often be achieved by dividing the calculations into two stages. In the first stage, the panel is loaded up to $\varepsilon/\varepsilon_y = 2$, which normally spans the entire pre-collapse regime, as well as the first part of the post-collapse regime. In the second stage the loading is continued through the range $2 \leq \varepsilon/\varepsilon_y \leq 6$, which normally spans the remainder of the post-collapse regime. This load-step size is reset to a larger value at $\varepsilon/\varepsilon_y = 2$, which allows the solution algorithm to advance more quickly over the post-collapse regime. The maximum growth of the step size is controlled by using $\alpha = 3$ in the first stage, and $\alpha = 10$ in the second stage.

Table 3: Nonlinear solution strategy

Pass	κ	μ	Initial step size $_1\Delta l /a\varepsilon_y$	α	N_d
1	0.005	0.5	1/24	(3, 10)	4
2	0.005	0.075	1/24	(3, 10)	4
3	0.005	0.01	1/24	(3, 10)	4
4	0.005	0.01	1/48	(3, 10)	4

2.6   Automated curve library generation

Because of the large number of load-shortening curves to be calculated, the entire curve generation process must be automated as much as possible. This is done using a master computer program called LSCGenerator, which calls subprograms for generating the FE models (LSPanel), performing the FE analysis (VAST), and extracting the load-shortening curve from the results (LSCurveReader). The precise sequence of steps is as follows:

1. The basic parameters defining the composition of the curve library are input: values for β, λ, and γ, stiffener types (tee, angle, flatbar), and imperfection levels (slight, average, severe);

2. Panel dimensions are determined for all possible combinations of the basic parameters;

3. FE models are generated using panel dimensions and the mesh parameter, *P*; distortion imperfections are applied to the model geometry, and residual stresses are applied to the elements as an initial stress distribution;

4. A linear buckling analysis is performed, and a linear buckling mode is selected which predominantly consists of local plate and/or web deformations; a small amplitude of this mode is added to the model geometry;

5. Nonlinear solution parameters are selected from Table 3 for the given pass number;

6. Nonlinear FE analyses are performed using the VAST;

7. The load-shortening curve is extracted from the FEA results and a diagnostic step is performed in which the curve is checked for validity;

8. Steps 5-7 are repeated until either a valid curve is obtained, or until the maximum number of passes has been performed (4); and

9. If the curve is still invalid, steps 3-8 are repeated using progressively larger values of mesh parameter P until a valid curve is obtained.

3   Curve library results

The methodology of Section 2 was used to generate a library of 525 curves, all for an "average" level of imperfection. The curve library can be viewed in its entirety in Figure 35 – Figure 55 in Annex A. The present section summarizes main features of the library.

3.1   Effect of plate and column slenderness

The effect of plate slenderness β and column slenderness λ on the load-shortening behaviour can most easily be seen from Figure 5 and Figure 6. The former shows the ultimate strengths, i.e., peak values, from all the library curves for tee-stiffened panels. The latter gives the area under the curves, which is determined using a numerical approximation of the integral,

$$U_a = (1/\bar{\varepsilon}_0)\int_0^{\bar{\varepsilon}_0} \bar{\sigma} d\bar{\varepsilon} \tag{13}$$

where $\bar{\sigma} = \sigma/\sigma_y$ is the normalized axial stress, $\bar{\varepsilon} = \varepsilon/\varepsilon_y$, is the normalized axial strain, and $\bar{\varepsilon}_0 = 6$ is the maximum normalized strain. Note that U_a is a measure of the normalized strain energy in axial compression (elastic plus plastic strain combined). The strain energy complements ultimate strength in that it provides a measure of the shape of the curves, rather than just the peak value.

The results in Figure 5 show that ultimate strength decreases both with increasing β and with increasing λ. The loss of strength between $\beta = 1$ and $\beta = 1.5$ is often negligible for $\lambda > 0.4$. The energies (areas) also decrease both with increasing β, but this is most notable for $\lambda < 0.5$. The decline in energy with λ is much more marked than the decline in ultimate strength, reflecting the more pronounced load-shedding, or steepness of the post-buckling unloading, that occurs at higher values of λ. These observations are consistent with what has been observed in other studies [2].

3.2   Effect of area ratio

The effect of the area ratio γ on load-shortening behaviour has received much less attention in the literature than the effect of β and λ. In Figure 7 and Figure 8 the results of the two previous figures are re-plotted to better reveal the effect of γ. Overall the strengths and energies vary weakly with γ, showing slight increases in both strength and energy with increasing λ, a trend which is somewhat more pronounced at higher β. Similar behaviour is observed for angle and flatbar curves. The area ratio, which measures the relative importance of the stiffener to the overall load carrying capacity of a panel, therefore appears to be much less of a determining factor for the load-shortening behaviour than β and λ.
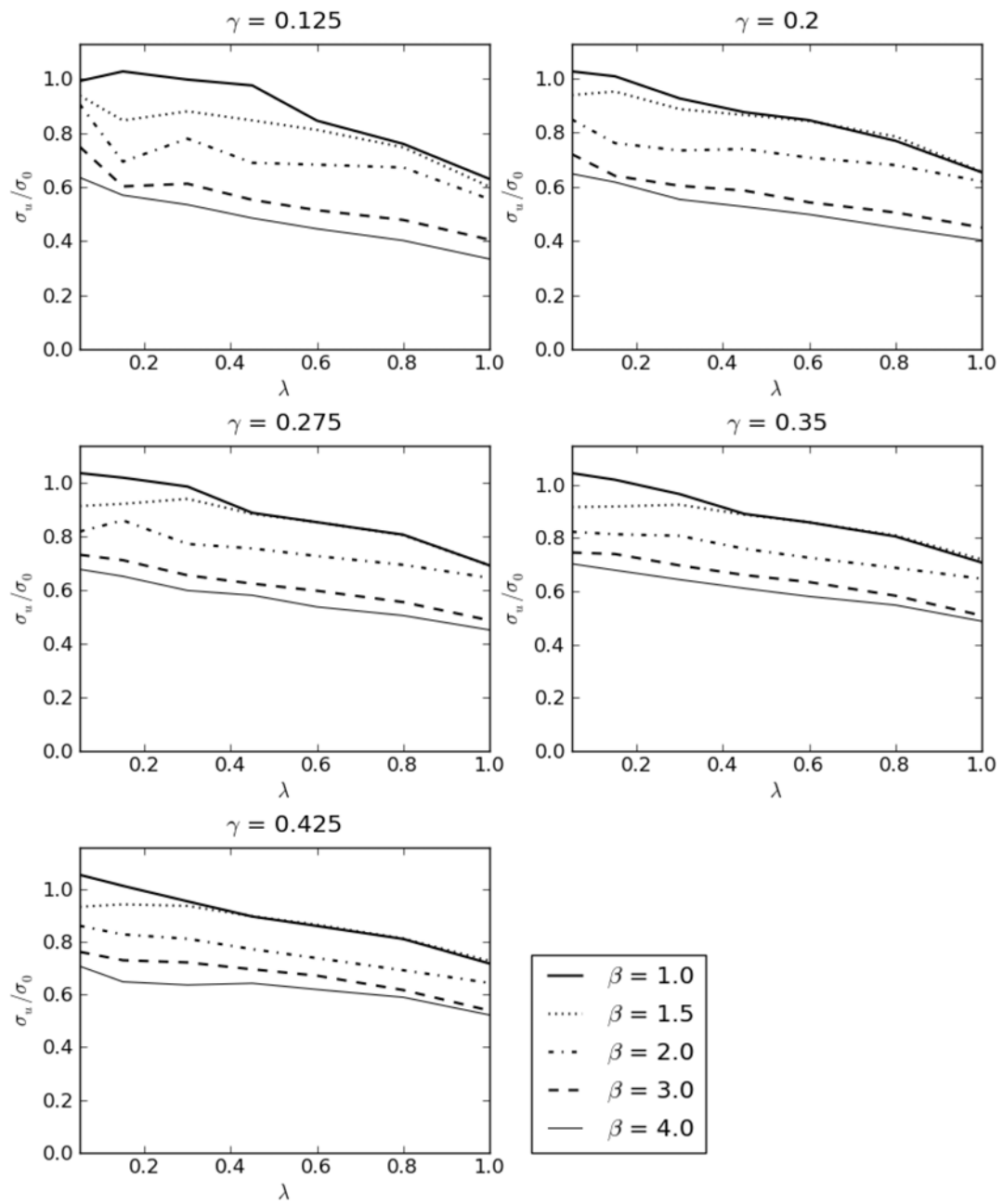
DRDC Atlantic TM 2010-140

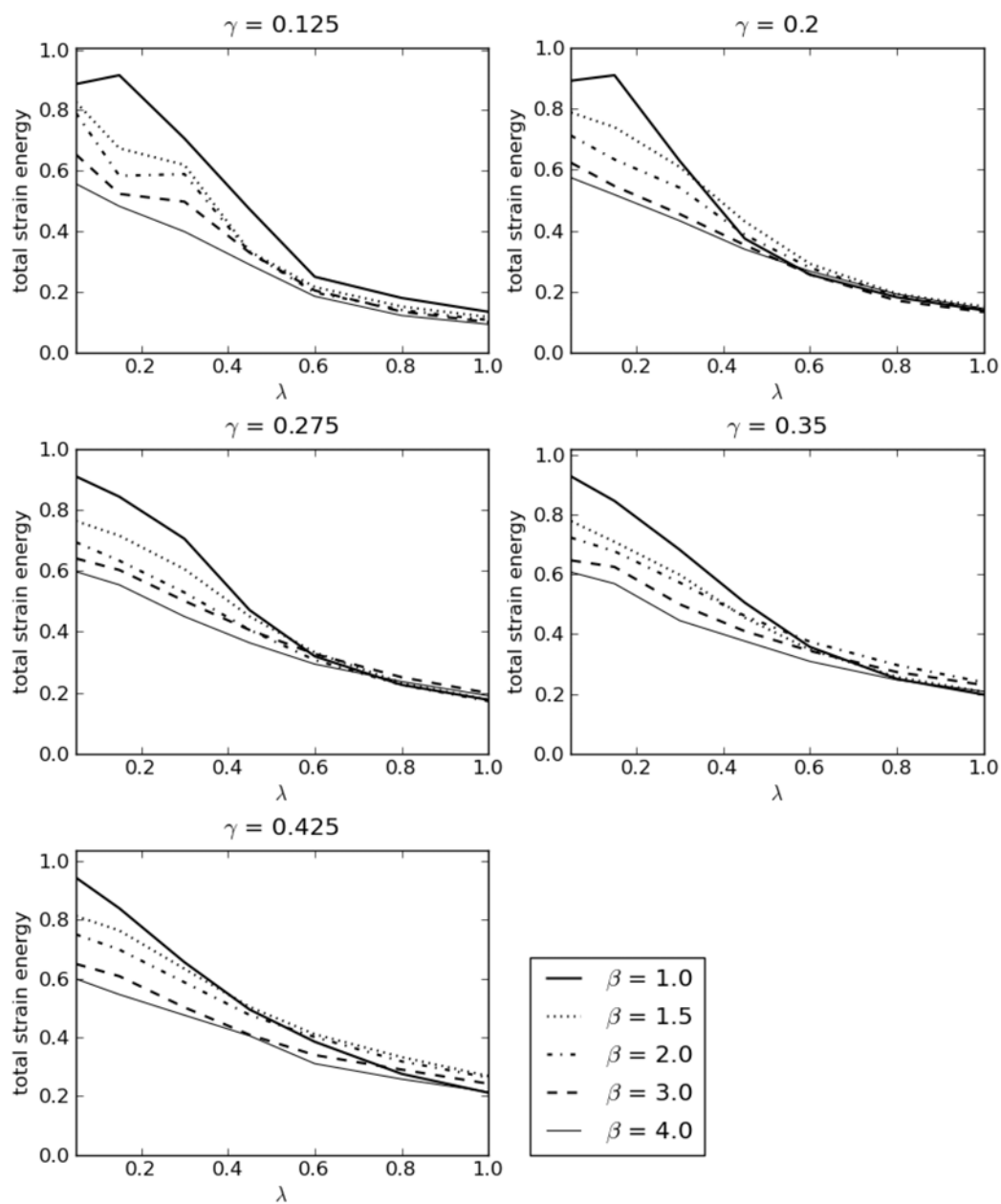*Figure 5: Ultimate strengths of tee-stiffened panels.*

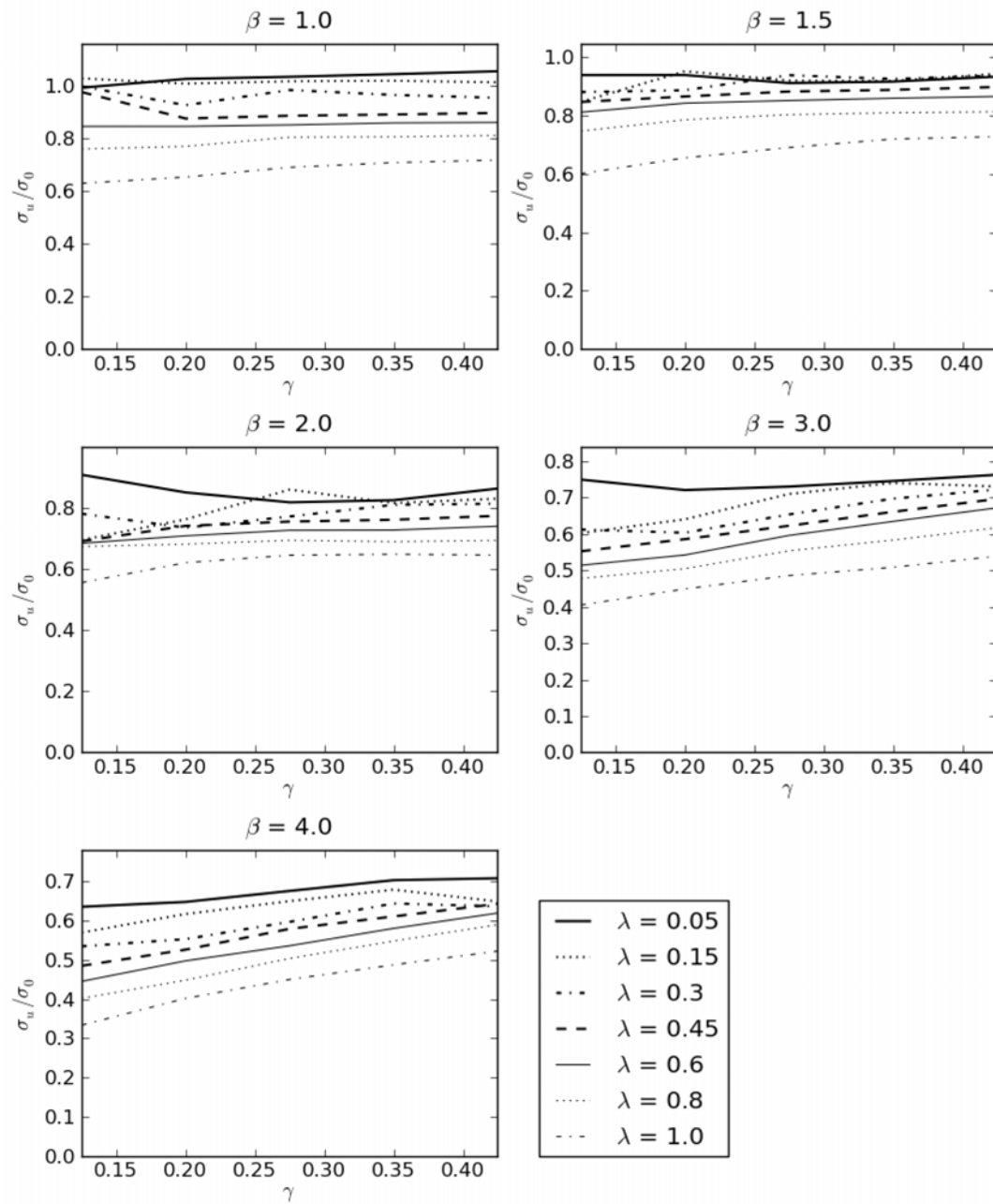*Figure 6: Normalized strain energies of tee-stiffened panels.*

Figure 7: Ultimate strengths of tee-stiffened panels showing the effect of γ.
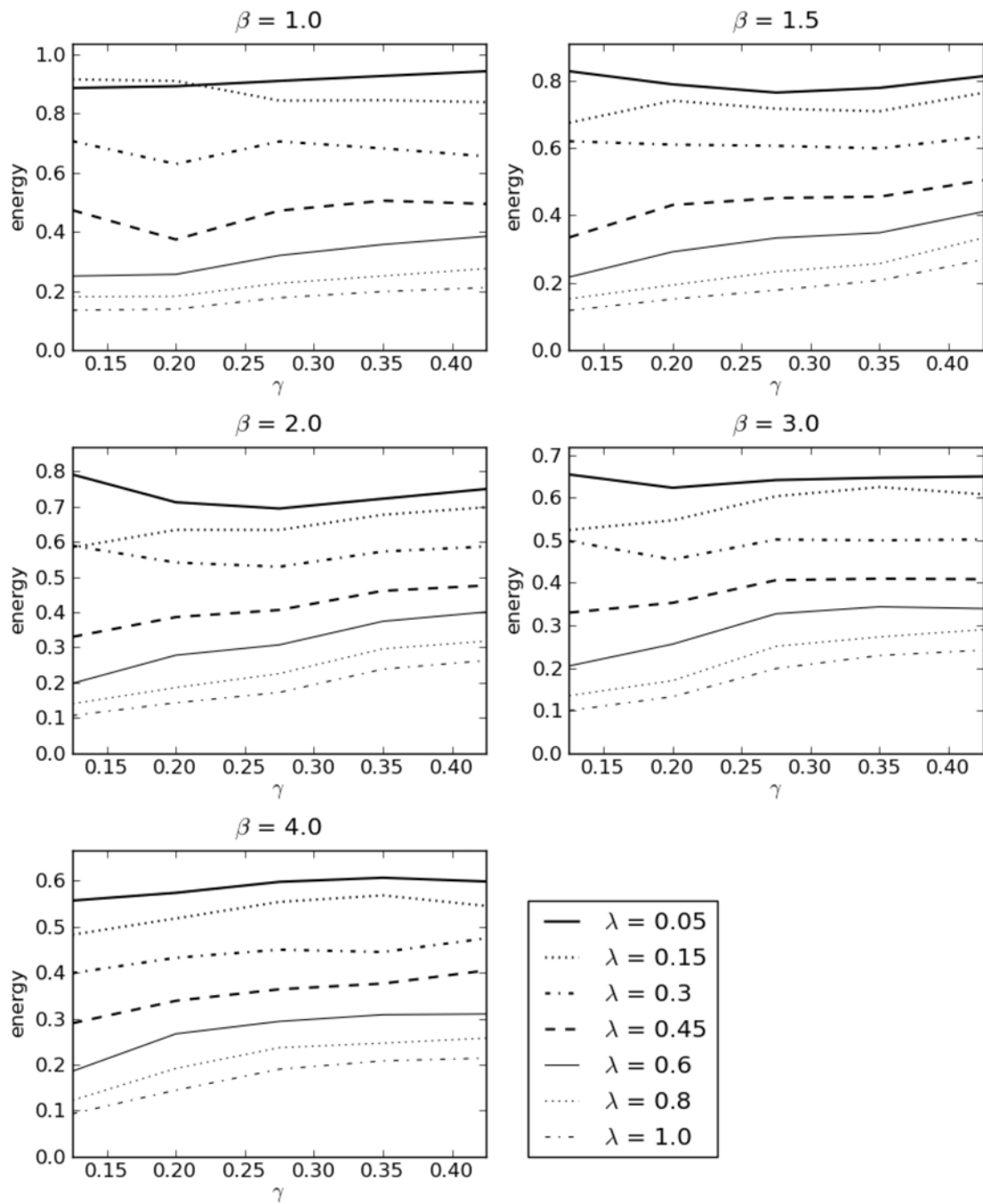
Figure 8: Normalized strain energies of tee-stiffened panels showing the effect of γ.

3.3   Effect of stiffener shape

Visual comparisons of the load-shortening curves in Annex A or of the ultimate strength and energy values depicted in Figure 9 and Figure 10 do not immediately reveal significant differences related to stiffener shape. To better bring out these effects, some further processing is performed on the strength and energy results. Consider a strength bias factor X_σ and an energy bias factor X_U defined using the results for tee-stiffeners as a reference. Thus for angle stiffeners

$$X_\sigma = \frac{[\bar{\sigma}_u]_{angle}}{[\bar{\sigma}_u]_{tee}} \qquad\qquad X_U = \frac{[U_a]_{angle}}{[U_a]_{tee}} \qquad\qquad (14)$$

with similar expressions for flatbars.

Plots of the resulting strength and energy bias factors are given in Figure 11 – Figure 14. Figure 11 shows that strengths of angle-stiffened panels are generally less than the corresponding tee-stiffened panels. Although for a wide range of parameters, strength bias factors are very close to 1.0, they fall to as little as 0.85 for combinations of high β and high γ. Greater variation can be seen in the energy bias factors, where the bias varies between 0.85 and 1.2 (Figure 12). No clear trend can be discerned here except that the more extreme values occur at higher values of γ. The flatbar biases show variation in the strength bias factors between 0.85 and 1.2, with no discernable trend (Figure 13). Even greater variation in the energy ratios can be seen, with values ranging between 0.7 and 1.8, but again with no apparent trend (Figure 14). As might be expected, the load-shortening behaviour of tee-stiffened panels is more akin to angle-stiffened panels than flatbar-stiffened panels. These differences seem large enough to warrant separate sets of library curves according to stiffener shape.
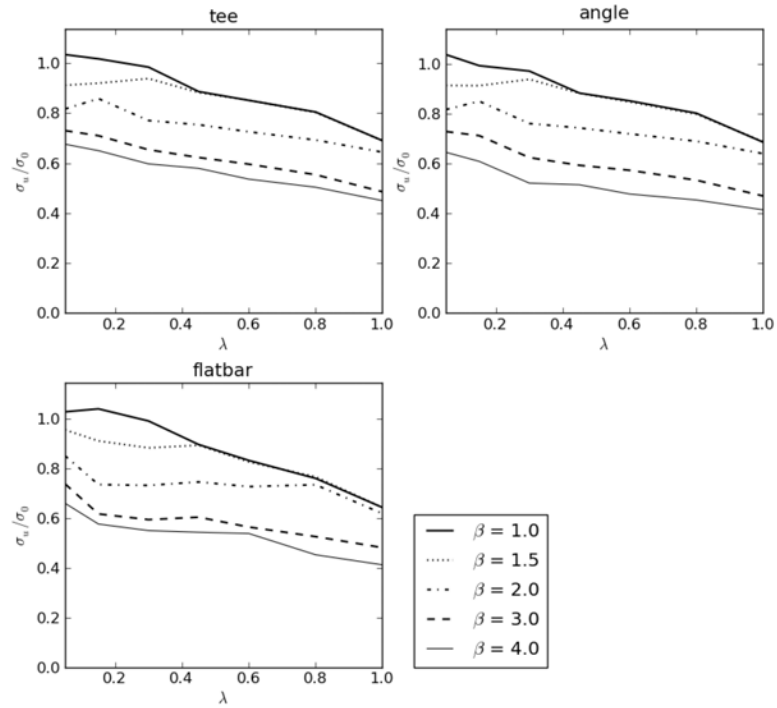
Figure 9: Strengths for $\gamma = 0.275$ compared for different stiffener shapes.
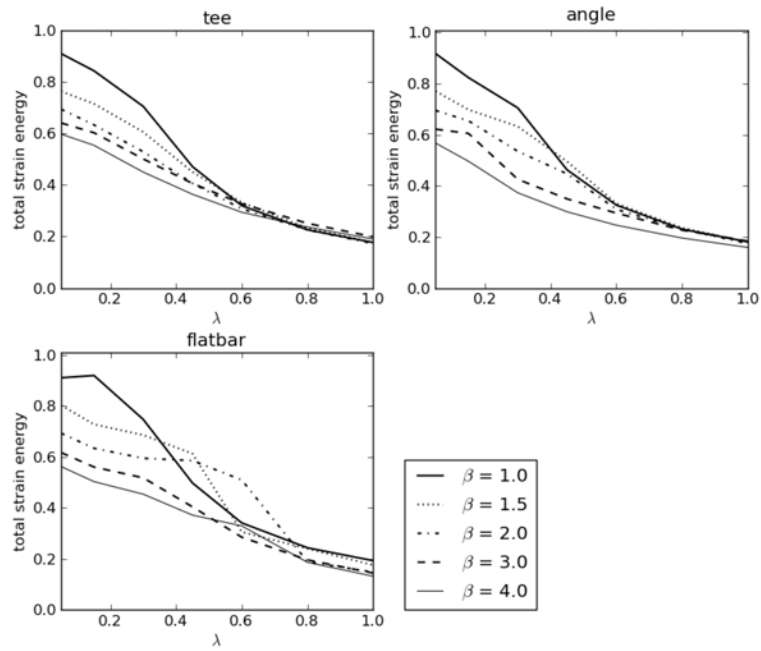
Figure 10: Strain energies for $\gamma = 0.275$ compared different stiffener shapes.
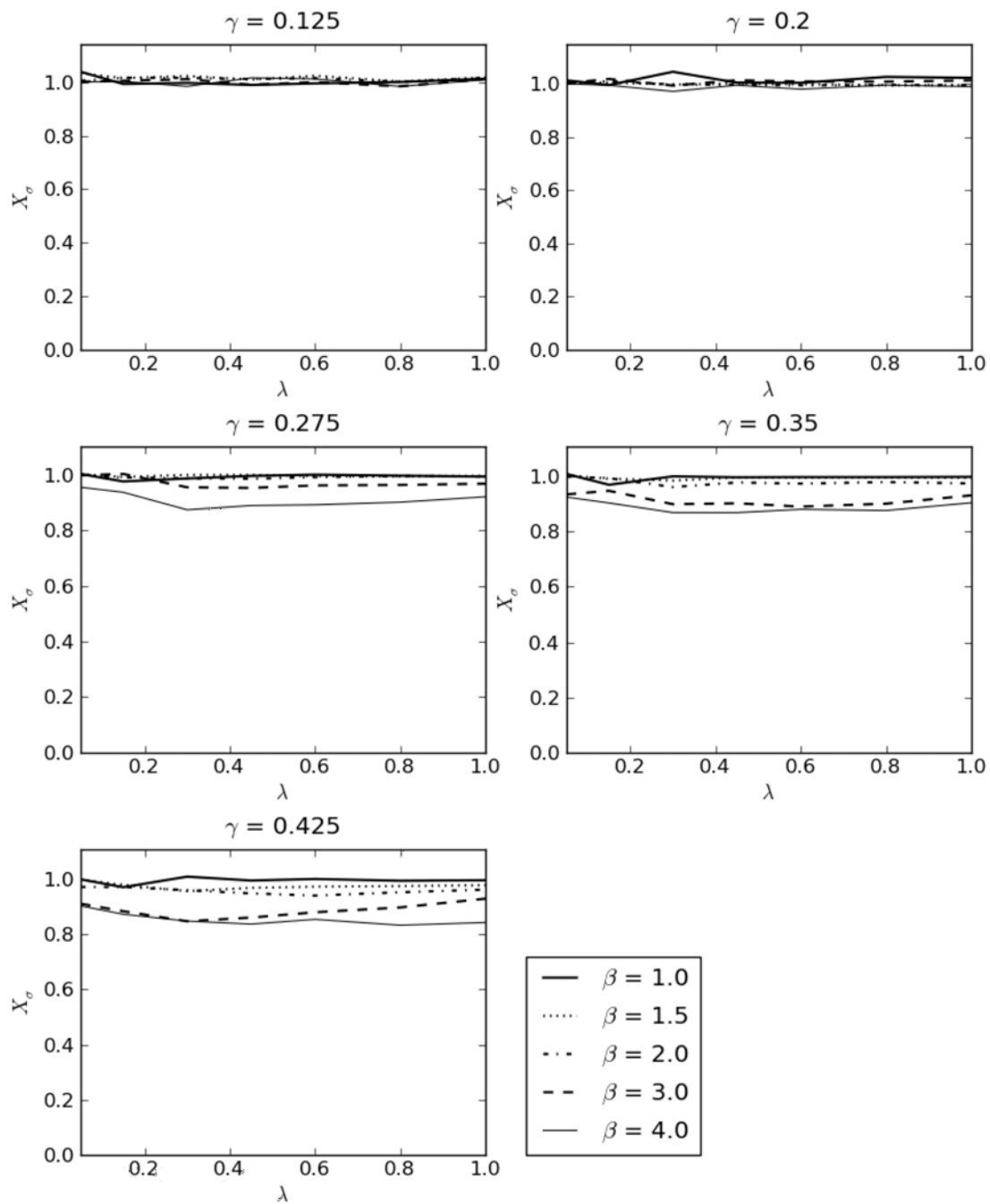
DRDC Atlantic TM 2010-140

Figure 11: Strength bias factors for angle-stiffened panels.
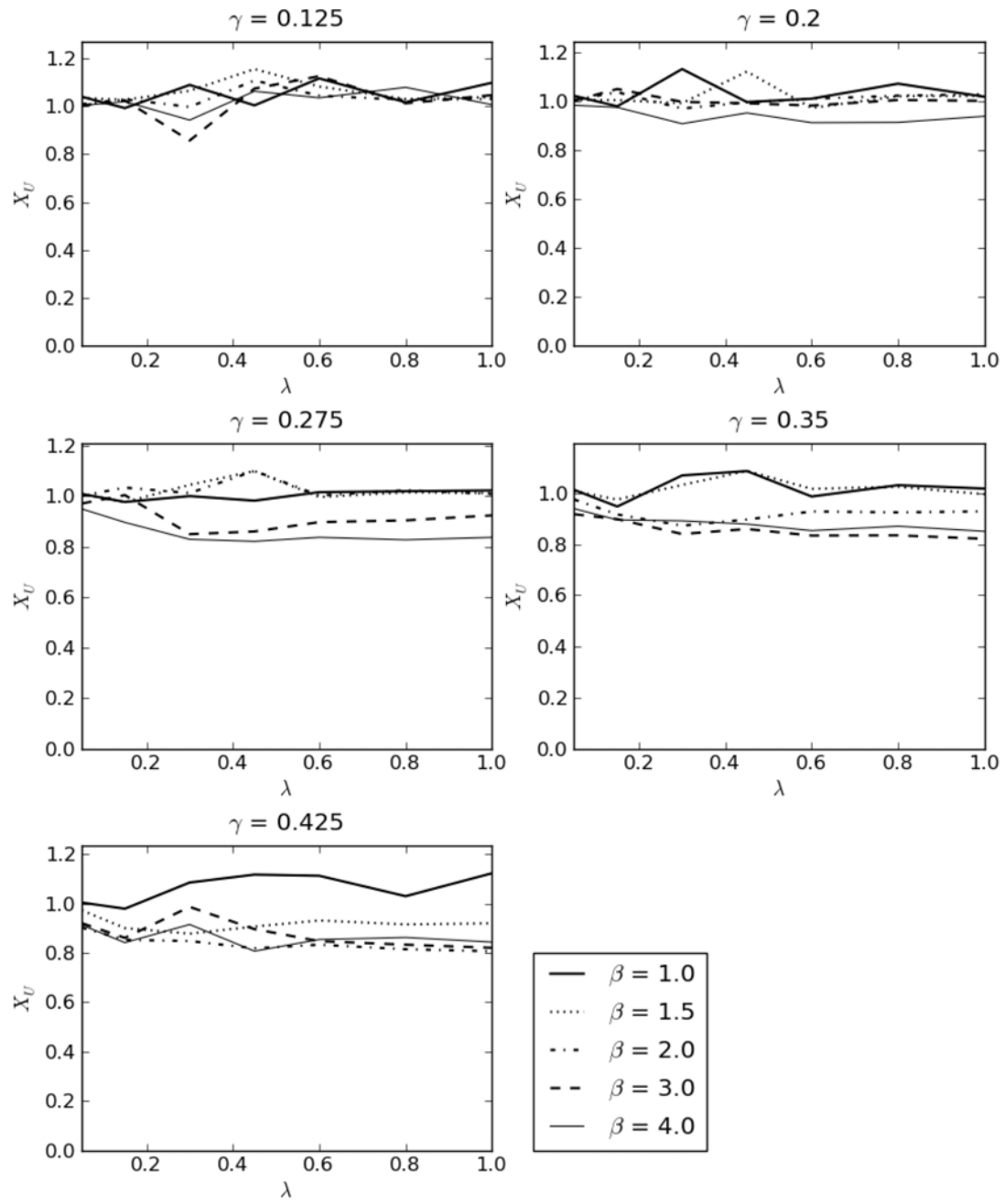
Figure 12: Energy bias factors for angle-stiffened panels.
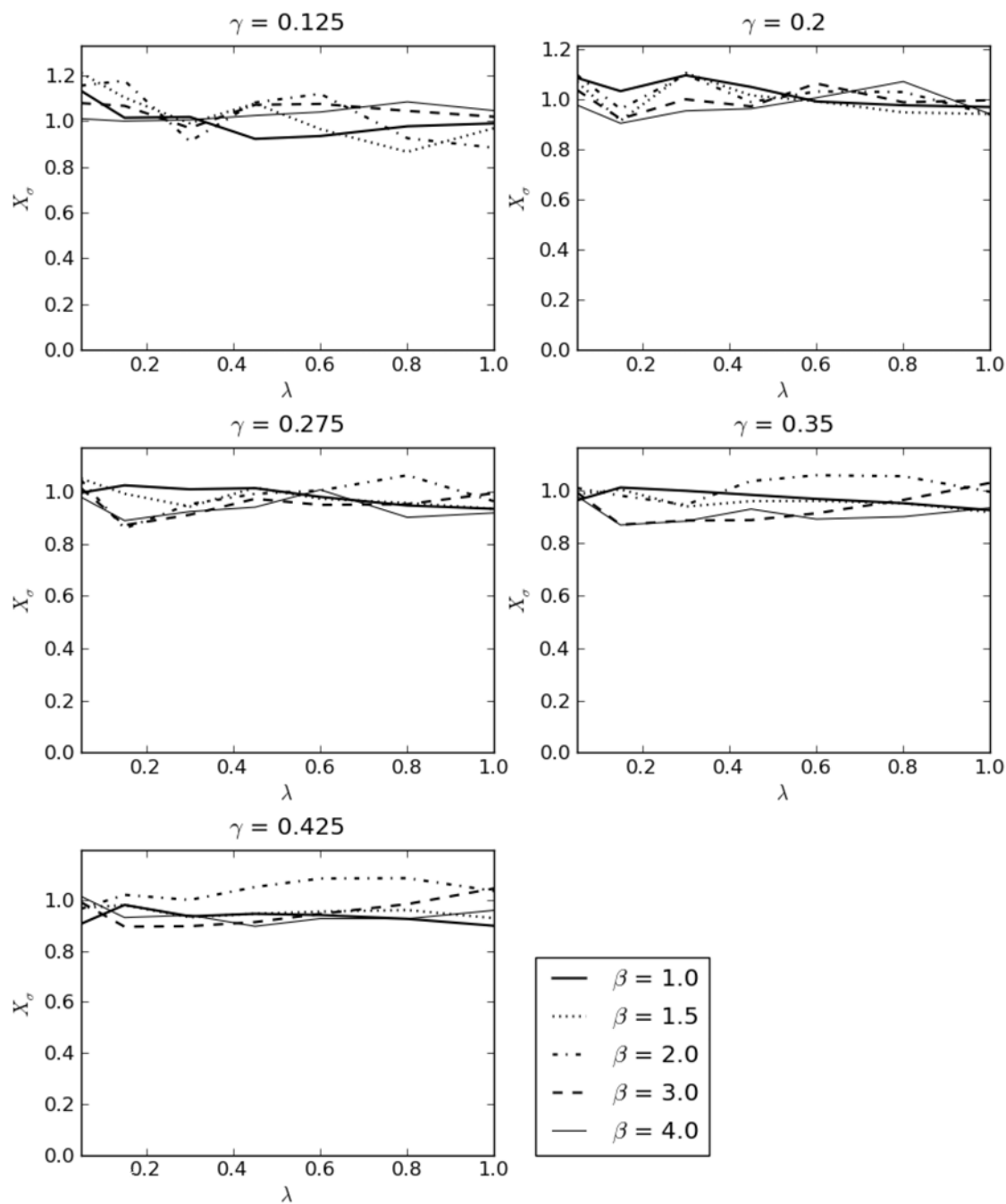
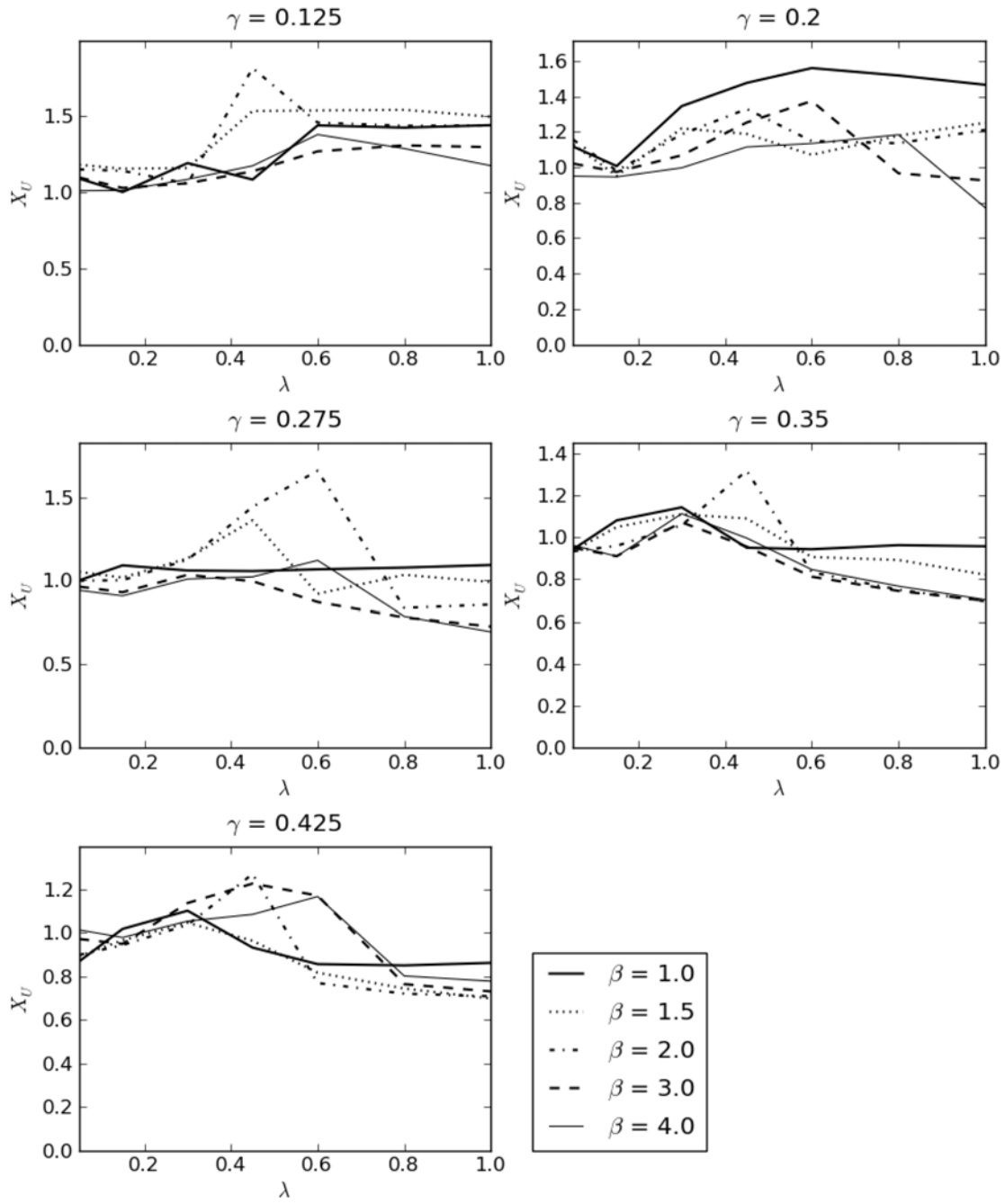*Figure 13: Strength bias factors for flatbar-stiffened panels.*

Figure 14: Energy bias factors for flatbar-stiffened panels.

4 Application to benchmark stiffened panels

In the present section the accuracy of interpolating load-shortening curves from the new curve library is evaluated using the results of twenty benchmark longitudinally stiffened panels. Load-shortening curves were calculated for each panel by three methods: direct calculation using nonlinear FEA, direct calculation using the IACS rules, and interpolation from the library curves. To generate these results, the new curve library presented in Section 3 was implemented in ULTMAT 2.3 and used in conjunction with ULTMAT's existing interpolation algorithm. ULTMAT 2.3's implementation of the IACS formulas for load-shortening curves is also used for the results presented in this section.

The properties of the benchmark panels are listed in Table 4. Panels A through H are based on naval ship designs and are all tee stiffened panels; panel J is from a 1/3 scale model of a naval vessel [16]; panels K through U are taken from various commercial designs (bulk carriers, tankers and container ships), and include a variety of tee, angle and flatbar stiffener geometries. A wide range of design parameters are represented in the benchmark panels.

Table 4: Properties of benchmark longitudinally stiffened panels

Name	a (mm)	b (mm)	t (mm)	Beam section $d \times w \times t_w \times t_f$ (mm)	σ_{yp} (MPa)	σ_{yb} (MPa)	β	λ	γ
A	1000	350	9.0	200×140×6.4×8.8 T	350	350	1.589	0.159	0.438
B	2000	350	9.0	200×140×6.4×8.8 T	350	350	1.587	0.318	0.438
C	2000	550	9.0	128×102×6.1×8.4 T	350	350	2.495	0.538	0.243
D	1000	450	9.0	128×102×6.1×8.4 T	350	350	2.041	0.264	0.281
E	2000	550	5.0	76×25×4.4×6.4 T	350	310	4.491	1.038	0.146
F	1000	550	5.0	76.2×25.4×4.4×6.4 T	350	310	4.491	0.519	0.146
G	2000	500	7.0	127×68×4.0×5.2 T	350	350	2.916	0.587	0.194
H	1000	450	9.0	127×68×4.0×5.2 T	350	350	2.041	0.317	0.172
J	457.2	202.7	2.0	38.1×14×1.78×3.3 T	245	245	3.487	0.373	0.211
K	5100	925	23.5	847×180×15×25 A	235.2	313.6	1.317	0.185	0.436
L	5100	925	23.5	549×125×11.5×22 A	235.2	235.2	1.317	0.289	0.288
M	5100	1000	25	830×200×15×33 T	313.6	313.6	1.546	0.198	0.426
N	5220	880	24.5	390×27 FB	392	392	1.411	0.612	0.349
O	860	880	25.5	395×25.5 FB	350	350	1.409	0.097	0.310
P	5100	1000	25	480×32 FB	313.6	313.6	1.546	0.429	0.381
Q	830	830	20	300×90×13×17 A	313.6	313.6	1.604	0.106	0.239
R	830	830	20.5	575×150×12×25 T	313.6	313.6	1.565	0.047	0.378
S	3270	880	14	300×90×13×17 A	313.6	313.6	2.429	0.365	0.306
T	5220	880	18	333×100×9×16 T	352.8	352.8	2.004	0.587	0.225
U	830	820	14	400×150×11×14 T	313.6	352.8	2.263	0.069	0.362

Figure 15 – Figure 18 give the load-shortening curves calculated by the three analysis methods. For the interpolated results, a nested four-level linear interpolation scheme, based on the values of β, λ, and γ, is applied to the library curves. Where parametric values fall outside of the ranges represented in the curve library (e.g., $\beta = 4.491$, and $\lambda = 1.038$, for Panel E), the library curves are instead extrapolated using the curves for the two closest values of each out-of-range parameter (e.g., $\beta = 3,4$, and $\lambda = 0.8,1.0$). Details of the nested interpolation/extrapolation scheme are given in Annex B.

An average level of imperfections was assumed for all of the direct FEA and interpolation calculations. While IACS formulas do not explicitly define the imperfection level, it is assumed that imperfections are implicitly included in the formulas consistent with typical levels found in ship panels.

A FE modelling approach identical to that used for the library curves was adopted for the direct nonlinear FEA calculations. Direct calculation of a single load-shortening curve with VAST typically required about fifteen minutes of analysis time on a standard desktop computer. In comparison, all of the interpolated and IACS curves were generated in less than a second of computer time. This illustrates the much greater efficiency that can be gained through the use of the two approximate methods.

Visual comparison of the curves in Figure 15–Figure 18 suggests that for the naval structural panels (A-J) the interpolated curves are a better approximation to the direct FEA curves than the IACS rules. However, for the commercial structural panels (K-U) results are more mixed. In some instances interpolated curves give better results; in others the IACS rules are better; and in a few cases (K, L) neither method gives a good approximation.

For a more quantitative measure of accuracy, the strength and energy ratios defined in Section 3.3 are reintroduced here in a slightly different form. The strength bias factor X_σ is here defined as the ratio of the approximate strength (from an interpolation or IACS prediction) to a reference strength value, which here is taken to be the direct FEA result:

$$X_\sigma = \frac{\left[\bar{\sigma}_u\right]_{approx}}{\left[\bar{\sigma}_u\right]_{ref}} \qquad (15)$$

An energy bias factor X_U can be defined in a similar manner.

Results for the strength and energy bias factors are given in Table 5 and Table 6, respectively. Also given are the means and standard deviations of the calculated bias values. The results show that in one instance (panel E), the interpolated curves overestimate the strength by 18%, while the IACS formulae overestimate the strength by 11%. The interpolated method is more than 10% in error for panels E and K, whereas the IACS formulas are more than 10% in error for four of the panels. Overall, the mean of the interpolated strength predictions is 1.01, indicating that on average it overestimates the direct FEA strength prediction by 1%. For the IACS results, the mean value indicates an average overestimate of the strength of 6.1%. The standard deviations for the two methods are similar: 0.066 and 0.052 for the interpolation and IACS methods, respectively.

The energy results are revealing in that they show that the interpolation method overall does a much better job of predicting the shapes of the curves than does the IACS method. This is largely due to the approximations used in the IACS formulas. For example, the IACS formulas assume that the peak strength occurs at a relative strain very close to 1.0, whereas both the direct FEA and interpolation methods often locate the peak values at relative strains that are greater or less than 1.0, depending on the column slenderness. Another significant assumption in the IACS method is that post-collapse response follows a load shedding path determined by a two bar mechanism joined by plastic hinges. This is a somewhat crude approximation to the real three-dimensional post-collapse response, and it appears to lead to some large errors in the post-collapse response (e.g., panels N and T).

Table 5: Predicted strength bias factors for twenty stiffened panels

Panel	Interpolation	IACS	EE	CC
A	0.998	1.025	0.925	0.985
B	0.992	1.030	0.882	0.928
C	0.992	1.093	0.903	0.921
D	1.023	1.096	0.963	0.979
E	1.184	1.112	0.907	0.820
F	0.948	1.043	0.754	0.782
G	0.987	1.130	0.867	0.868
H	1.041	1.147	1.048	0.983
J	0.987	1.068	0.846	0.877
K	1.166	1.158	1.151	1.190
L	0.997	1.030	0.914	0.908
M	1.061	1.012	0.965	1.022
N	0.941	1.036	0.915	0.921
O	0.942	0.948	0.917	0.963
P	0.937	1.007	0.859	0.875
Q	0.982	1.017	0.922	0.967
R	1.030	1.043	0.993	1.068
S	0.974	1.093	0.912	0.951
T	0.975	1.058	0.939	0.915
U	1.044	1.081	0.999	1.096
Mean	**1.010**	**1.061**	**0.929**	**0.951**
Std. Dev	**0.066**	**0.052**	**0.081**	**0.095**

Because both the direct FEA curves and the library curves underlying the interpolation method were calculated using identical finite element modelling methods and analysis programs, it is perhaps not surprising that the interpolation method gives on average a better correspondence with the direct FEA results. Indeed, besides the error that arises from the interpolation (or extrapolation) of the library curves, the only other possible sources of error include differences in the material properties and the panel sizing ratios of Eqns (7)-(10). As the latter can generally be

assumed to be quite small, the main source of error in most cases can be assumed to arise from interpolation/extrapolation. In instances where the panel sizing ratios differ widely from those assumed for the library curves, these may also be a contributing factor.

It is also of interest to evaluate the accuracy of the present interpolation method and curve library, with those used in previous versions of ULTMAT. Table 5 and Table 6 each report two other sets of results obtained with curve libraries developed by Wallace et al [17] and Jiang and Chernuka [18], and which were implemented in versions 2.2 and earlier of the ULTMAT code [19]. The same interpolation scheme was used to obtain the results in columns EE and CC (these refer to the end-to-end and center-to-centre stiffened panel models used to populate those curve libraries). Interpolation with the older libraries on average underestimates the strengths by 5-7% and the energies by 3-5%, and gives predictions with standard deviations that are somewhat larger than those obtained with the new curve library. Based on these results, it can be concluded that the new curve library represents a modest but significant improvement over the older libraries.

Table 6: Predicted energy bias factors for twenty stiffened panels

| Panel	Interpolated	IACS	EE	CC
A	1.028	0.962	0.810	0.878
B	1.049	1.147	0.904	0.952
C	0.867	1.121	0.914	0.844
D	0.908	0.966	0.794	0.806
E	1.024	1.535	1.169	0.970
F	0.929	1.080	0.897	0.858
G	0.994	1.414	1.177	1.004
H	1.003	1.024	0.926	0.849
J	0.944	0.953	0.830	0.823
K	1.224	1.043	1.118	1.186
L	0.953	0.947	0.951	0.903
M	1.170	0.891	0.966	1.031
N	1.023	1.654	1.491	1.283
O	0.935	0.748	0.876	0.898
P	1.012	1.123	0.974	0.953
Q	0.986	0.899	0.957	0.950
R	1.061	0.881	0.911	0.977
S	0.860	1.009	0.809	0.825
T	1.034	1.587	1.278	1.115
U	1.044	0.863	0.794	0.877
Mean	**1.002**	**1.093**	**0.977**	**0.949**
Std. Dev	**0.089**	**0.256**	**0.182**	**0.126**
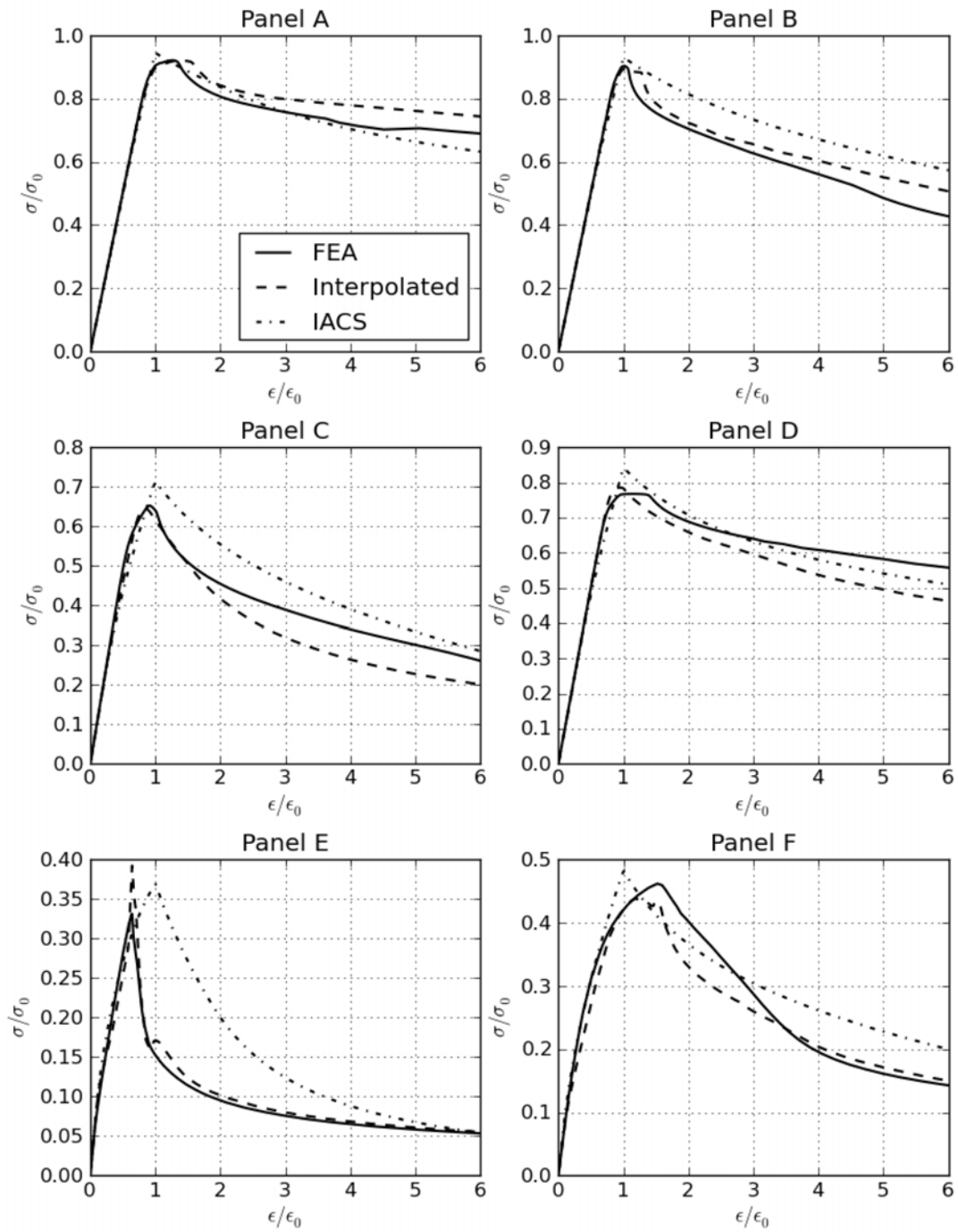
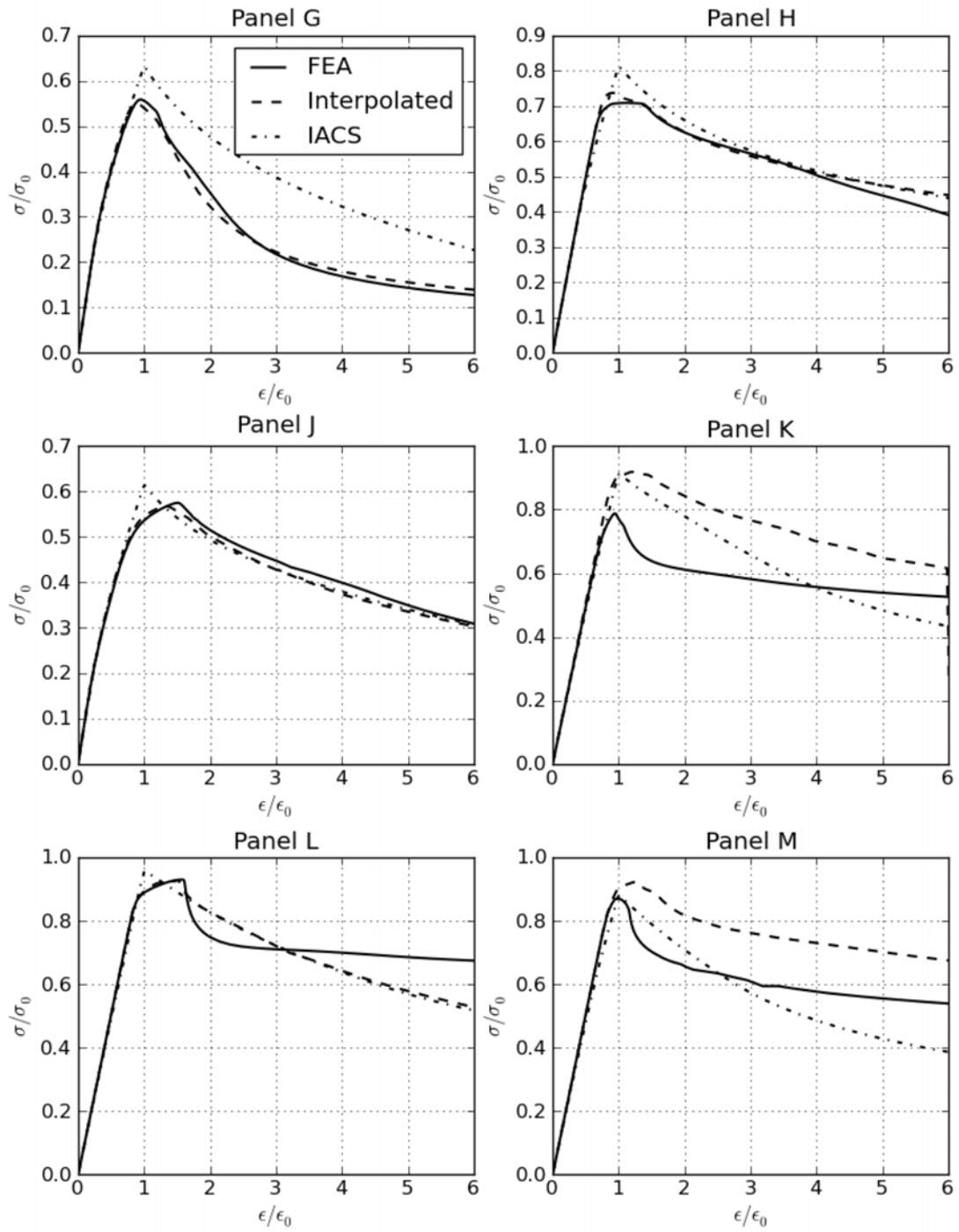*Figure 15: Load-shortening curves for panels A-F*

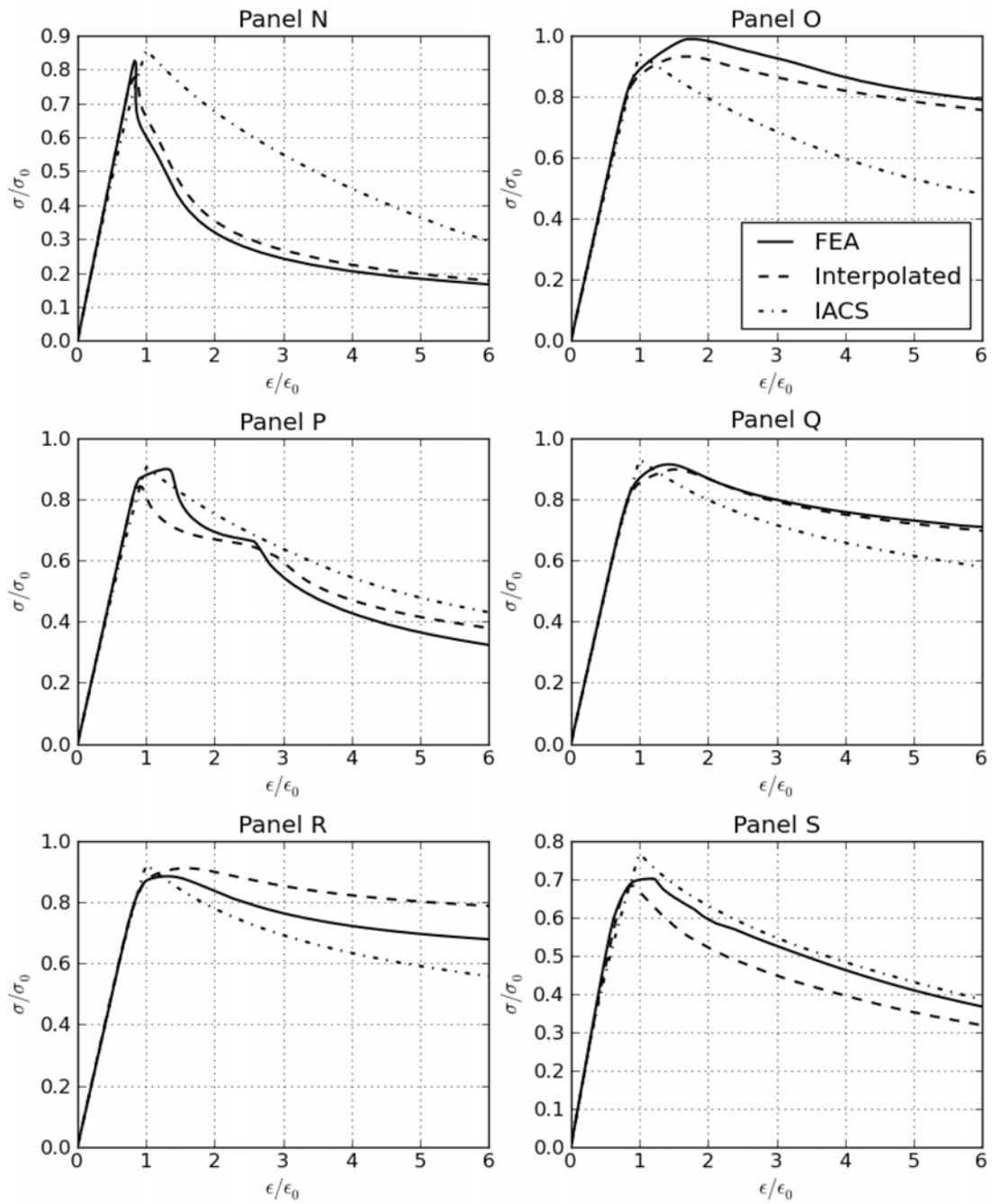*Figure 16: Load-shortening curves for panels G-M.*

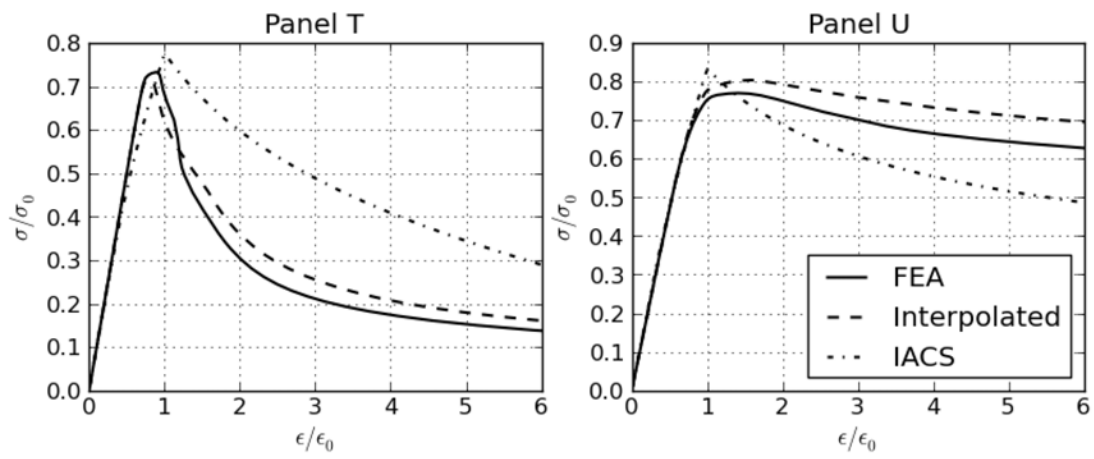*Figure 17: Load-shortening curves for panels N-S.*

Figure 18: Load-shortening curves for panels T-U.

5   Hull girder strength evaluation of intact ships

Interpolated load shortening curves using the new curve library are now applied to the prediction of the ultimate strength of ship hull girders. For this purpose, a total of eight benchmark hull girder models are considered. Five of these models are taken from an ISSC report [20], while another model was taken from Paik [21]. The two other benchmark cases are derived from naval structural designs. Detailed descriptions of model development and validation for most of these models were presented in an earlier report [10].

The present section provides updated hull girder ultimate strength analysis results calculated with ULTMAT 2.3, using both the new curve library and IACS formulas to determine load shortening properties. These results are compared to previously published results where appropriate.

5.1   Bulk Carrier 1

The cross sectional model of a bulk carrier is shown in Figure 19 for which hog and sag ultimate strength predictions are given in Figure 20. ULTMAT 2.3 results are shown for two cases: those based on IACS load shortening formulas, and those based on interpolated library curves. For comparison, results from the earlier study obtained with ULTMAT 2.2 using the IACS formulas are also given [10]. The other results shown are those contributed by other researchers to the ISSC study [20].

The new ULTMAT predictions for hog strength are in good agreement with the lower group of ISSC results, and are a considerable improvement over the ULTMAT 2.2 results. The differences between the two IACS-based results can be attributed to the fact that since the earlier study, errors were discovered and corrected in ULTMAT's implementation of the IACS formulas, and errors were also discovered in the bulk carrier model that caused the weather deck and top side tank to be undersized. The two sources of error caused both hog and sag strength to be underestimated in the earlier study.

The new IACS-based predictions for sag strength are also in good agreement with the ISSC results. However, the sag strength prediction using interpolated curves is significantly lower than the main body of ISSC results. Sag strength predictions depend to a large extent on the accuracy of the load shortening response of the weather deck. In this model, the weather deck stiffened panels are essentially identical to Panel N of Section 4. It was shown in Figure 17 that, in comparison to the direct FEA curve, the interpolated load-shortening curve agrees very well, whereas the IACS formulas considerably overestimate the entire post-buckling portion of the response. Table 5, on the other hand, indicated that the interpolated curve underestimated the peak strength of Panel N by 6%, while the IACS curve overestimated it by about 4%. The 10% spread in peak strength of Panel N results in a 10% difference in the sag strength of the bulk carrier.
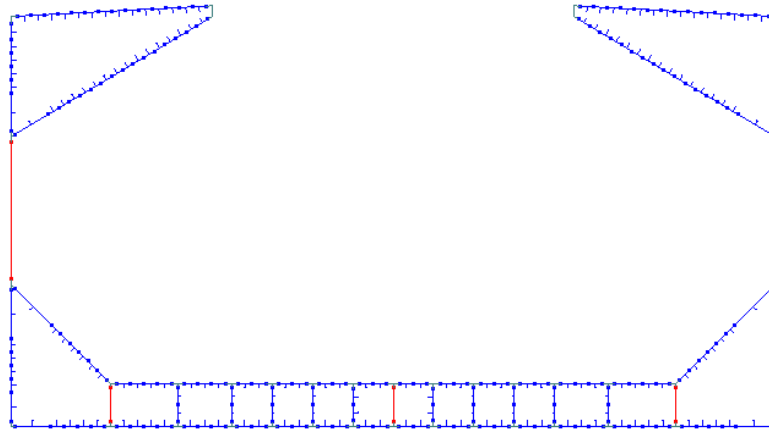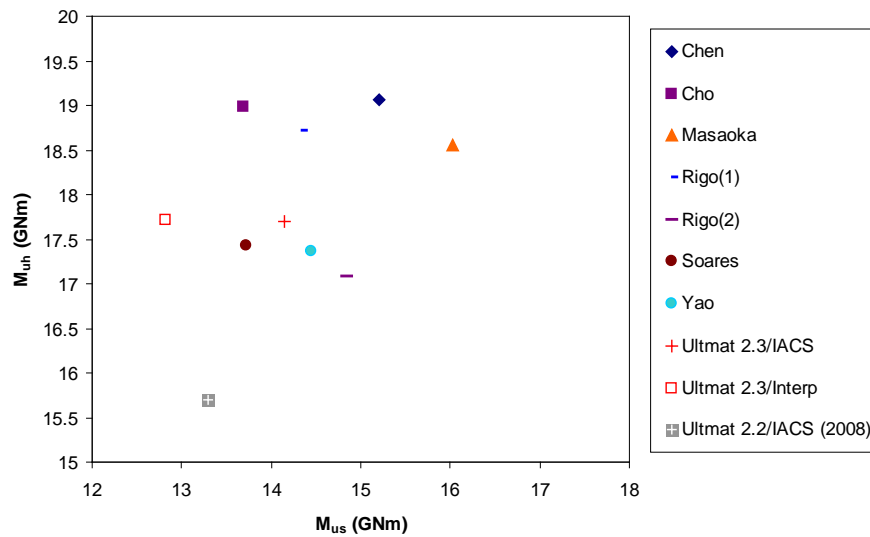
Figure 19: Cross section model for bulk carrier 1.

Figure 20: Ultimate strength in hog and sag for the bulk carrier 1 model.

5.2 Container ship

Figure 21 shows the cross section model of a container ship, and Figure 22 provides the ultimate strength predictions from ULTMAT and from the ISSC study. The ULTMAT results are in good agreement with the main body of ISSC results, with the ULTMAT predictions for hog and sag strength based on IACS, being slightly larger than those obtained from interpolated curves.
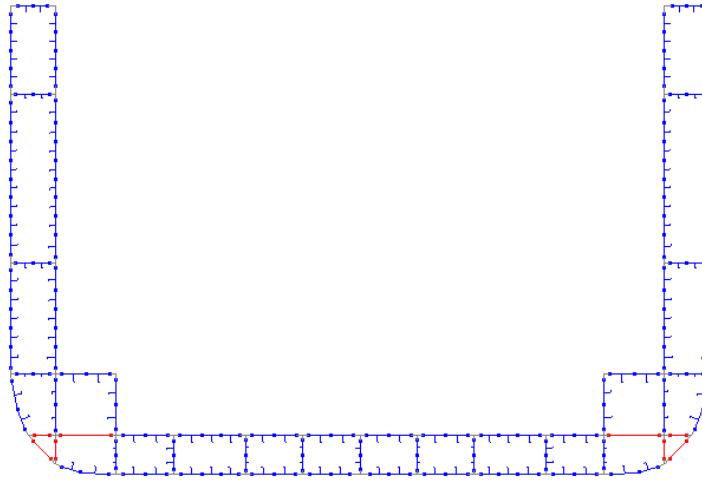
Figure 21: Container ship cross section model.
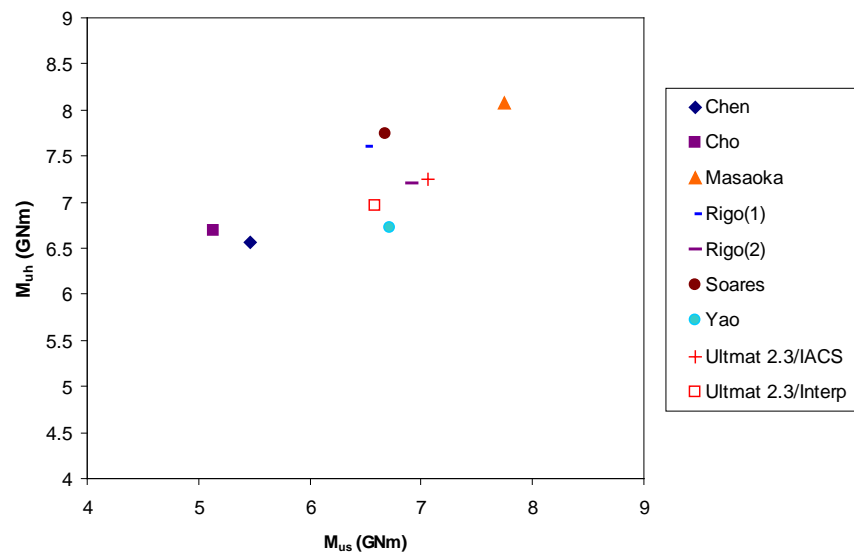
Figure 22: Ultimate strength in hog and sag for the container ship model.

5.3   Double Hull Tanker

The cross section model for a double hull tanker is shown in Figure 23. The results in Figure 24 indicate that ULTMAT 2.3 sag strength predictions are significantly higher than the main body of ISSC results, whereas hog strength predictions are more in line with the bulk of the ISSC results. The differences between the ULTMAT 2.3 predictions are approximately 3% in hog and 5.5% in

sag. Also shown is the ULTMAT 2.2 prediction using IACS, which gives a sag strength that is 20% lower than the results obtained with ULTMAT 2.3.

Figure 23: Double hull tanker cross section model.
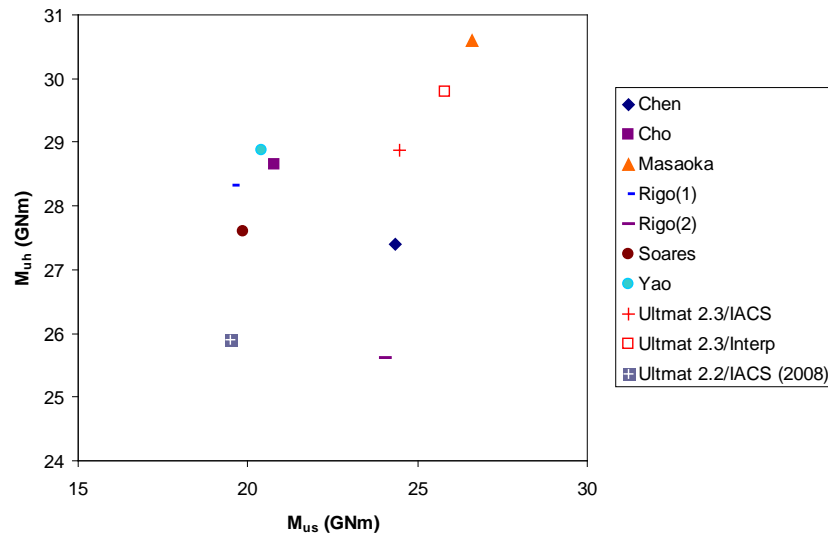
Figure 24: Ultimate strength in hog and sag for the double hull tanker model.

5.4   Single Hull Tanker

The single hull tanker is in this case VLCC *Energy Concentration*, which broke in half in Rotterdam in 1981. The cross section model of this vessel is shown in Figure 25. A forensic investigation by Rutherford and Caldwell [22] established the state of loading of the vessel at the time of failure. This is the dotted line shown in Figure 26, indicating that the ship failed in hog.

The plotted results have taken into account the estimated amount of corrosion in the vessel at the time of the accident by uniformly reducing the thickness of the plating and stiffener webs by 1 mm and the stiffener flanges by 2 mm from their nominal values.
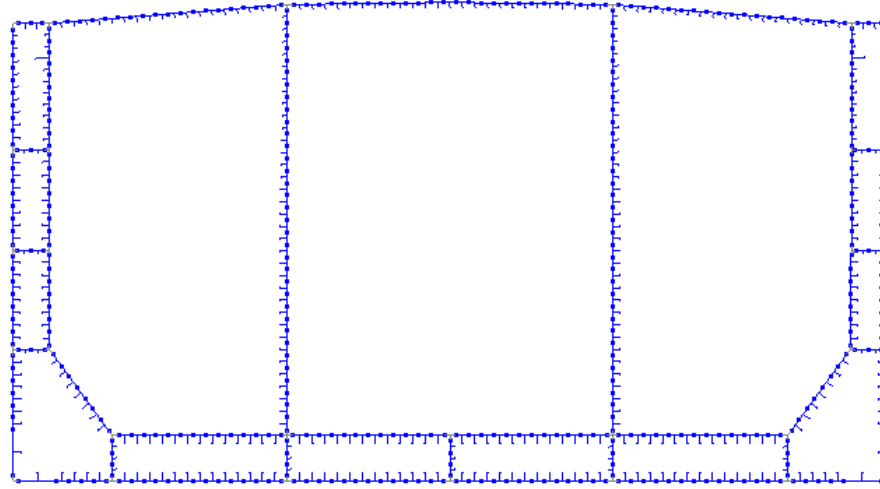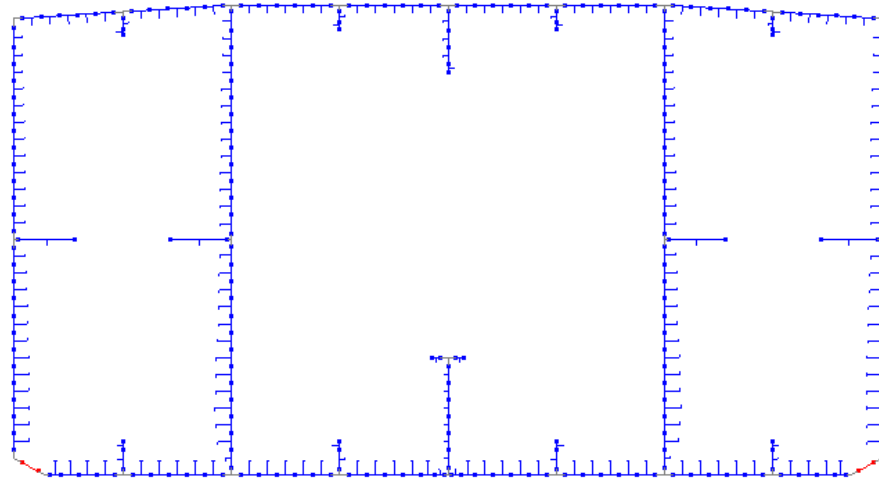

Figure 25: Single hull tanker cross section model.
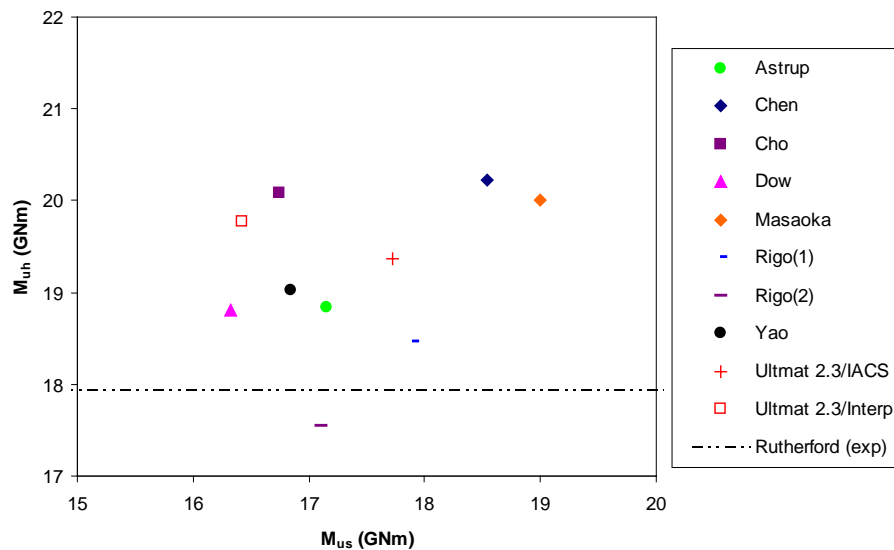
Figure 26: Ultimate strength in hog and sag for the single hull tanker model.

The ULTMAT hog results are in agreement with the body of ISSC results, and are about 10% larger than Rutherford and Caldwell's estimate of the failure load. The two ULTMAT predictions differ from each other by 2%. The hog strength is primarily governed by the strength of the bottom structure, which is mainly comprised of stiffened panels identical to Panel M. Figure 16 showed that, in comparison with the direct FEA curve, the IACS formulas agree better than the

interpolated curve. The lower hog strength prediction obtained with the IACS method can therefore be expected to be more accurate in this case. It should also be noted that the ULTMAT predictions do not take into account the lateral pressure in the bottom structure.

The ULTMAT sag strength results fall in the same range as the ISSC results, but differ from each other by 8%. The sag strength is primarily governed by the weather deck structure, which is mainly comprised of panels identical to Panel P. Table 5 shows that the peak strength of this panel was better predicted by the IACS formulas, whereas Figure 17 showed that the shape of the direct FEA curve was better predicted by interpolation. The difference in the peak strengths predicted by the two methods is 7%, which is close to the 8% difference seen in the sag strengths.

5.5   1/3 scale frigate

The cross section model for the 1/3 scale frigate model is shown in Figure 27. The results in Figure 28 indicate ULTMAT's predictions are in very good agreement with the ISSC results and with Dow's experimental result. The sag strength predicted using the IACS method is in fact identical to the measured sag strength. The ULTMAT predictions by the two methods agree with each other quite well, differing by less than 3%.
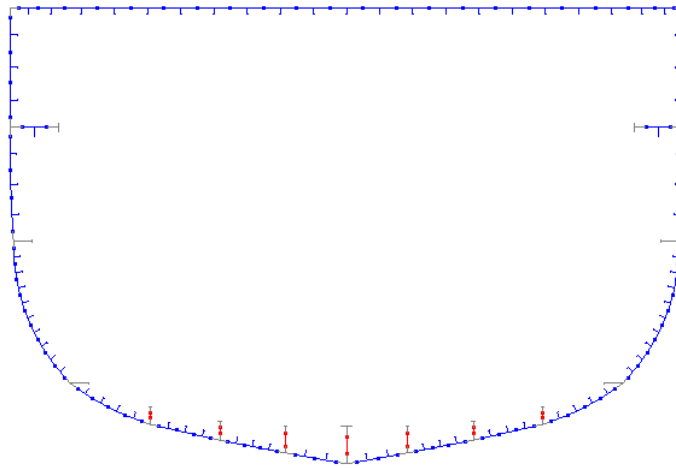

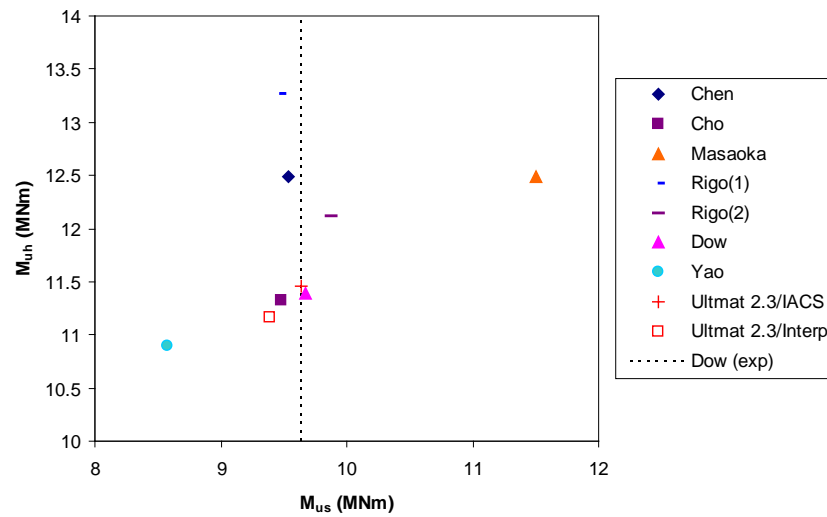*Figure 27: 1/3 scale frigate cross section model.*

Figure 28: Ultimate strength in hog and sag for the 1/3 scale frigate.

5.6 Bulk Carrier 2

A second bulk carrier model is shown in Figure 29. ULTMAT results given in Figure 30 are compared with Paik's result [21] based on the ISUM code ALPS [12]. ULTMAT 2.3's hog strength predictions are higher than Paik's result by about 8%. ULTMAT 2.3's sag strength predictions are on the other hand 6% to 11% lower than Paik's result for the interpolation and IACS methods, respectively. Note the results obtained with the IACS method, are quite different from those from the 2008 study, again owing to the aforementioned implementation errors in ULTMAT 2.2.

Considering again the sag strength, the main deck of this ship is comprised of stiffened panels identical to Panel O of Section 4. Figure 17 indicated that the interpolation method gave a better representation than the IACS method of the direct FEA curve. From Table 5, the peak of the interpolated curve is 6% lower than that of the direct FEA curve, which corresponds closely to the difference between the sag strength results obtained by the interpolation method and by Paik.
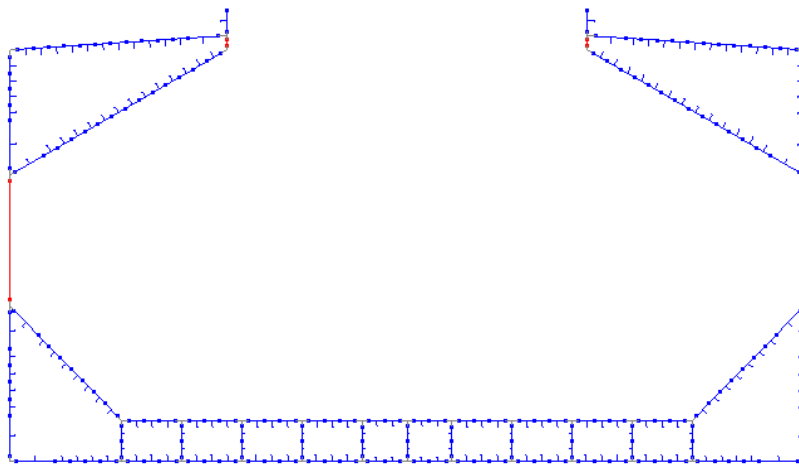
Figure 29: Bulk carrier 2 cross section model.
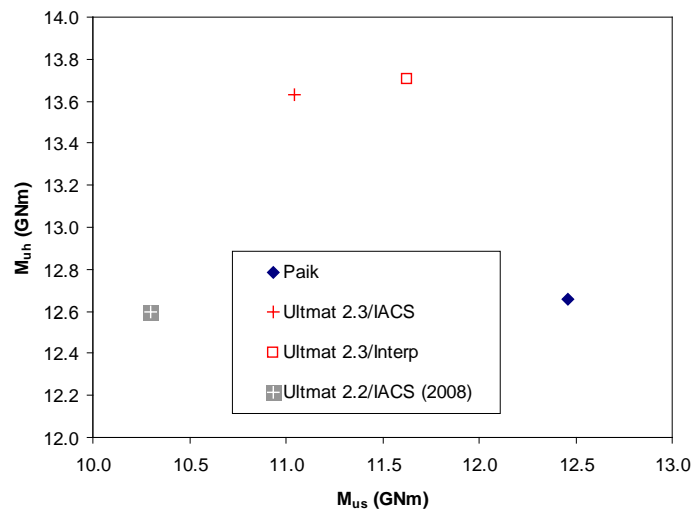
Figure 30: Ultimate strength in hog and sag for the bulk carrier 2 model.

5.7   Naval frigate

A cross sectional model of a naval frigate is shown in Figure 31. In Figure 32, new results obtained with ULTMAT 2.3 are compared with a number of previously published results for the same ship. The strength results are normalized to the vertical plastic bending moment of the ship, which is the maximum bending moment that can be resisted with fully developed plasticity in the structure and neglecting buckling. The ULTMAT 2.3 results based on the interpolation method

are in good agreement with ULTMAT 2.1, ULTMAT 2.2 and NS94B results obtained from previous studies, although the hog strength is slightly higher than previous results. The IACS method in ULTMAT 2.3, however, gives a sag strength that is significantly higher than previous results, and more than 15% higher than the result with the interpolation method.

Figure 31: Cross section model of a naval frigate

Figure 32: Normalized hog and sag strength results for the naval frigate model.

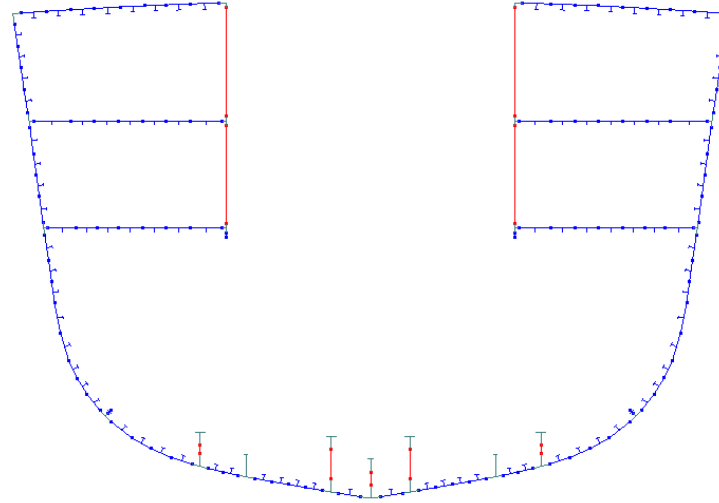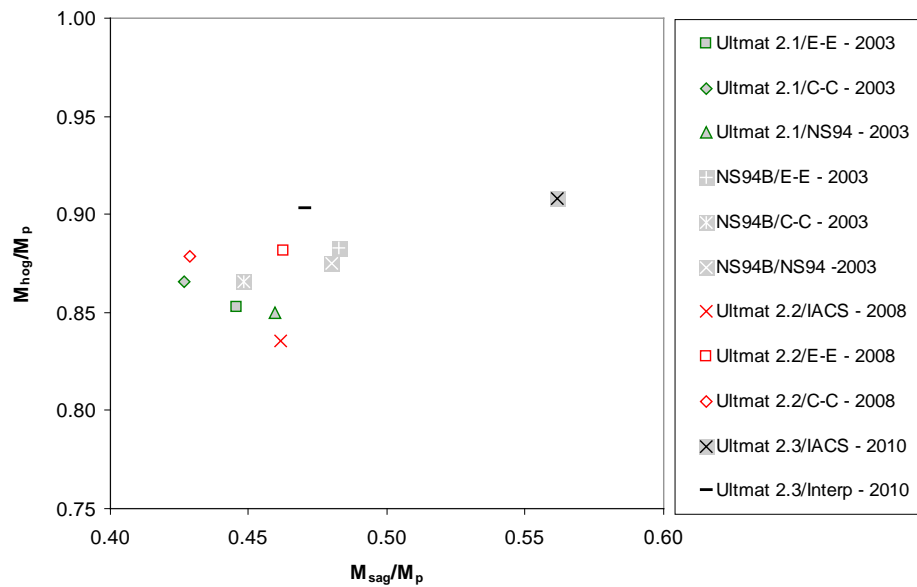To understand this wide discrepancy in the sag strength, the structure of the main deck of the frigate can be considered more closely. The stiffened panels of the main deck have properties

very similar to those of Panel C. The peak of the direct FEA for that panel was predicted quite accurately by the interpolation method, but was overestimated by the IACS formulas by 10%. The IACS method also overestimated the post-collapse part of the curve. Together, this could account for much of the large discrepancy in the sag strengths.

5.8   Naval destroyer

A cross sectional model of a naval destroyer is shown in Figure 33 in which the lower deck and the longitudinal bulkheads have been made ineffective because of their lack of structural continuity. In Figure 34, new results obtained with ULTMAT 2.3 are compared with previous results for the same ship, and these are again normalized to the vertical plastic bending moment of the ship. The ULTMAT 2.3 results are in good agreement with all of the previously obtained results, with the exception the ULTMAT 2.2 results based on the IACS method. The ULTMAT 2.3 predictions agree with each other within 2%.
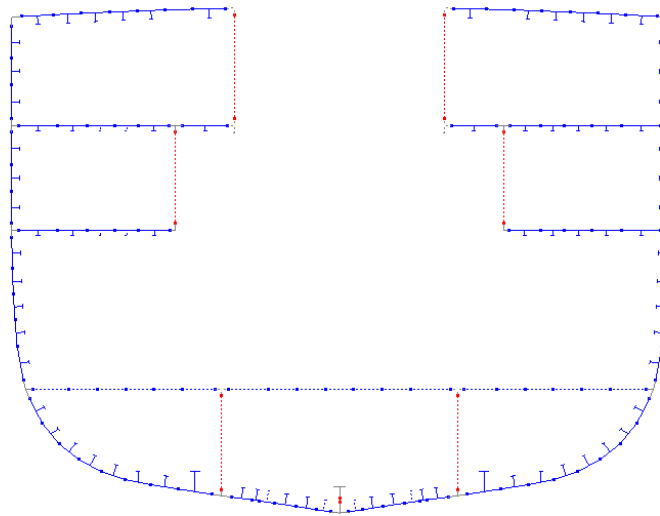
Figure 33: Cross section model of a naval destroyer.

5.9   Analysis of results

In Table 7, ratios of the interpolated strength to IACS strength, as predicted with ULTMAT 2.3, are recorded for each of the hull girder models. The interpolation method generally predicts smaller sag strengths than the IACS method (on average by 4.2%) while the hog strengths predicted by the two methods are on average the same. The standard deviations show that, compared with the hog strength results, the variability among the sag strengths is about three times greater. This is indicative of the greater uncertainty associated with the collapse behaviour of weather deck structure, which is typically more slender, as compared with the hull bottom structure.
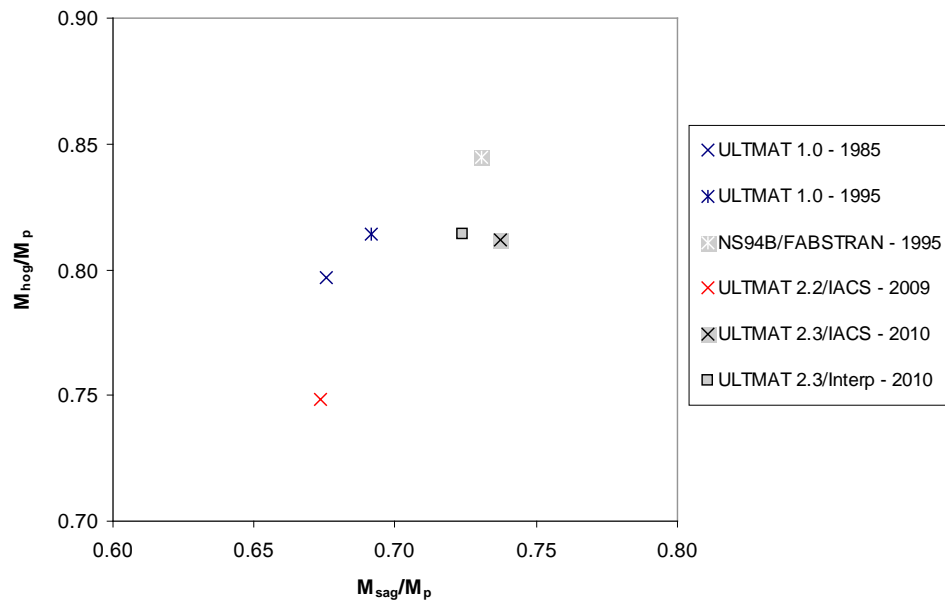
Figure 34: Normalized hog and sag strength results for the naval destroyer model.

Table 7: Ratios of ULTMAT strength predictions (interpolation strength over IACS strength)

Ship	Sag	Hog
Bulk carrier 1	0.906	1.001
Containership	0.932	0.959
Double hull	1.055	1.031
Single hull	0.927	1.020
1/3 scale frigate	0.974	0.975
Bulk carrier 2	1.052	1.006
Naval frigate	0.838	0.994
Naval destroyer	0.982	1.003
Mean	**0.958**	**0.999**
Std Dev	**0.074**	**0.023**

If a normal distribution about the mean is assumed, the standard deviation for sag ratios indicates that this ratio will differ from the mean by more than 7.4% about 31% of the time, and by more than 10% about 17% of the time. In fact, in both hog and sag, three out of eight of the predictions differ from the mean by more than one standard deviation, which is slightly greater than what is predicted by a normal distribution.

These statistics are of course only a measure of the spread between the two methods, and not of their absolute accuracy. For this, an independent reference value is needed for comparison. Among the eight benchmark models, two independent reference values are in fact available (measured sag strength for the 1/3 scale frigate and the estimated hogging failure load of the single hull tanker). To evaluate the accuracy of Smith's method for all cases, reference values for the other cases are taken to be the mean value of all the predictions available for a particular model, regardless of the method used.

Table 8 summarizes all of the Smith's methods results available for the eight benchmark models. From the ISSC study, these are the results of Cho, Dow, Rigo(1), Soares and Yao. ULTMAT 2.1, 2.3 and NS94B results are included for the naval frigate and destroyer models. ULTMAT 2.2 results using the IACS method have not been included because of the previously noted inaccuracies. The strength values have all been normalized with respect to the reference values, which are also recorded in the table.

The factor of safety recommended by IACS for ultimate strength with Smith's method is 1.1. Normalized strength values over 1.1 therefore indicate strength predictions that could potentially lead to an unsafe design. These are indicated by the five red squares in Table 8. Of theses, three are ULTMAT 2.3 predictions. In particular, the interpolation method gives an unsafe result for the double hull tanker model (1.13) and a marginally safe value for the single hull tanker (1.102); while the IACS method gives an unsafe prediction for the naval frigate (1.19). There therefore appears to be some tendency with ULTMAT 2.3 to overestimate the strength in comparison to other methods. This could be mitigated by always choosing the lower of the two ULTMAT predictions. Note, however, that for bulk carrier 1, the interpolation method gives an excessively conservative result in comparison to the reference value.

Table 8: Normalized strength results for all Smith's method predictions.

Bulk Carrier 1	Sag	Hog	Containership	Sag	Hog
Cho	0.953	1.051	Ultmat 2.3/IACS	1.081	1.007
Rigo(1)	0.999	1.036	Ultmat 2.3/Interp	1.007	0.966
Soares	0.955	0.965	Cho	0.785	0.929
Yao	1.006	0.961	Rigo(1)	0.996	1.056
Ultmat 2.3/IACS	0.985	0.980	Soares	1.022	1.076
Ultmat 2.3/Interp	0.893	0.981	Yao	1.028	0.933
Reference (GNm)	**14.36**	**18.07**	**Reference (GNm)**	**6.53**	**7.20**
Std Dev	**0.043**	**0.038**	**Std Dev**	**0.104**	**0.063**
Double hull			**Single hull**		
Ultmat 2.3/IACS	1.069	1.016	Ultmat 2.3/IACS	1.020	1.080
Ultmat 2.3/Interp	`1.128`	1.048	Ultmat 2.3/Interp	0.945	`1.102`
Cho	0.909	1.009	Cho	0.964	`1.120`
Rigo(1)	0.855	0.997	Dow	0.939	1.048
Soares	0.868	0.972	Rigo(1)	1.030	1.029
Yao	0.893	1.016	Yao	0.969	1.061
Reference (GNm)	**22.88**	**28.41**	**Reference (GNm)**	**17.37**	**17.94**
Std Dev	**0.121**	**0.025**	**Std Dev**	**0.039**	**0.034**
1/3 scale frigate			**Bulk carrier 2**		
Ultmat 2.3/IACS	1.000	0.967	Ultmat 2.3/IACS	0.943	1.022
Ultmat 2.3/Interp	0.973	0.943	Ultmat 2.3/Interp	0.993	1.028
Cho	0.983	0.956			
Dow	1.003	0.962			
Rigo(1)	0.982	`1.120`			
Yao	0.890	0.920			
Reference (MNm)	**9.64**	**11.84**	**Reference (GNm)**	**11.71**	**13.33**
Std Dev	**0.042**	**0.073**	**Std Dev**	**0.036**	**0.004**
Naval frigate			**Naval destroyer**		
Ultmat 2.3/IACS	`1.190`	1.038	Ultmat 2.3/IACS	1.045	1.005
Ultmat 2.3/Interp	0.997	1.031	Ultmat 2.3/Interp	1.026	1.008
Ultmat 2.1/E-E	0.945	0.974	NS94B/FABSTRAN	1.036	1.045
Ultmat 2.1/C-C	0.905	0.989	Ultmat 2.2/CC	0.894	0.941
Ultmat 2.1/NS94	0.974	0.971			
NS94B/E-E	1.022	1.009			
NS94B/C-C	0.950	0.989			
NS94B/NS94	1.018	0.999			
Reference	**0.472**	**0.875**	**Reference**	**0.706**	**0.808**
Std Dev	**0.086**	**0.025**	**Std Dev**	**0.071**	**0.043**

6   Summary and conclusions

The present study was undertaken as a follow-on investigation to an earlier study that found that significant discrepancies were arising among ultimate strength predictions of benchmark hull girders. Based on the recommendations of that study, a new library of load-shortening curves was developed that was designed to be suitable for both naval and commercial structures. The curve library was implemented in a new version of DRDC's ultimate strength code ULTMAT (version 2.3). In the course of this work it was also discovered that the ULTMAT 2.2 implementation of the IACS formulas for load-shortening curve had some significant errors, which were subsequently corrected for version 2.3.

The curve library developed for this study contained 525 curves, and was determined using a fully automated FE modelling and analysis procedure. Separate sets of curves are provided for tee, angle and flatbar stiffened panels, and all curves are for an "average" level of geometric and residual stress imperfections. Whereas plate and column slenderness properties both had a major effect on the load-shortening behaviour, it was found that the area ratio had only a modest effect.

To verify the new curve library and the corrected implementation of the IACS formulas, the load-shortening responses of twenty benchmark stiffened panels were calculated by direct nonlinear FEA, by interpolation of the library curves, and by calculation with the IACS formulas. Results showed that interpolated curves were generally closer to the direct FEA curves, in terms of peak value and the curve shape. Moreover, the IACS load-shortening curves are not always conservative and can in some instances significantly overestimate the post-collapse response. Based on the twenty benchmark panels, the IACS formulas predict a mean peak strength that is 6% higher than that predicted by direct FEA calculations.

The interpolation and IACS methods (implemented in ULTMAT 2.3) were then applied to ultimate strength predictions for eight benchmark hull girder models. Overall, it was found that the interpolation method predicted lower sag strengths than the IACS method (by about 4%), while hog strengths were about the same. In most cases, the strength predictions were within the range of previously published results for the same models.

A fairly high level of scatter is nonetheless observed, both in the ULTMAT predictions and among all Smith's method results taken from the ISSC study. The standard deviation among just the ULTMAT results was found to be 7.4% in sag and 2.3% in hog. Among a wider class of Smith's method predictions derived from the ISSC study plus predictions with ULTMAT and similar methods (88 predictions in total), five were found to have normalized strengths in excess of 1.1, the recommended safety factor for Smith's method.

In future ultimate strength assessments, it is recommended that both the interpolation method and the IACS method implemented in ULTMAT 2.3 be used. Whichever is the lower of the two results could safely be used as the working value for ultimate strength. If there are large differences between the two results, some further investigation using direct FEA evaluation of load-shortening curves is recommended.

References

[1]   Smith, C. S. (1977), Influence of Local Compression Failure on Ultimate Longitudinal Strength of a Ships Hull, In *Proceedings of the International Symposium on Practical Design in Shipbuilding*, 73–79, Tokyo.

[2]   Smith, C. S., Anderson, N., Chapman, J.C., Davidson, P.C., and Dowling, P.J., (1992), Strength of Stiffened Plating under Combined Compression and Lateral Pressure. *Transactions of RINA*, 134, 131-147.

[3]   International Association of Classification Societies (2006), Common Structural Rules for Double Hull Oil Tankers. http://www.iacs.org.uk/.

[4]   International Association of Classification Societies (2006), Common Structural Rules for Bulk Carriers. http://www.iacs.org.uk/.

[5]   Caldwell, J. B. (1965), Ultimate Longitudinal Strength, *Transactions of RINA*. 107, 411–230.

[6]   Paik, J. K., and Mansour, A. E. (1995), A Simple Formulation for Predicting the Ultimate Strength of Ships, *Journal of Marine Science and Technology*, 1, 52–62.

[7]   Paik, J. K., Hughes, O. F., and Mansour, A. E. (2001). Advanced Closed-Form Ultimate Strength Formulation for Ships. *Journal of Ship Research*, 45 (2), 111-132.

[8]   Ueda, Y. and Rashed, S. M. H. (1984), The Idealized Structural Unit Method and Its Application to Deep Girder Structures, *Computers & Structures*, 18 (2) 277–293.

[9]   Chen, Y-K., Kutt, L. M., Piaszczyk, C. M., and Bieniek, M. P. (1983), Ultimate Strength of Ship Structures, *SNAME Transactions*, 91, 149-168.

[10]   Smith, M. J. (2008), Ultimate strength assessment of naval and commercial ships, (DRDC Atlantic TM 2008-059), Defence R&D Canada – Atlantic.

[11]   Stredulinsky, D., Oakey, S. (2010), STRUC II User's Manual, (DRDC Atlantic ECR 2010-048), Defence R&D Canada – Atlantic. In Draft. Limited Distribution.

[12]   Paik, J. K. and Thayamballi, A. K. (2003), *Ultimate Limit State Design of Steel-Plated Structures*, Chichester, England: John Wiley & Sons.

[13]   Chalmers, D. W. (1993). *Design of Ships' Structures*. London: Her Majesty's Stationery Office.

[14]   Smith, C. S., Davidson, P. C., Chapman, J. C., Dowling, P. J. (1988), Strength and Stiffness of Ships' Plating Under In-Plane Compression and Tension, *Transactions of RINA*, 130, 277-296.

[15]   Martec Limited (2006), VAST— Vibration and Strength Analysis Program (VAST), Version 8.8 User's Manual.

[16]   Dow, R. S. (1991), Testing and Analysis of a 1/3-Scale Welded Steel Frigate Model, In C. S. Smith and R. S. Dow (Eds.), *Advances in Marine Structures—2*, pp. 749–773, London: Elsevier.

[17]   Wallace, J. C., Jiang, L., and Chernuka, M. (1997), Generation of a Normalized Effective Stress-Strain Curve Database of Stiffened Panels for the Halifax Class Frigate, (Technical Report TR 97-39), Martec Limited. Halifax, Canada.

[18]   Jiang, L., and Chernuka, M. (1998), Continued Development of a Normalized Effective Stress-Strain Curve Database of Stiffened Panels for the Halifax Class Frigate, (Technical Report TR 98-08), Martec Limited. Halifax, Canada.

[19]   Smith, M. J. (2006), ULTMAT 2.1 User's Manual, (DRDC Atlantic TM 2006-049), Defence R&D Canada – Atlantic.

[20]   Ohtsubo H. and Sumi. Y., eds. (2000), Ultimate Hull Girder Strength, In *Proceedings of the 14th International Ship and Offshore Structures Congress*, Vol. 2, 321-391, Kidlington England: Elsevier Science Ltd.

[21]   Paik, J. K. (1993), Hull Collapse of an Aging Bulk Carrier Under Combined Longitudinal Bending and Shearing Force, *Transactions of RINA*, 135, 217-228.

[22]   Rutherford, S. E., and Caldwell, J. B. (1990), Ultimate Longitudinal Strength of Ships: a Case Study, SNAME Transactions, 90, 441-471.

Annex A   Load-shortening curve library

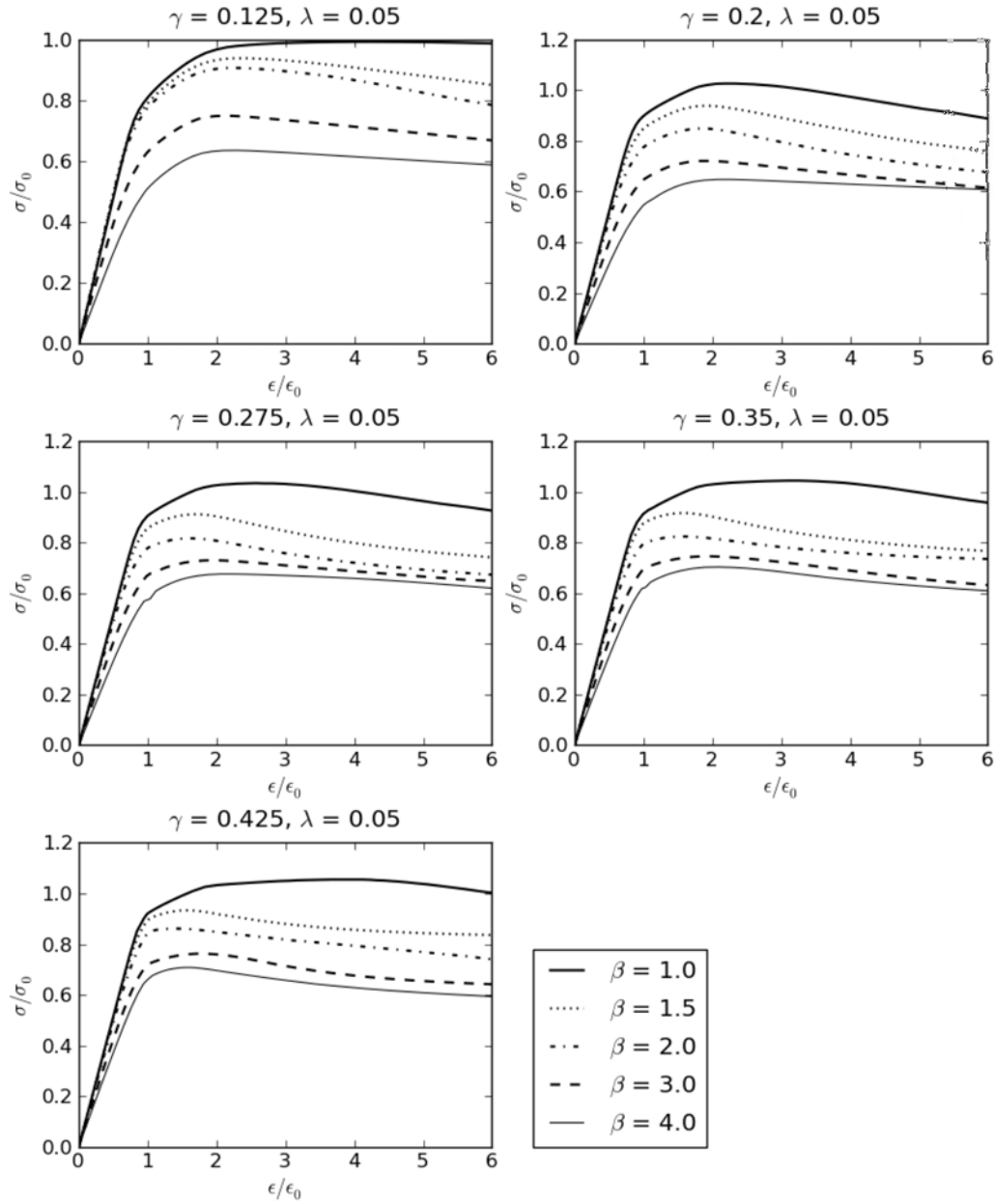## A.1   Load-shortening curves for tee-stiffened panels

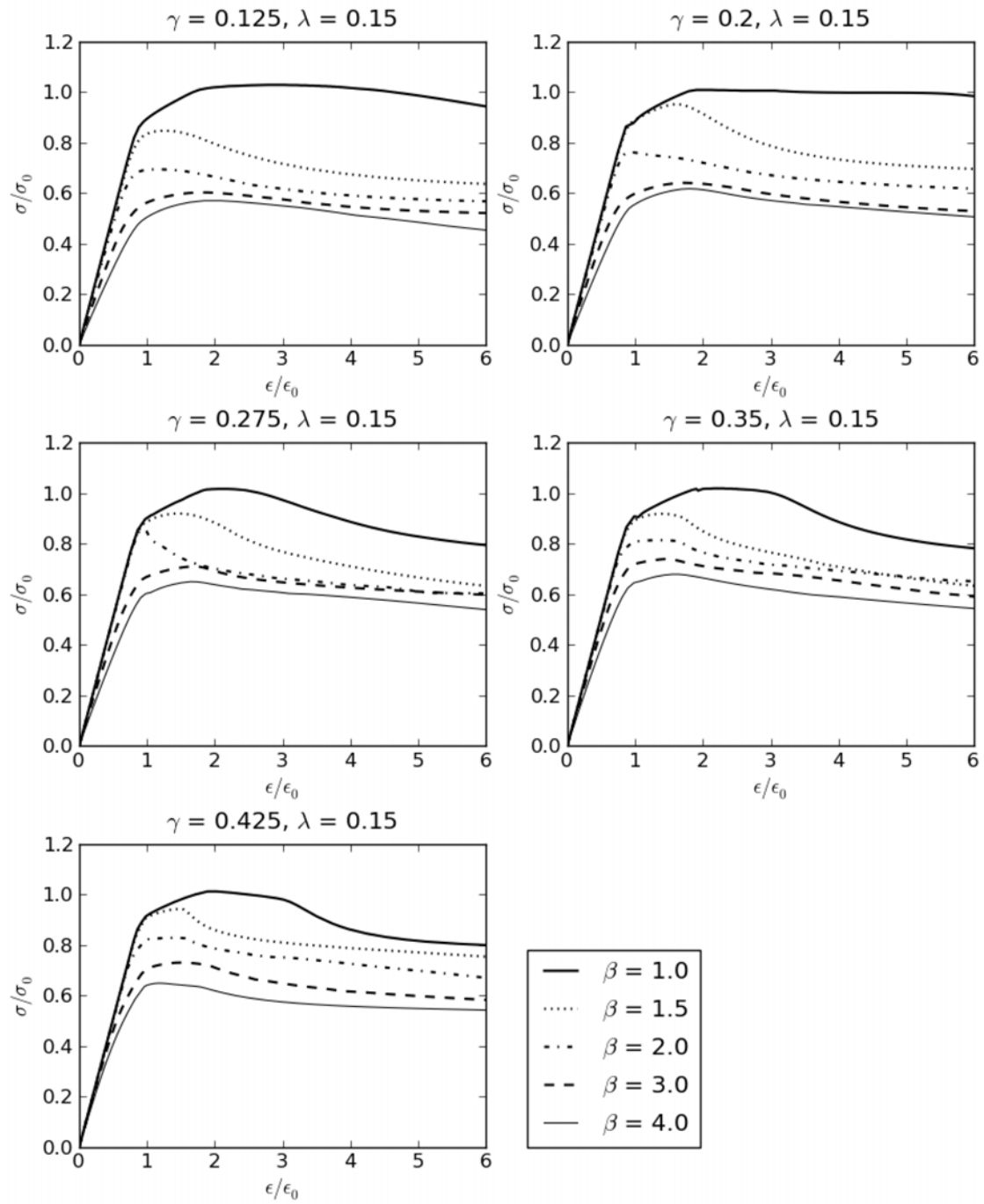*Figure 35: Load shortening curves for tee-stiffened panels with λ = 0.05.*

Figure 36: Load shortening curves for tee-stiffened panels with $\lambda = 0.15$.

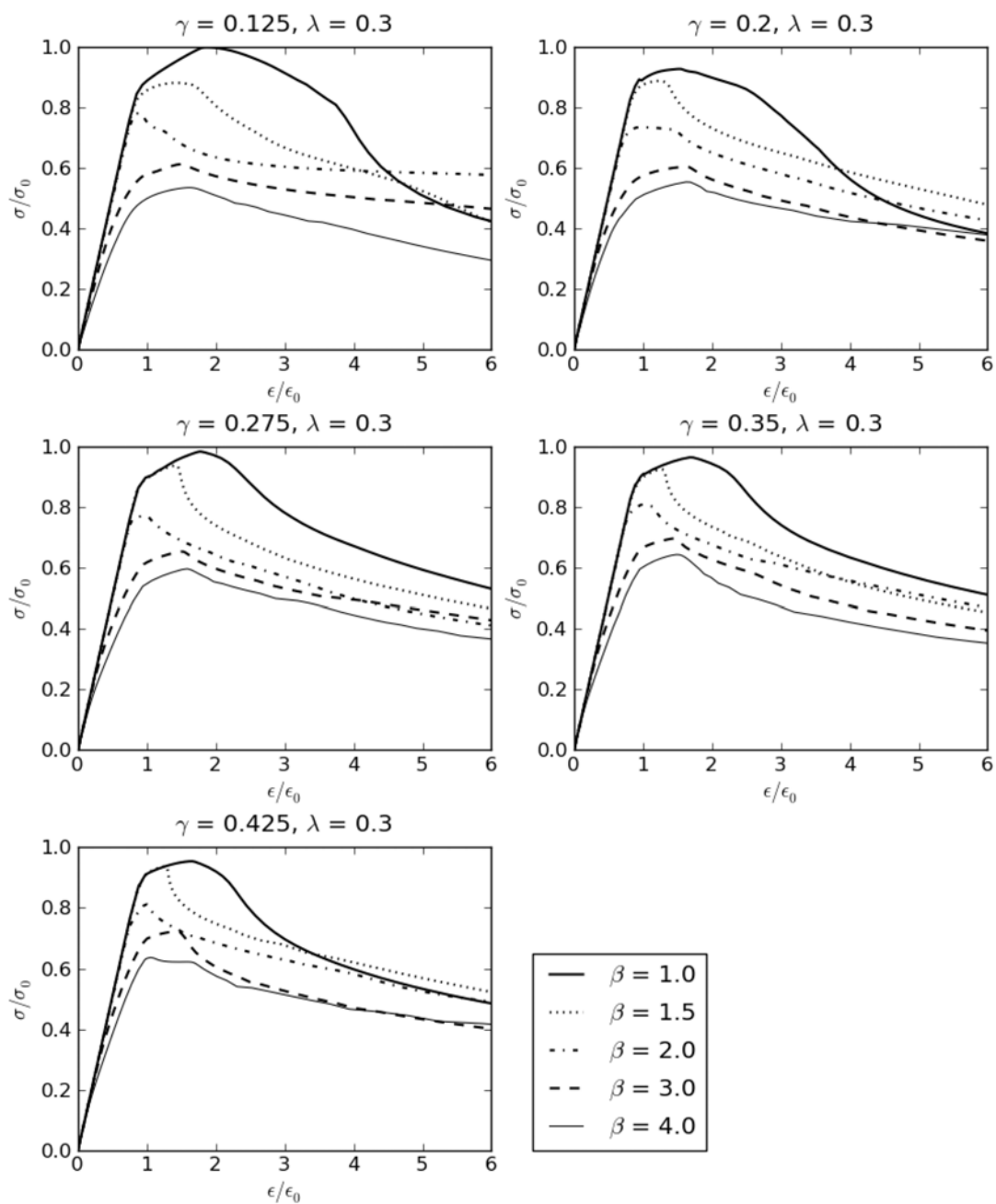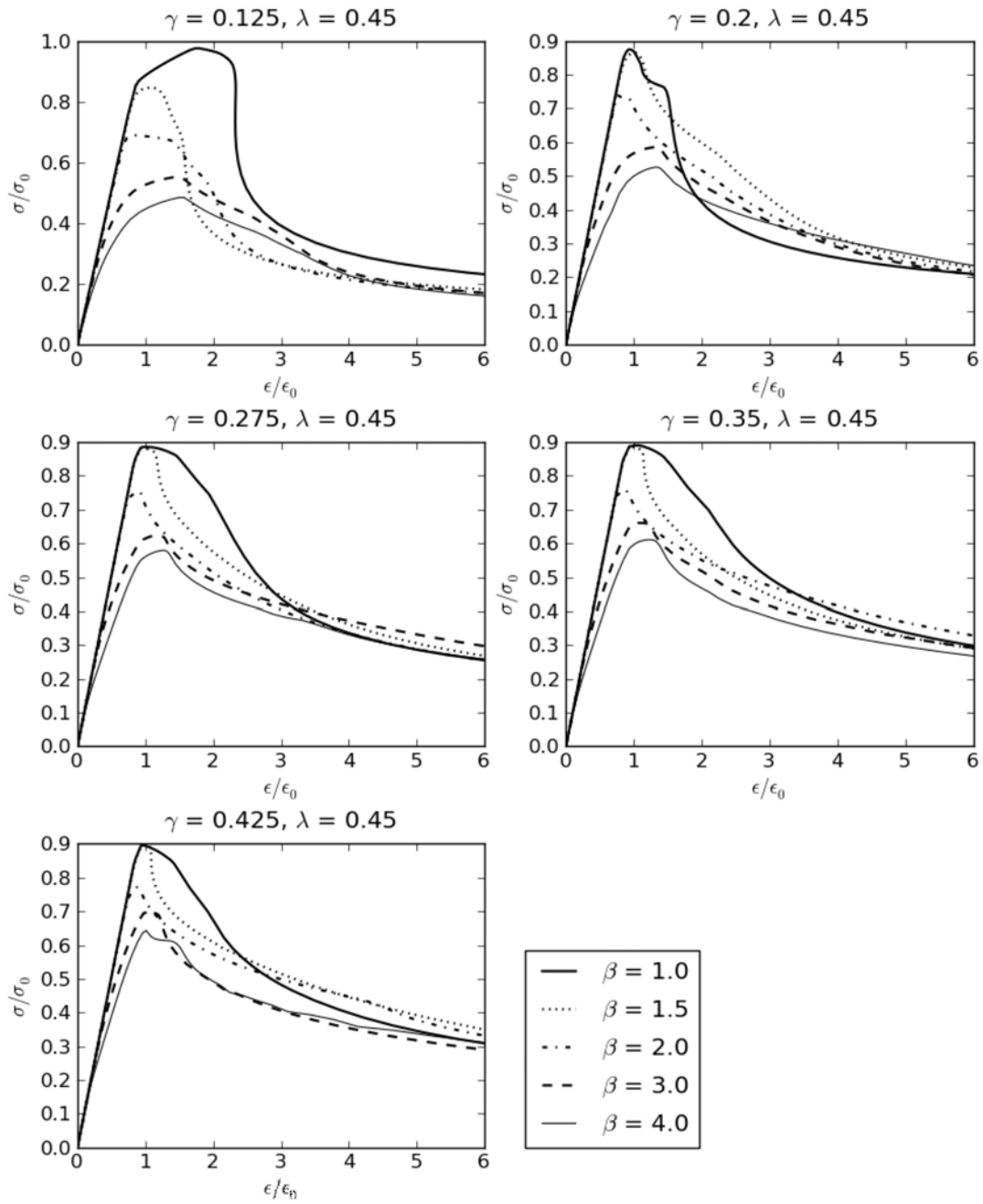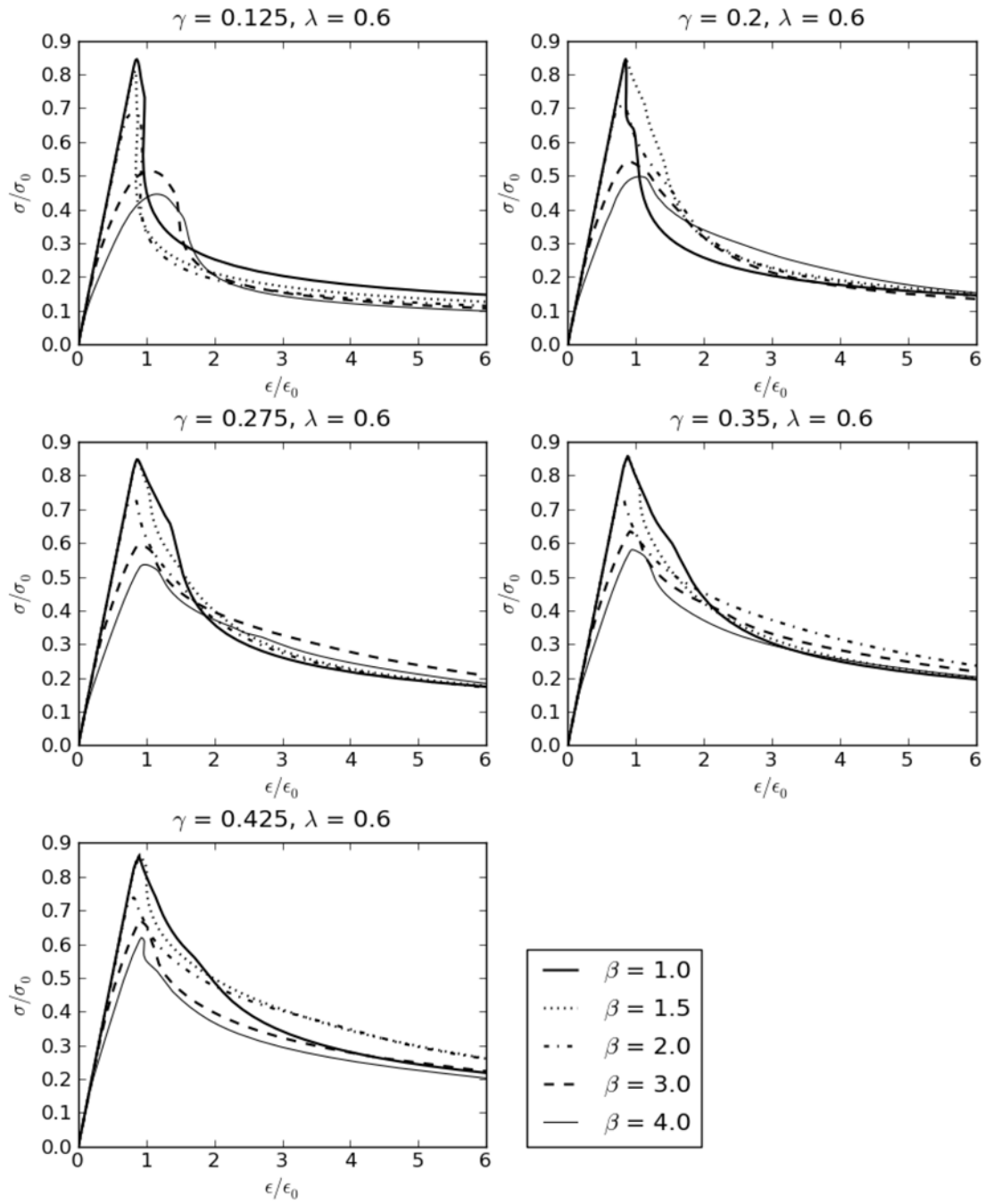*Figure 37: Load shortening curves for tee-stiffened panels with λ = 0.3.*

Figure 38: Load shortening curves for tee-stiffened panels with λ = 0.45.

Figure 39: Load shortening curves for tee-stiffened panels with λ = 0.6.

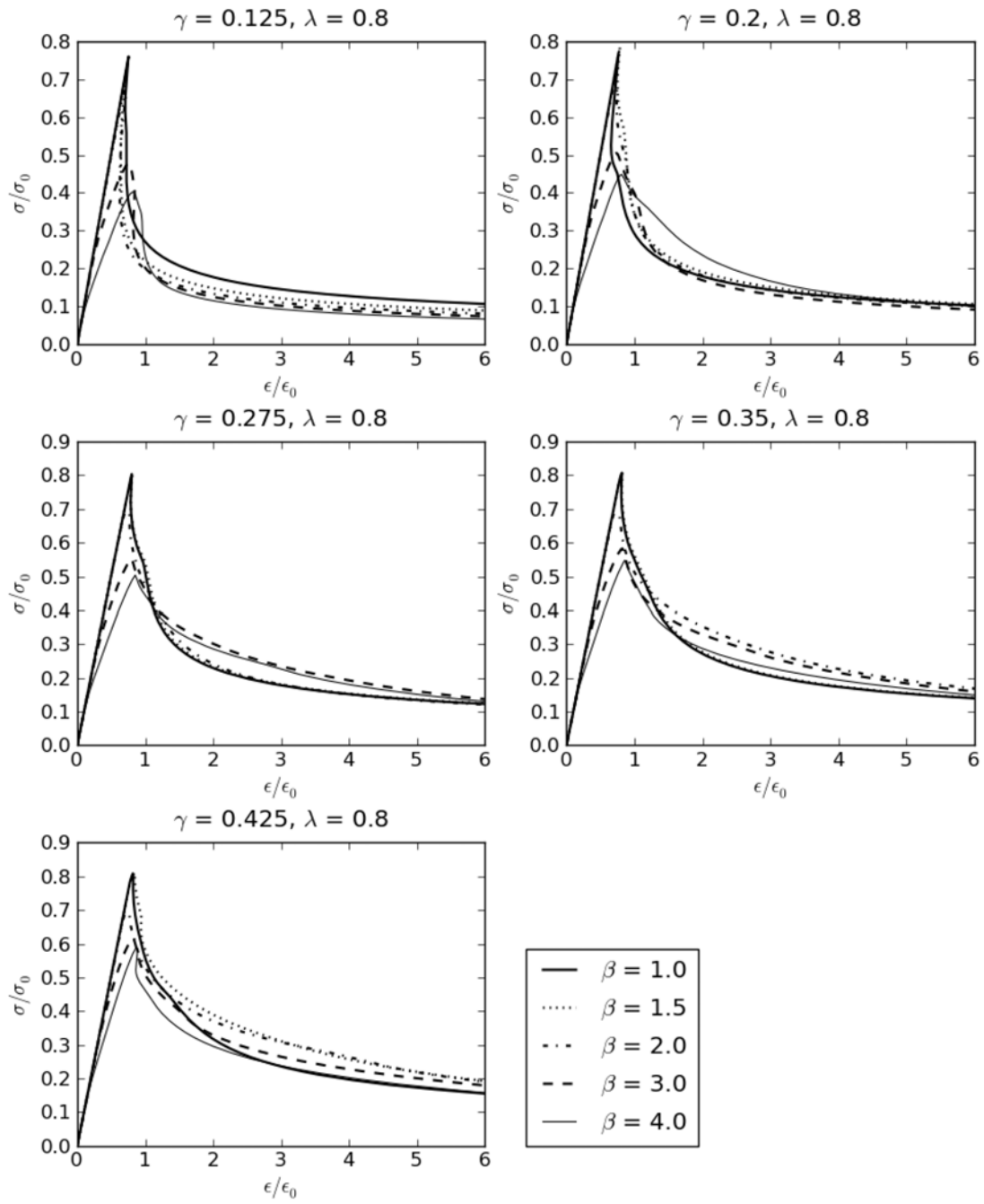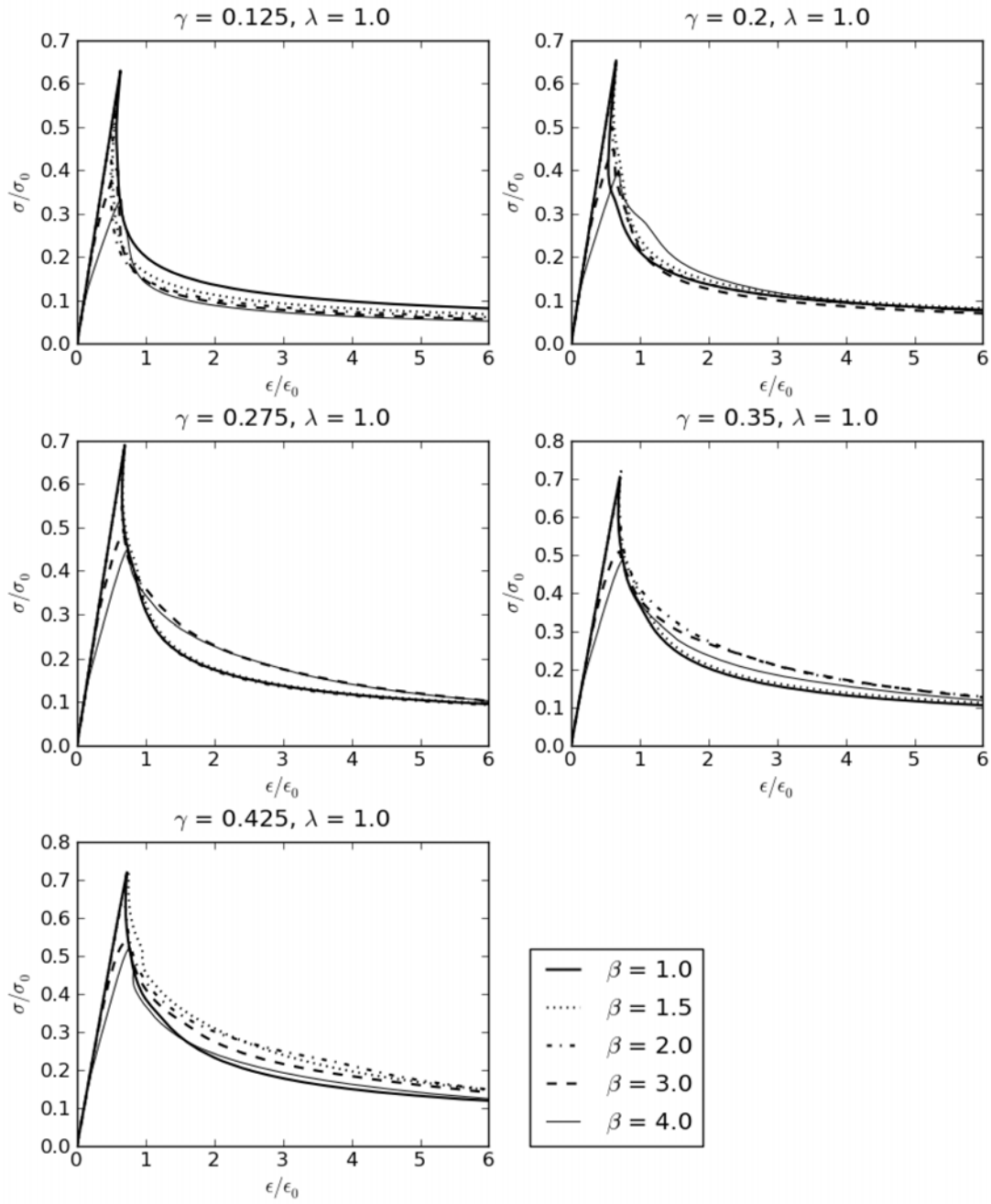*Figure 40: Load shortening curves for tee-stiffened panels with λ = 0.8.*

Figure 41: Load shortening curves for tee-stiffened panels with λ = 1.0.

A.2 Load-shortening curves for angle-stiffened panels

Figure 42: Load shortening curves for angle-stiffened panels with λ = 0.05.

Figure 43: Load shortening curves for angle-stiffened panels with λ = 0.15.

Figure 44: Load shortening curves for angle-stiffened panels with λ = 0.3.

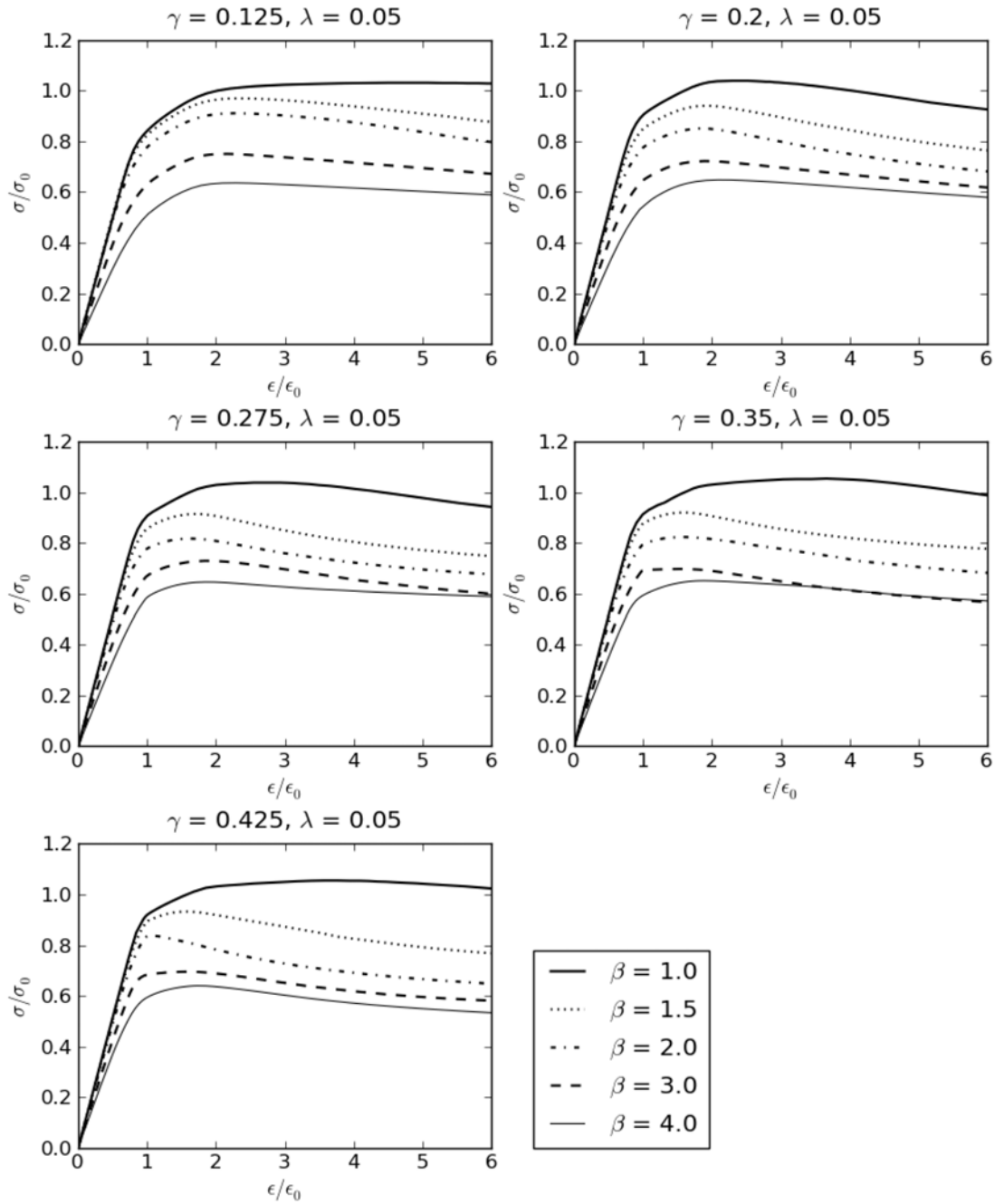*Figure 45: Load shortening curves for angle-stiffened panels with λ = 0.45.*

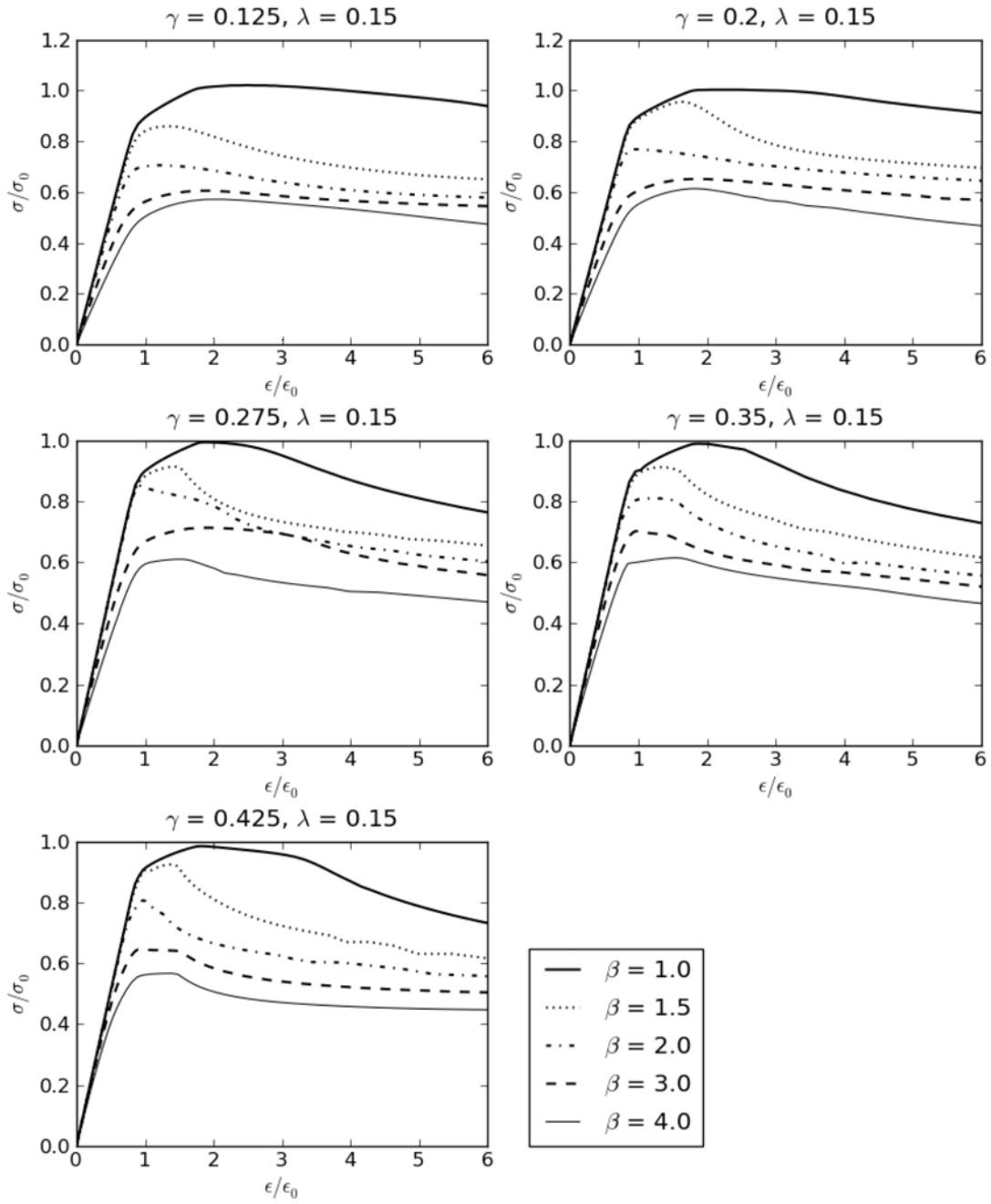*Figure 46: Load shortening curves for angle-stiffened panels with λ = 0.6.*

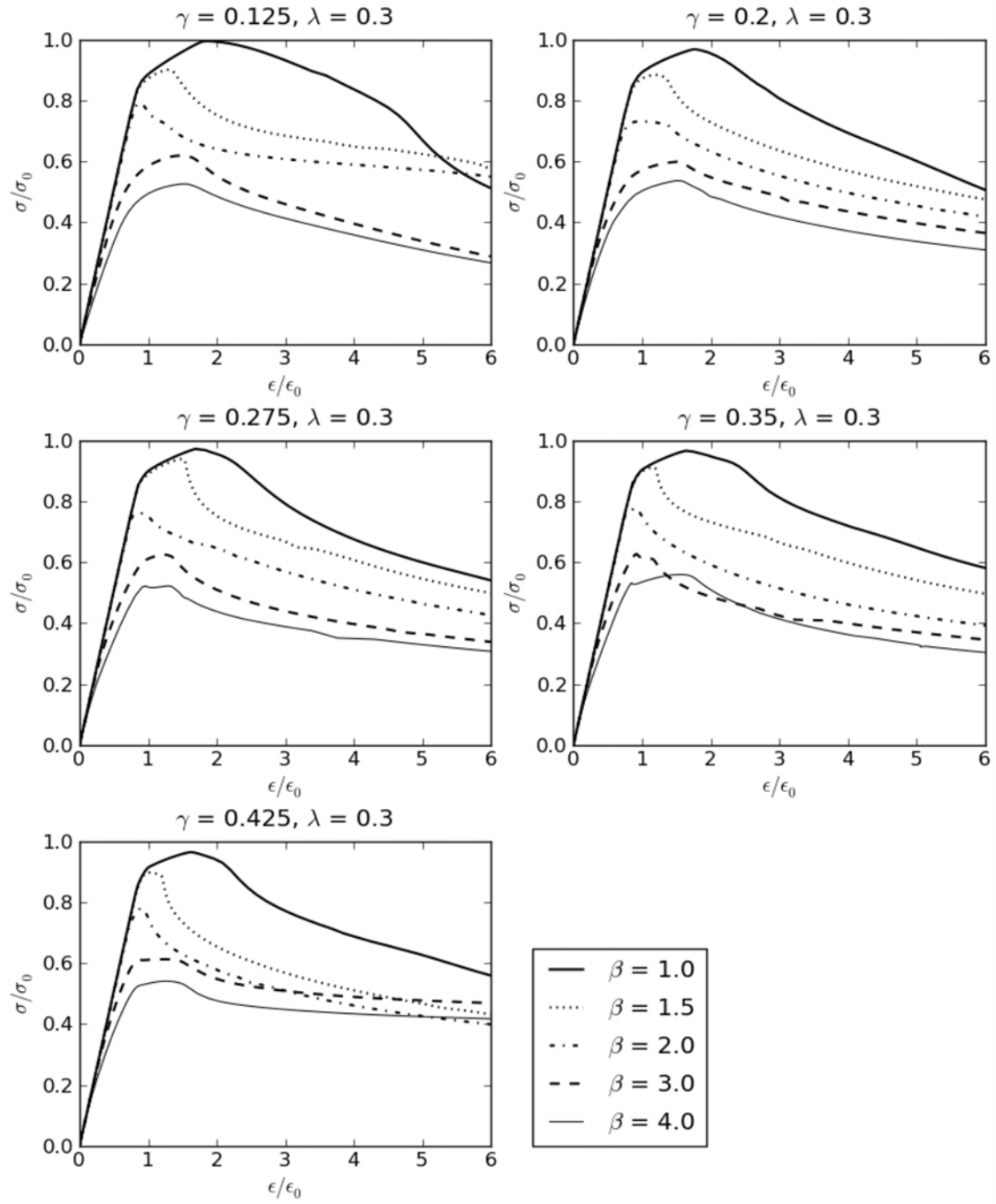*Figure 47: Load shortening curves for angle-stiffened panels with λ = 0.8.*
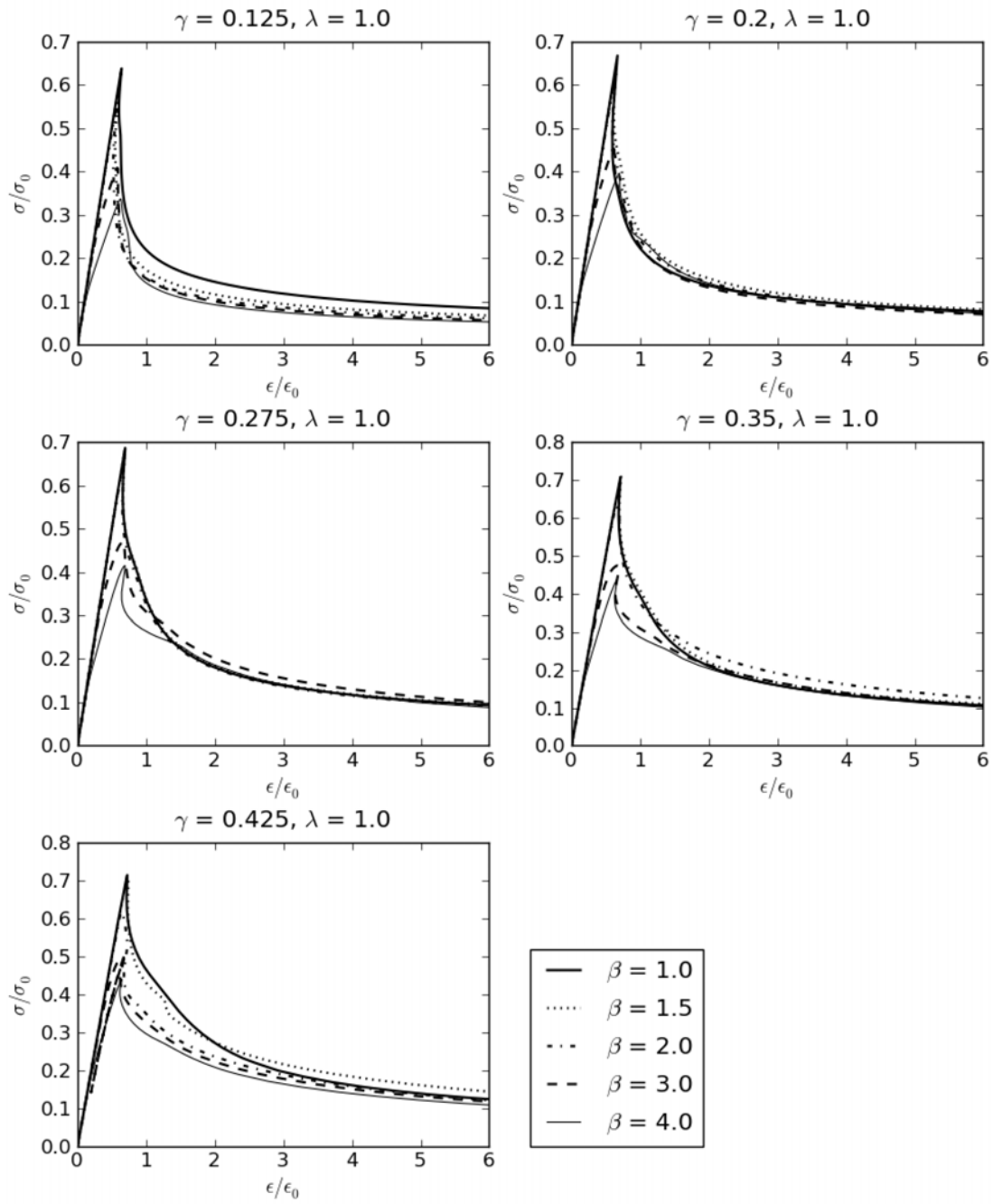
Figure 48: Load shortening curves for angle-stiffened panels with λ = 1.0.

A.3 Load-shortening curves for flatbar-stiffened panels

Figure 49: Load shortening curves for flatbar-stiffened panels with λ = 0.05.

Figure 50: Load shortening curves for flatbar -stiffened panels with λ = 0.15.

Figure 51: Load shortening curves for flatbar -stiffened panels with λ = 0.3.
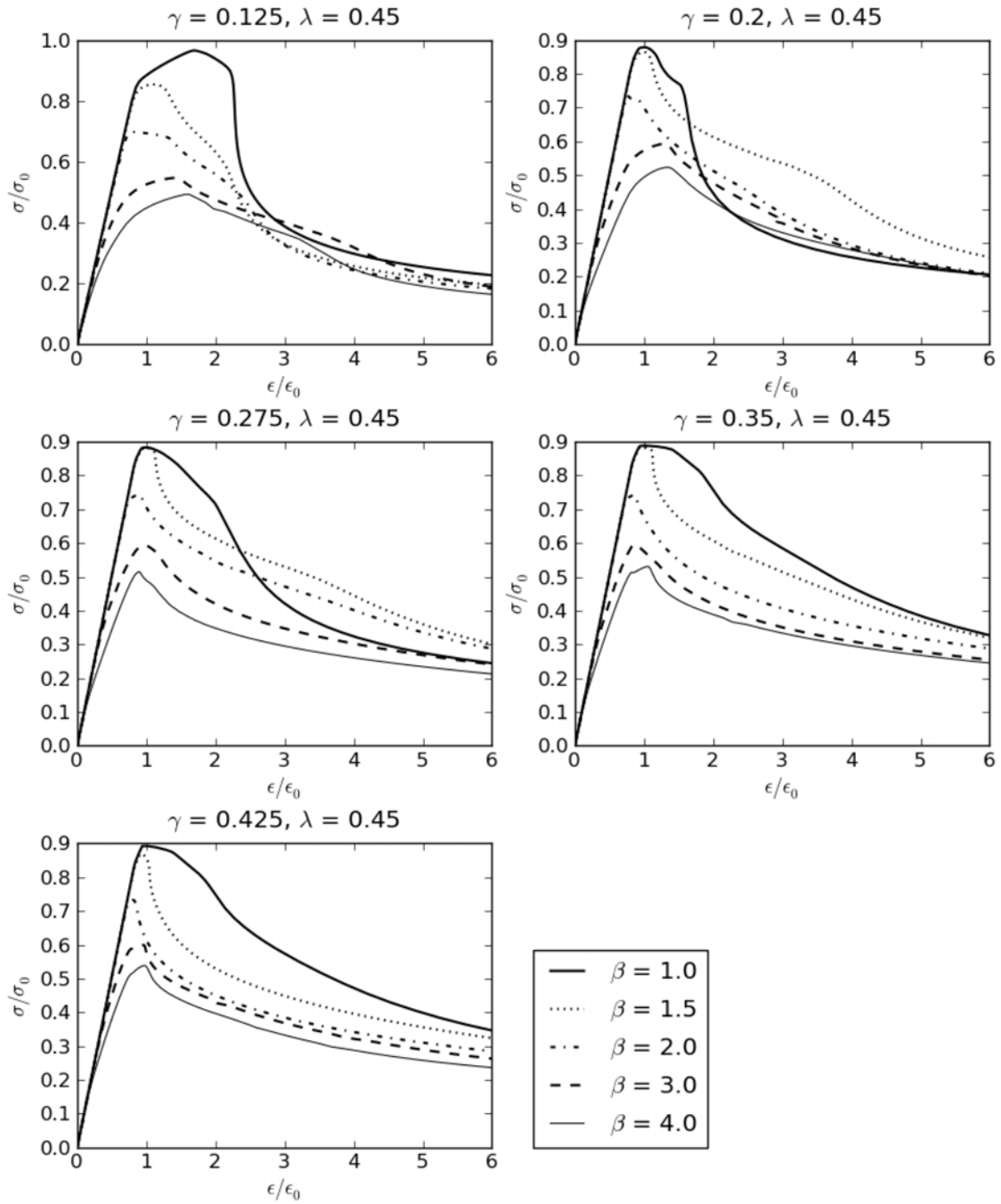
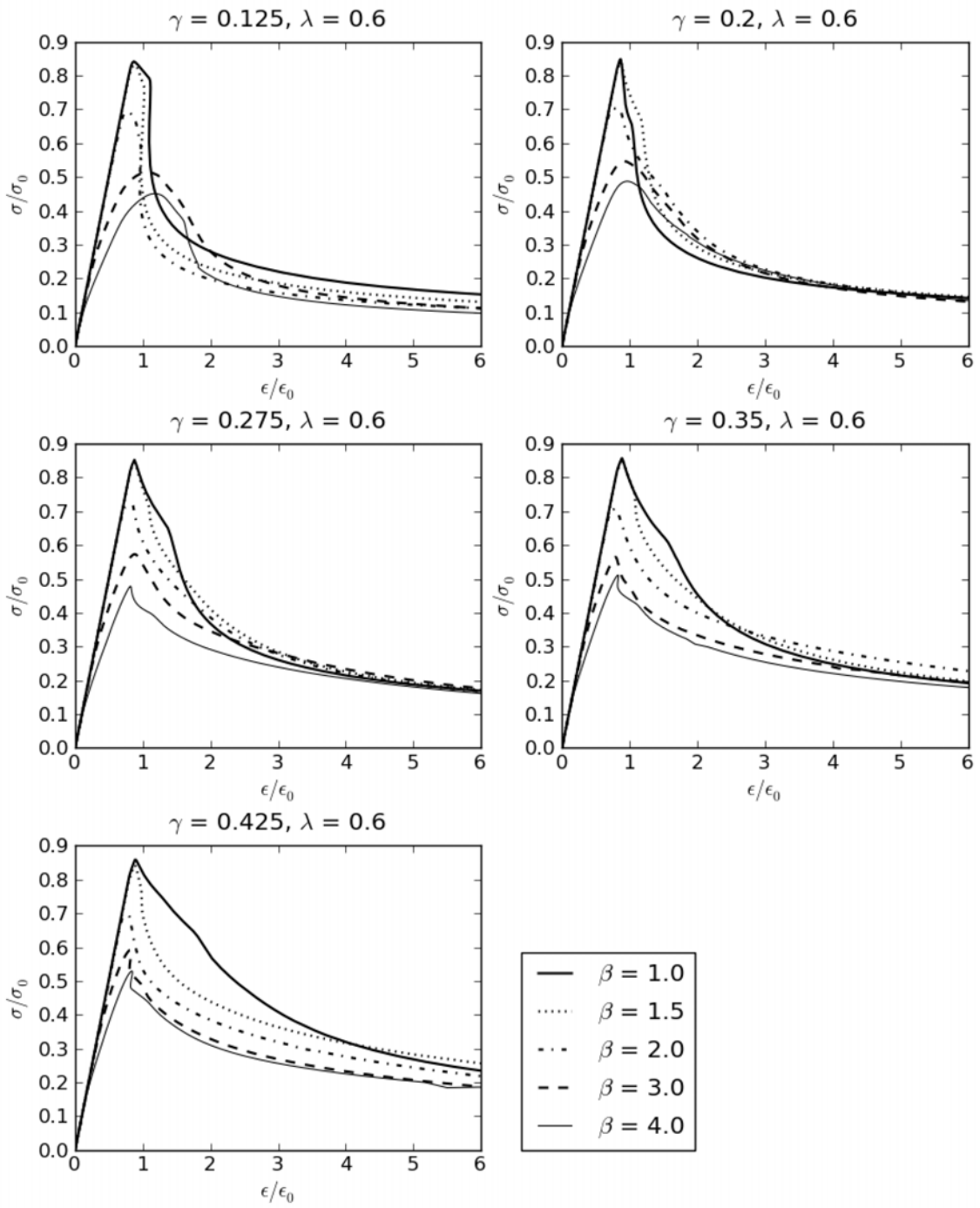*Figure 52: Load shortening curves for flatbar -stiffened panels with λ = 0.45.*

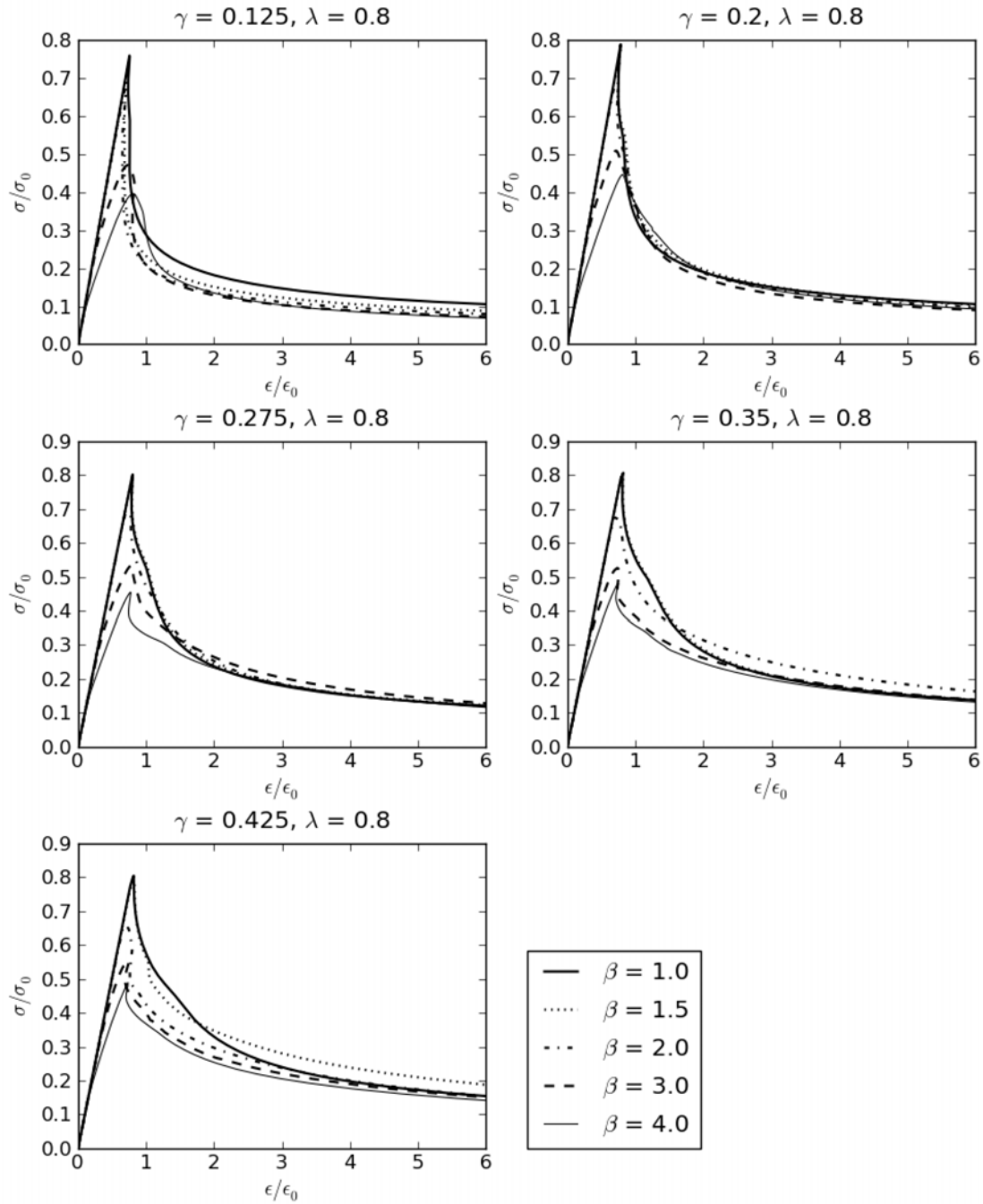*Figure 53: Load shortening curves for flatbar -stiffened panels with λ = 0.6.*

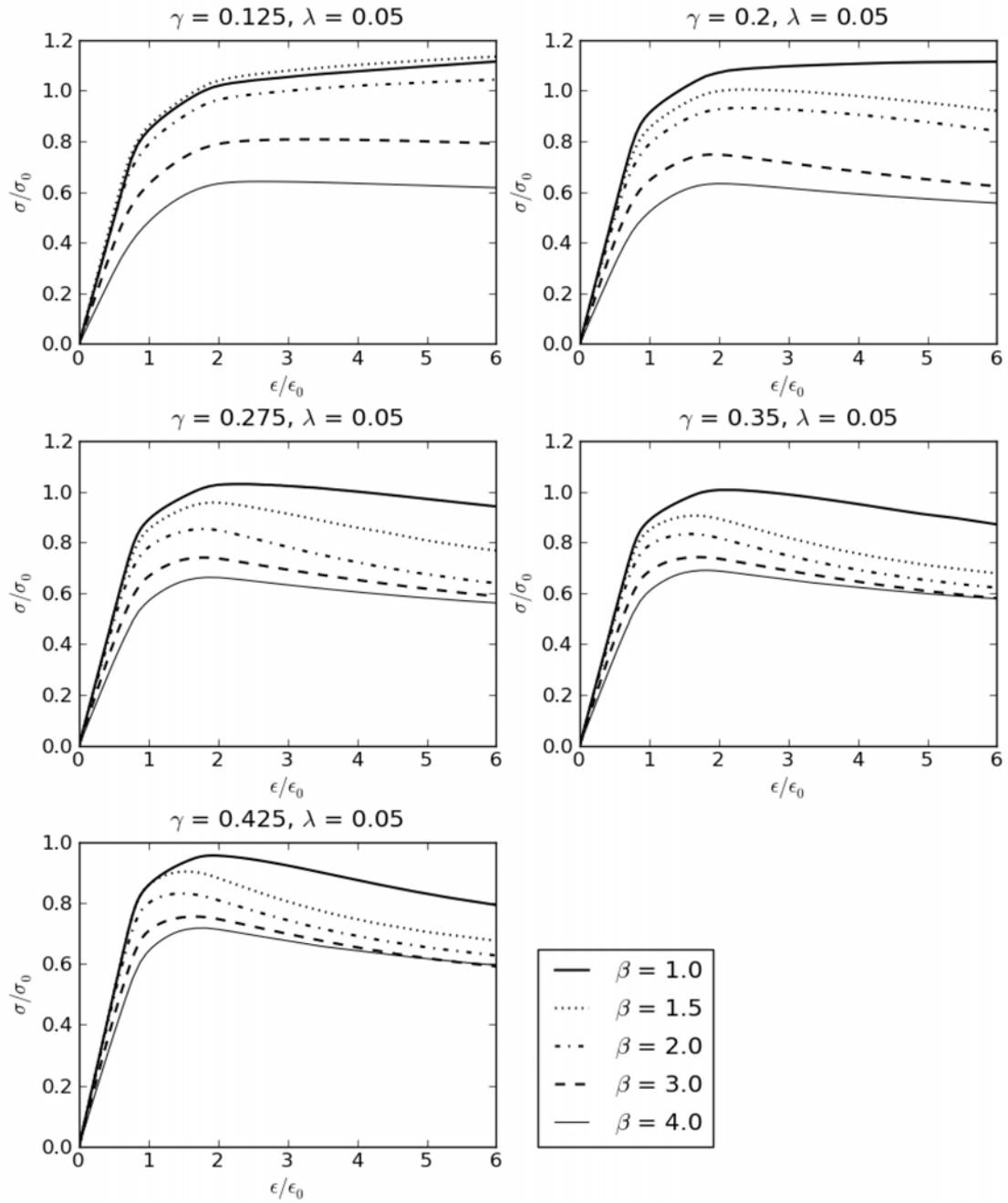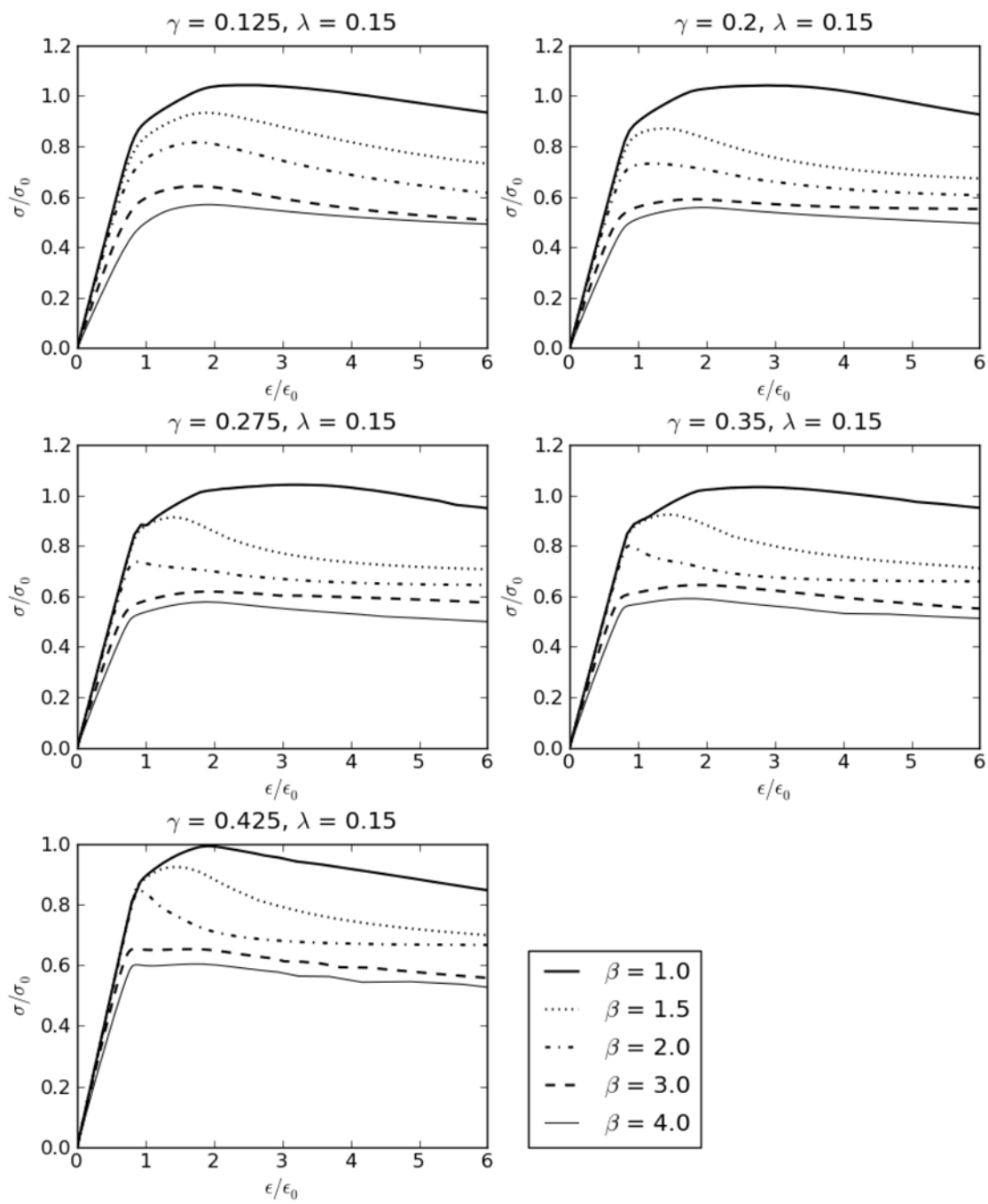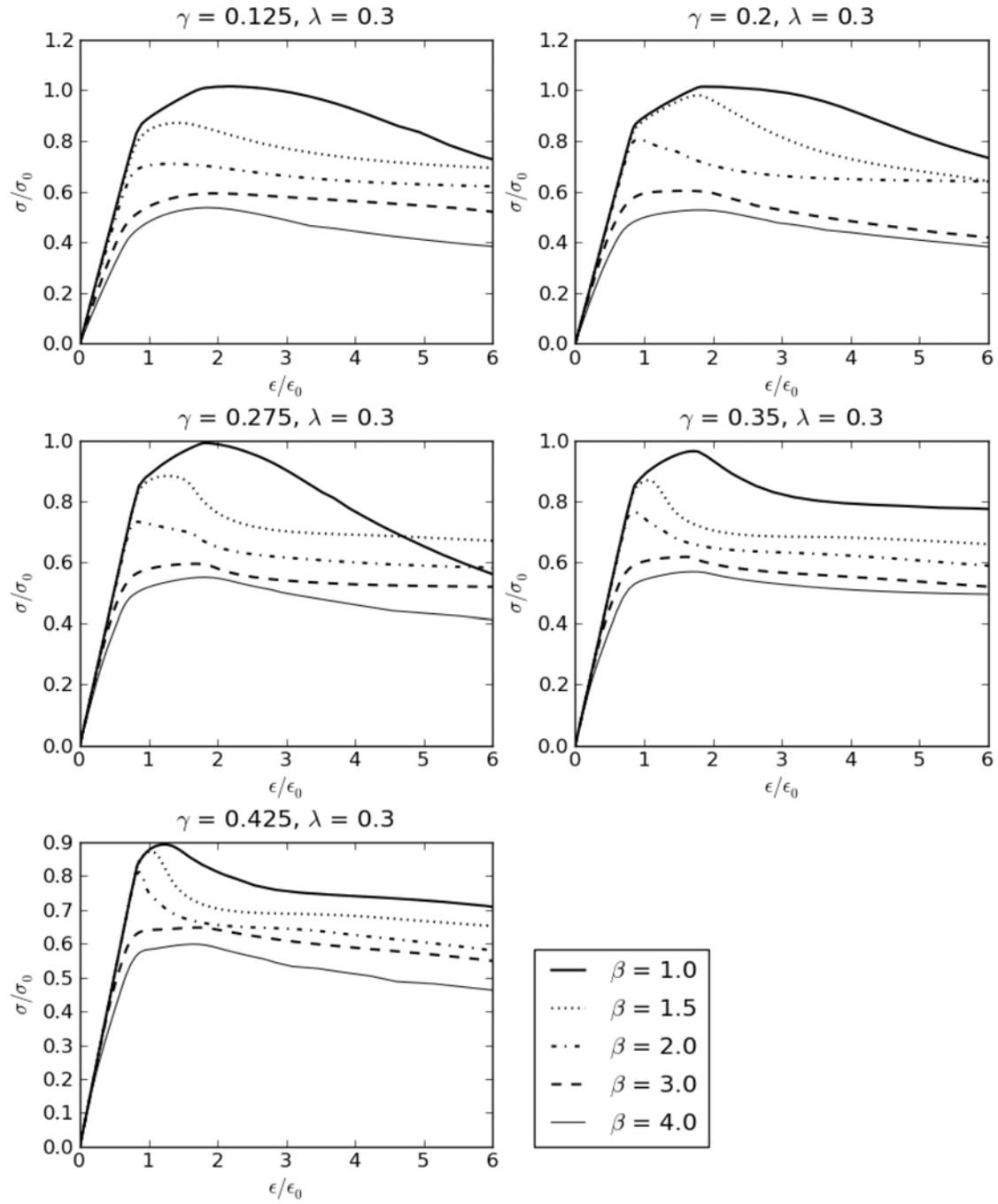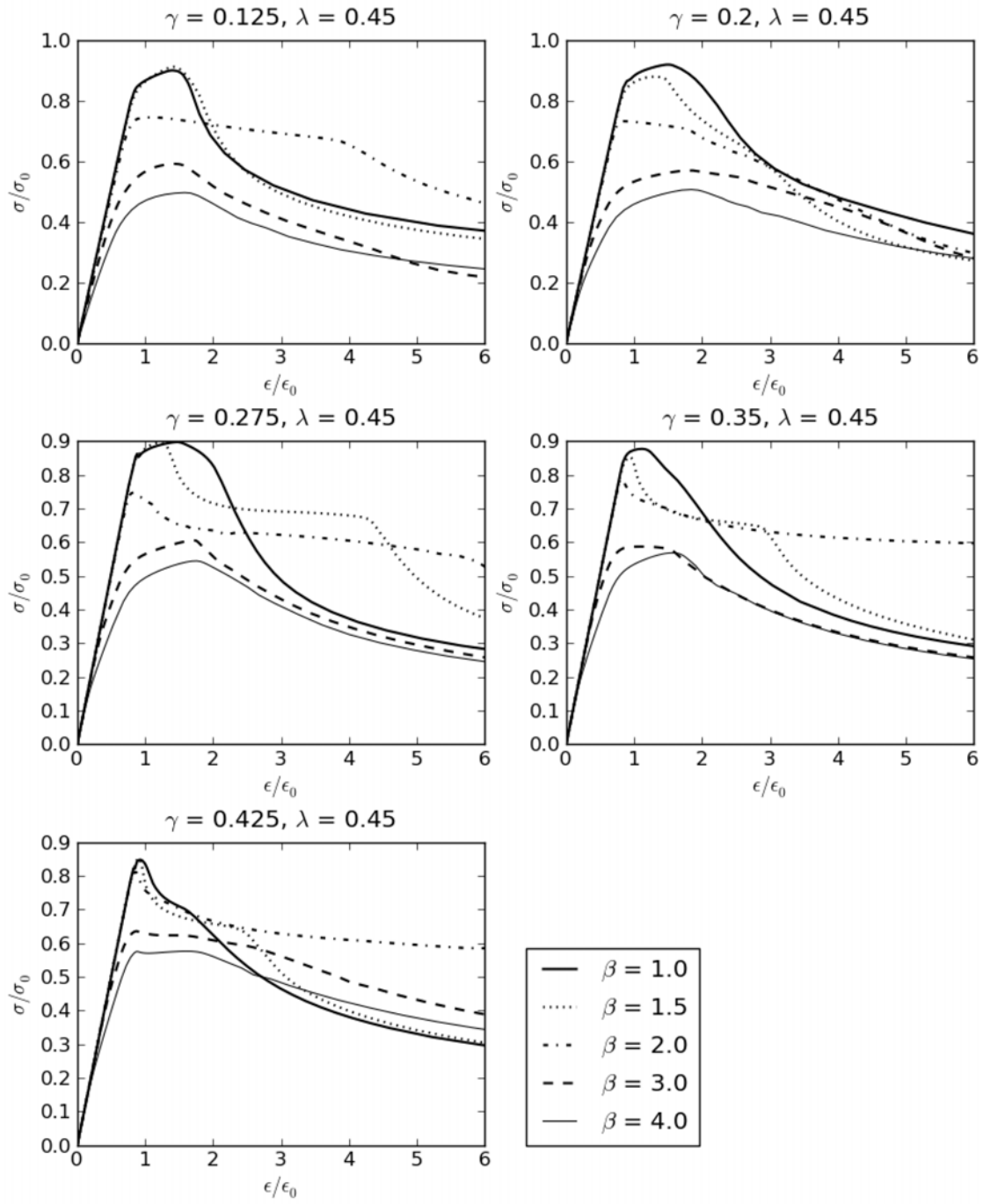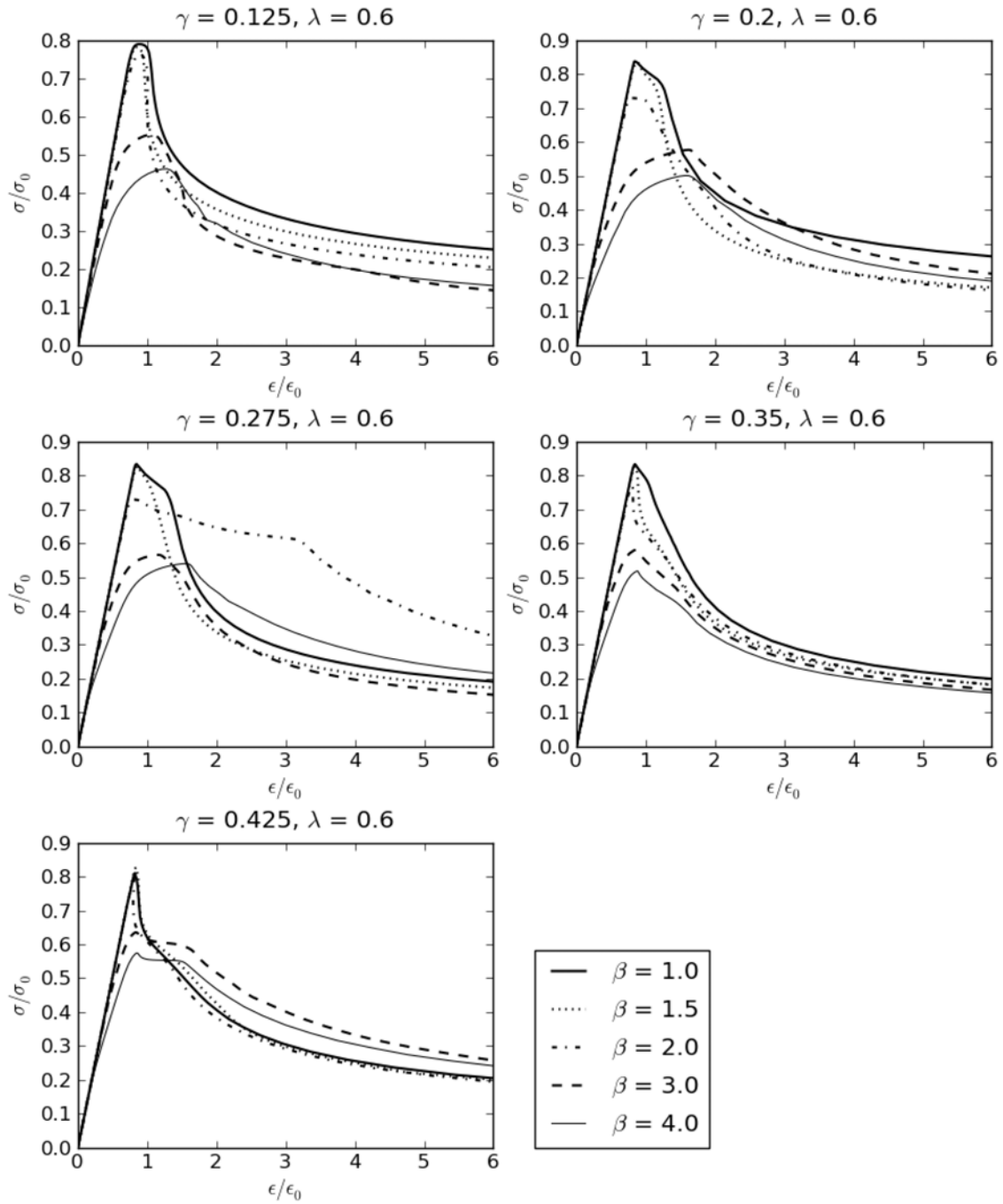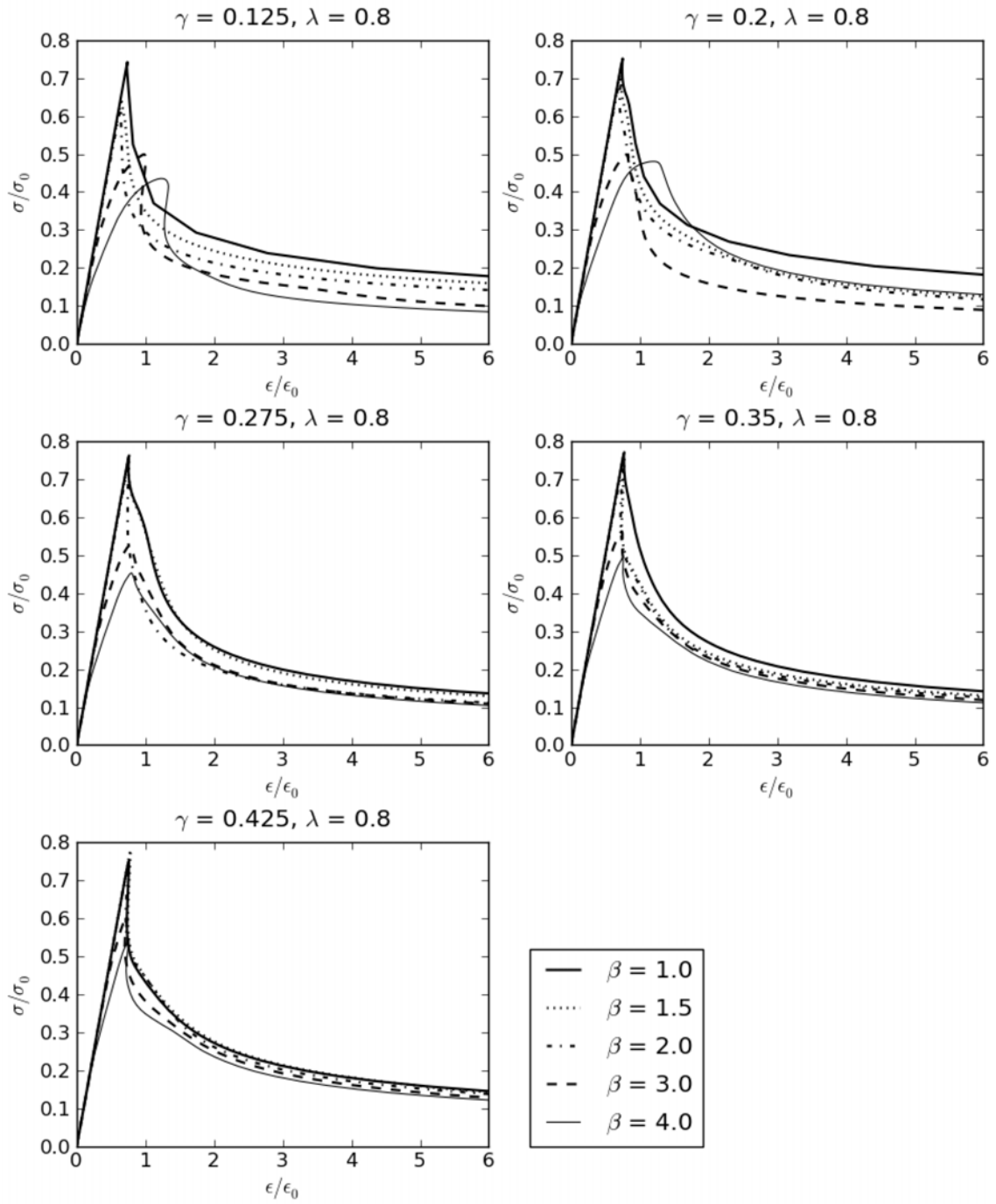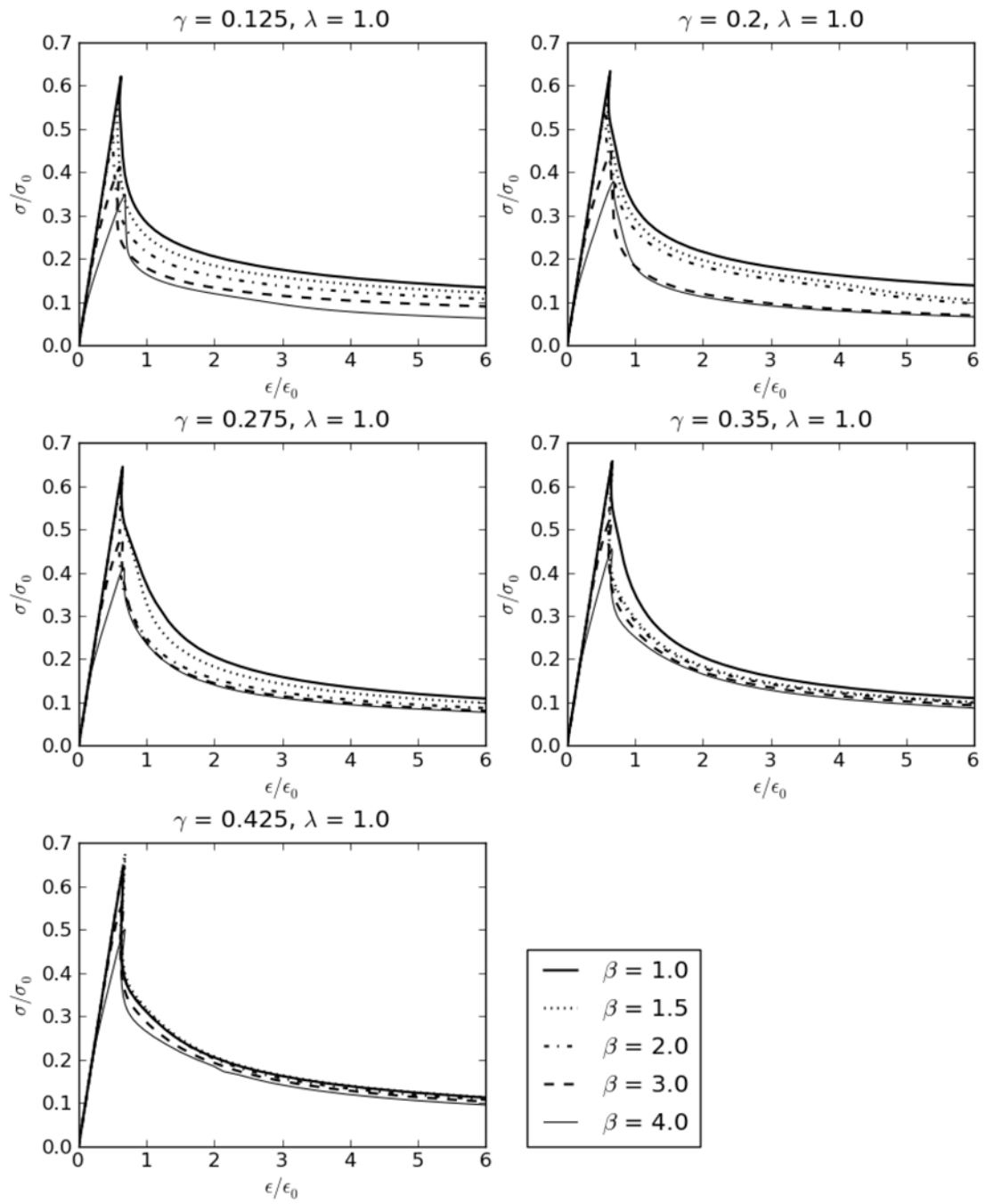*Figure 54: Load shortening curves for flatbar -stiffened panels with λ = 0.8.*

Figure 55: Load shortening curves for flatbar -stiffened panels with λ = 1.0.

This page intentionally left blank.

Annex B   Interpolation method

The compressive axial stress in a stiffened panel is expressed as a function of compressive strain, plate slenderness, column slenderness, and area ratio:

$$\sigma = \sigma(\varepsilon, \beta, \lambda, \gamma) \tag{16}$$

In the interpolation method, the stress function is approximated using stresses obtained from pre-calculated curves for discrete values of β, λ, and γ. Consider first the approximation introduced by discrete values of γ. If it is assumed that $\gamma_i \le \gamma \le \gamma_{i+1}$, where γ_i and γ_{i+1} represent discrete values of area ratio for pre-calculated curves, then linear interpolation over γ gives the following approximate stress:

$$\sigma(\varepsilon, \beta, \lambda, \gamma) = \sigma(\varepsilon, \beta, \lambda, \gamma_i)\frac{(\gamma_{i+1} - \gamma)}{\Delta\gamma} + \sigma(\varepsilon, \beta, \lambda, \gamma_{i+1})\frac{(\gamma - \gamma_i)}{\Delta\gamma}, \tag{17}$$

where $\Delta\gamma = \gamma_{i+1} - \gamma_i$.

If linear interpolation is now applied to λ, such that $\lambda_j \le \lambda \le \lambda_{j+1}$, each of the stress functions on the right-hand side of Eqn (17) can be replaced by the following approximate form:

$$\sigma(\varepsilon, \beta, \lambda, \gamma_i) = \sigma(\varepsilon, \beta, \lambda_j, \gamma_i)\frac{(\lambda_{j+1} - \lambda)}{\Delta\lambda} + \sigma(\varepsilon, \beta, \lambda_{j+1}, \gamma_i)\frac{(\lambda - \lambda_j)}{\Delta\lambda}, \tag{18}$$

where $\Delta\lambda = \lambda_{j+1} - \lambda_j$, and λ_j, λ_{j+1} are discrete values of column slenderness for which pre-calculated curves are available.

If the interpolation is extended to β, such that $\beta_k \le \beta \le \beta_{k+1}$, each of the stress functions on the right-hand side of Eqn (18) can be replaced by the following approximate form:

$$\sigma(\varepsilon, \beta, \lambda_j, \gamma_i) = \sigma(\varepsilon, \beta_k, \lambda_j, \gamma_i)\frac{(\beta_{k+1} - \beta)}{\Delta\beta} + \sigma(\varepsilon, \beta_{k+1}, \lambda_j, \gamma_i)\frac{(\beta - \beta_k)}{\Delta\beta}, \tag{19}$$

where $\Delta\beta = \beta_{k+1} - \beta_k$, and β_k, β_{k+1} are discrete values of plate slenderness for which pre-calculated curves are available. Substitution of (19) into (18) and (18) into (17) allows the stress to be expressed entirely in terms of discrete values of β, λ, and γ.

Pre-calculated curves used in computation are generally not represented as continuous functions of the strain. Rather, they are digitized into sets of discrete pairs $(\varepsilon_l, \sigma_l)$, for $l = 1, \ldots, n$. Provided n is large enough, a reasonably good approximation is obtained by assuming that the stress-strain curves are linear piecewise continuous between discrete pairs $(\varepsilon_l, \sigma_l)$. The stress functions on the right hand side of (19) can then be replaced the following approximate form:

$$\sigma(\varepsilon, \beta_k, \lambda_j, \gamma_i) = \sigma(\varepsilon_l, \beta_k, \lambda_j, \gamma_i) \frac{(\varepsilon_{l+1} - \varepsilon)}{\Delta \varepsilon} + \sigma(\varepsilon_{l+1}, \beta_k, \lambda_j, \gamma_i) \frac{(\varepsilon - \varepsilon_l)}{\Delta \varepsilon}, \qquad (20)$$

where $\varepsilon_l \leq \varepsilon \leq \varepsilon_{l+1}$ and $\Delta \varepsilon = \varepsilon_{l+1} - \varepsilon_l$. The stress terms on the right-hand side of (20) are now in the form of discrete stress values taken directly from the pre-calculated curve for β_k, λ_j, γ_i.

If any of the values for β, λ, and γ lie outside of the range of discrete values, extrapolation rather than interpolation of the pre-calculated curves is required. An example of this is if $\lambda < \lambda_1 < \lambda_2$, where λ_1 and λ_2 are the two lowest discrete values of column slenderness. The formulas required for extrapolation over γ, λ, and β are identical to (17) – (19), so no further modification is required. Eqns (17) – (20) therefore fully described the interpolation method for load shortening curves.

List of symbols/abbreviations/acronyms/initialisms

6.1.1   Abbreviations/acronyms/initialisms

ALPS	Analysis of Large Plated Structures (structural analysis program)
CC	Centre-to-centre
CRS	Cooperative Research Ships
DND	Department of National Defence
EE	End-to-end
Eqn	Equation
FABSTRAN	Frame and beam static or transient response analysis nonlinear (UK FE code)
FB	Flatbar stiffener
FE	Finite element
FEA	Finite element analysis
IACS	International Association of Classification Societies
ISSC	International Ship Structures Committee
ISUM	Independent Structural Unit Method
LSPanel	Program for generating stiffened panel models for FEA
NS94B	UK MoD ultimate strength codes
ULTMAT	Canadian ultimate strength code
VLCC	Very large crude carrier

6.1.2   Symbols

a	Panel length, or frame spacing
A_s	Stiffener cross sectional area
A	Panel cross sectional area
b	Plate width
d	Stiffener depth
I	Second moment of area
M_p	Plastic bending strength
M_{us}, M_{uh}	Ultimate strength in sag, hog
n_a	Number elements in the longitudinal direction
n_b	Number elements in the transverse direction
n_f	Number elements across the width of the flange

n_w	Number elements in across the depth of the stiffener web
$_iN$	Number of iterations per load step
N_d	Desired number of iteration per load step
P	Mesh parameter
r_g	Radius of gyration
t	Plate thickness
t_w	Web thickness
t_f	Flange thickness
U_a	Total strain energy in axial compression
w	Stiffener width
X_σ, X_U	Strength and energy bias factor
α	Ratio of maximum allowable arc length to the initial arc length
β	Plate slenderness
γ	Area ratio (stiffener area / panel cross-section area)
δ_p	Maximum plate imperfection
δ_{bv}, δ_{bh}	Maximum vertical, horizontal beam imperfection
$_1\Delta l$	Initial arc length
$_i\Delta l$	Arc length in load step i
ε	Strain
$\bar{\varepsilon}$	Normalized strain $= \varepsilon/\varepsilon_y$
ε_y	Yield strain
κ	Convergence tolerance
η	Parameter used to define width of heat-affect zone
λ	Column slenderness
μ	Arc length size exponent, material parameter
π	Pi
σ	Stress
$\bar{\sigma}$	Normalized stress $= \sigma/\sigma_y$
σ_r	Residual stress
σ_u	Ultimate strength
σ_y	Yield stress
σ_{yb}, σ_{yp}	Yield stress of beam, plate

Distribution list

Document No.:   DRDC Atlantic TM 2010-140

LIST PART 1 – Internal Distribution by Centre:

4   Author (2 paper copies, 2 CDs)
3   DRDC Atlantic Library (1 paper copy, 2 CDs)
_____
7   TOTAL LIST PART I

LIST PART II: External Distribution within Canada by DRDKIM

1   Library and Archives Canada, Attn: Military Archivist, Government Records Branch
1   NDHQ/DRDKIM 3
1   NDHQ/DMSS 2
_____
3   TOTAL LIST PART II

10   TOTAL COPIES (3 paper copies, 7 CDs)

This page intentionally left blank.

DOCUMENT CONTROL DATA

(Security classification of title, body of abstract and indexing annotation must be entered when the overall document is classified)

1. ORIGINATOR (The name and address of the organization preparing the document. Organizations for whom the document was prepared, e.g. Centre sponsoring a contractor's report, or tasking agency, are entered in section 8.) Defence R&D Canada – Atlantic 9 Grove Street P.O. Box 1012 Dartmouth, Nova Scotia B2Y 3Z7	2. SECURITY CLASSIFICATION (Overall security classification of the document including special warning terms if applicable.)	

3. TITLE (The complete document title as indicated on the title page. Its classification should be indicated by the appropriate abbreviation (S, C, R or U) in parentheses after the title.)

A load shortening curve library for longitudinally stiffened panels

4. AUTHORS (last name, followed by initials – ranks, titles, etc. not to be used)

Smith, Malcolm J.

5. DATE OF PUBLICATION (Month and year of publication of document.) August 2010	6a. NO. OF PAGES (Total containing information, including Annexes, Appendices, etc.) 88	6b. NO. OF REFS (Total cited in document.) 22

7. DESCRIPTIVE NOTES (The category of the document, e.g. technical report, technical note or memorandum. If appropriate, enter the type of report, e.g. interim, progress, summary, annual or final. Give the inclusive dates when a specific reporting period is covered.)

Technical Memorandum

8. SPONSORING ACTIVITY (The name of the department project office or laboratory sponsoring the research and development – include address.)

Defence R&D Canada – Atlantic
9 Grove Street
P.O. Box 1012
Dartmouth, Nova Scotia B2Y 3Z7

9a. PROJECT OR GRANT NO. (If appropriate, the applicable research and development project or grant number under which the document was written. Please specify whether project or grant.)11ge	9b. CONTRACT NO. (If appropriate, the applicable number under which the document was written.)
10a. ORIGINATOR'S DOCUMENT NUMBER (The official document number by which the document is identified by the originating activity. This number must be unique to this document.) DRDC Atlantic TM 2010-140	10b. OTHER DOCUMENT NO(s). (Any other numbers which may be assigned this document either by the originator or by the sponsor.)

11. DOCUMENT AVAILABILITY (Any limitations on further dissemination of the document, other than those imposed by security classification.)

(X) Unlimited distribution
(   ) Defence departments and defence contractors; further distribution only as approved
(   ) Defence departments and Canadian defence contractors; further distribution only as approved
(   ) Government departments and agencies; further distribution only as approved
(   ) Defence departments; further distribution only as approved
(   ) Other (please specify):

12. DOCUMENT ANNOUNCEMENT (Any limitation to the bibliographic announcement of this document. This will normally correspond to the Document Availability (11). However, where further distribution (beyond the audience specified in (11) is possible, a wider announcement audience may be selected.))

13. ABSTRACT (A brief and factual summary of the document. It may also appear elsewhere in the body of the document itself. It is highly desirable that the abstract of classified documents be unclassified. Each paragraph of the abstract shall begin with an indication of the security classification of the information in the paragraph (unless the document itself is unclassified) represented as (S), (C), (R), or (U). It is not necessary to include here abstracts in both official languages unless the text is bilingual.)

Efficient methods for determining the load versus end-shortening response of longitudinally stiffened panels are considered. A library of load-shortening curves for a wide range of design parameters is developed using an automated finite element analysis (FEA) procedure. The load-shortening response of twenty benchmark stiffened panels is estimated by interpolation of the library curves. These are compared with similar curves calculated using nonlinear FEA and using design formulas published by the International Association of Classification Societies (IACS). The ultimate strength of eight benchmark hull girders is predicted using the interpolation and IACS methods for estimating the load-shortening response of stiffened panel structure, all within the framework of a Smith's method algorithm implemented in ULTMAT. Comparisons with previously published results indicate that acceptable accuracy can usually be obtained with the approximate methods. The scatter in strength predictions using Smith's method is considered, and is sometimes found to be greater than the recommended safety factor of 1.1.

14. KEYWORDS, DESCRIPTORS or IDENTIFIERS (Technically meaningful terms or short phrases that characterize a document and could be helpful in cataloguing the document. They should be selected so that no security classification is required. Identifiers, such as equipment model designation, trade name, military project code name, geographic location may also be included. If possible keywords should be selected from a published thesaurus, e.g. Thesaurus of Engineering and Scientific Terms (TEST) and that thesaurus identified. If it is not possible to select indexing terms which are Unclassified, the classification of each should be indicated as with the title.)

Ultimate strength
Marine structures
Load shortening curves
Nonlinear finite element analysis
Hull girder bending moment
Stiffened panel
ULTMAT
Ship design

This page intentionally left blank.

Defence R&D Canada

Canada's leader in defence
and National Security
Science and Technology

R & D pour la défense Canada

Chef de file au Canada en matière
de science et de technologie pour
la défense et la sécurité nationale

DEFENCE R&D DÉFENSE